A peak into the mantle: primary magma generation beneath the Peak Range, central Queensland

Thesis submitted in accordance with the requirements of the University of Adelaide for an Honours Degree in Geology

Lauren Peters

November 2021

THE UNIVERSITY of ADELAIDE

A PEAK INTO THE MANTLE: PRIMARY MAGMA GENERATION BENEATH THE PEAK RANGE, CENTRAL QUEENSLAND

A PEAK INTO THE MANTLE BENEATH THE PEAK RANGE

ABSTRACT

The hotspot-related Tertiary Peak Range (central Queensland) consists of enriched peraluminous rhyolites in the north, and metaluminous trachytes and peralkaline rhyolites in the south. Further petrographical mapping of the southern Peak Range revealed consistency with Chandler (2018) model of an extended fractionation of an alkali basaltic melt as the source for the enriched intrusion, whereas a heterogeneous intrusion (Campbell's Peak; a phonolitic intrusion with a basaltic rim abundant in peridotite xenoliths and amphibole megacrysts) 20km NE of the central Peak Range executes a different evolutional pathway.

The peridotites are characteristic of metasomatised subcontinental lithospheric mantle (SCLM), enriched from the dehydration of fluids from the subducting slab along eastern Australia during the Late Devonian-Cretaceous, apparent in the growth of pargasitic amphibole (modal metasomatism), and high concentrations of Rb, La, Ta, U, and sodium-bearing pyroxenes (mild cryptic metasomatism). The amphibole megacrysts are assumed to be a cumulate or fractionation phase in the mantle, brought to the surface as xenocrysts in the basalt.

Melting models of the peridotite demonstrate a lack of correlation between the basaltic host rock (especially in TiO_2 levels), but a stronger correlation with the phonolitic intrusion when partially melted (<1%) at ~10kbar and if fractionation of ~15% amphibole was considered. Fractionation modelling of the trachybasalt revealed no direct relationship to the peridotites or phonolitic rocks, suggesting it is unrelated.

The spatial and temporal relation of Campbell's Peak to the Peak Range is similar to the Ernst & Bell (2010) model of linking large igneous provinces (LIPs) and carbonatites intrusions, if the central Peak Range is interpreted as the volcanic centre. It is proposed the phonolitic intrusion of Campbell's Peak is a result of low degree partial melting of the SCLM via low temperature magmatism at the outer edge of the mantle plume, with later basaltic eruption resembling more mantle plume, flood basalt mechanisms.

KEYWORDS

Peak Range, peridotite xenoliths, mantle melting modelling, mantle metasomatism, amphibole megacrysts

TABLE OF CONTENTS

LIST OF FIGURES

2. BACKGROUND/GEOLOGICAL SETTING

4. OBSERVATIONS AND RESULTS

5. DISCUSSION

LIST OF TABLES

2. BACKGROUND/GEOLOGICAL SETTING

4. OBSERVATIONS AND RESULTS

1. INTRODUCTION

The Peak Range is a breathtaking NW-SE volcanic chain amongst flat lying plains located near Clermont in central QLD, Australia. The range is divided into three groups: a central group of basaltic flat-topped mesas that are interpreted to be relic stacks of flood basalts that erupted during the Cenozoic, and the northern and southern group that are the Peak Range Volcanics, predominantly intermediate to felsic trachytes and rhyolites that intruded through the flood basalts during the Oligocene (Wellman & McDougall, 1974). The origin of this volcanic mountain chain is interpreted to be a result of mantle plume magma generation, as it lies along the Cosgrove hotspot track (Davies et al., 2015).

Previous work by Chandler (2018) on the southern Peak Range Volcanics focused on the diversity of rock types and concluded that fractional crystallisation was an important process in their diverse magmatic evolution. Highly fractionated rock bodies exhibited high rare earth metal enrichment, which formed from an alkali feldspar dominated fractionation of a low fO_2 alkali basalt parental melt at a shallow crustal position (Chandler, 2018). The origin of the parental melt was pre-emptively modelled as partial melting of a low fO_2 metasomatised source, although no mantle samples were observed.

A single intrusion located 20km NE of the central group is a heterogeneous plug by the name of Campbell's Peak, consisting of a trachyandesitic core gradually transitioning into tephriphonolite towards the edge. Exposed in the quarry is a trachybasaltic rim filled with spinel peridotite xenoliths and amphibole megacrysts. From what we have seen, this is the only locality in the Peak Range to contain them. The use of peridotite xenoliths could assist

in not only estimating the composition of the mantle, but also evaluating the dynamic processes involved in melt generation and segregation, and constraints on lithospheric evolution and mantle source beneath the Peak Range.

The primary aim of this thesis is to examine the well-preserved spinel peridotite xenoliths and amphibole megacrysts found at Campbell's Peak to understand the broad geodynamic origin and composition of the mantle beneath the Peak Range, and to further develop a model for the earlier stages of magmatic evolution of mantle to the highly evolved peralkaline magmas. These mantle xenoliths and amphibole megacrysts could also give information on not just the mantle source of the Peak Range but an insight to the Cosgrove hotspot chain and its characteristics.

The Newer Volcanics (Victoria) are assumed to be a result of the Cosgrove mantle plume as they also lay along the supposed track. Work by Powell (2004), Yaxley (1998), and O'Reilly & Griffin (1988) on mantle xenoliths in the Newer Volcanics have revealed evidence for metasomatic enrichment with increased concentrations of rare earth elements and specific trace elements, indicating that the mantle may be behind the rare earth metal enrichment for the Peak Range. It is likely that the trace element enrichment and high peralkalinity of the southern Peak Range was sourced from a metasomatised mantle, as amphibole phases present within mantle xenoliths are good indicators for mantle fluid interaction.

The secondary aim of this thesis is to briefly describe the newly mapped sections of the southern Peak Range and update the lithological map of the southern group.

These aims will be accomplished by a combination of field work, petrography, geochemistry, and mantle melting modelling described in detail in Section 2. Overall, further lithological mapping and examination on the origin and composition of the mantle beneath the Peak Range will improve the understanding of the geological and spatial origin of the Peak Range and give further insight to understanding the hotspot system beneath eastern Australia and other intracontinental hotspot volcanic systems.

2. BACKGROUND/GEOLOGICAL SETTING

2.1 MANTLE PETROLOGY

2.1.1 MANTLE COMPOSITION

The mantle exhibits physical layering but there is a debate whether the mantle is chemically homogenous, or heterogeneously layered remains undecided. During the formation of the Earth, chemical layering may have occurred either as a direct result of heterogeneous accretion without successive mixing, or by some process analogous to crystal fractionation from an early magma ocean (the latter is in favour) (Palme & O'Neil, 2005). Although, evidence from mineral inclusions in diamonds that formed in the lower mantle show that they were in equilibrium with a mantle of having a similar bulk composition of the upper mantle (Kesson & Fitz Gerald, 1991). Furthermore, seismic evidence for subducted slabs penetrating the lower crust indicate that there is considerable mass transfer between the upper and lower mantle, suggesting the upper and lower mantle are similar (Creager and Jordan, 1984; Van der Hilst et al, 1997).

Estimation on the composition of the mantle originates from models comparing CI chondrites compositions with upper mantle rocks and finding similarities between them (Table 2.1) (Palme & O'Neil, 2005). Although not exactly alike, it is believed that the Earth's mantle composition can be replicated from CI chondrites, suggesting that the mantle is

Table 2.1: Composition of the Earth's mantle assuming average solar system element ratios for the whole Earth

	Earth's mantle based on CI chondrite	Earth's mantle based on upper mantle rocks
MgO	35.80	36.77
SiO2	51.20	45.50
FeO	6.30	8.10
Al2O3	3.70	4.49
CaO	3.00	3.65

essentially magnesium, silicon, and iron, with minor calcium and aluminium (McCall, 2005; Palme & O'Neill, 2005). The spinel peridotite found at Campbell's Peak reflects a slightly different composition of the upper mantle, likely due to metasomatic enrichment within the mantle beneath the Peak Range.

2.1.2 THE SUBCONTINENTAL LITHOSPHERIC MANTLE & METASOMATISM

The Earth's continental crust is underlain by the subcontinental lithospheric mantle (SCLM), ranging from a few tens of kilometres beneath rift zones to >250km beneath some Archean cratons (Griffin & O'Reilly, 2007). It consists of mainly ultramafic rocks, ranging from lherzolites, dunites and harzburgites. Variation in compositions originate from progressive removal of basaltic components during partial melting events of the SCLM, and broadly related to the age of the overlying crust. From Archean though to Proterozoic and Phanerozoic times, the composition of the SCLM has become progressively less depleted in terms of Al, Ca, Mg# and Fe/Al (Poudjom Diomani et al., 2001). Thickness and density of the SCLM seems to also correlate with age, ranging from about 250-180km, 180-150km, and 140-60km for Archean, Proterozoic and Phanerozoic terranes respectively.

Off-cratonic regions tend to host abundant varieties of metasomatic effects, predominantly in the tectonically young Phanerozoic terranes (O'Reilly and Griffin, 2013). Metasomatism refers to the compositional changes in the mantle rock because of an interaction with a mantle fluid(s), either by the addition of new mineral phases (modal), or a change in composition of existing phases without the addition of new phases (cryptic) (O'Reilly and Griffin 2013). Metasomatic processes in the SCLM are evident in peridotite xenoliths, presented as the addition of amphibole, mica, carbonates, apatite, sulphides, titanite, ilmenite or zircon, or changes in trace and rare earth element abundances.

Enriched fluids are believed to originate from the melting and dehydration of recycled oceanic crust (Pilet et al., 2008), producing a variety of fluid types: silicate melts ranging from mafic to ultramafic, carbonatite melts, sulphide melts, C-O-H fluids ranging from water to CH_4 and CO_2, dense brines and hydrosilicic fluids, and hydrocarbon-bearing fluids (O'Reilly and Griffin, 2013), which later metasomatise the overlying SCLM. It is possible for liquids to become miscible with one another, but this has not yet been fully understood.

2.2 BRIEF TECTONIC HISTORY OF EASTERN AUSTRALIA

The Peak Range is a product of Cenozoic intraplate volcanism, assumingly connected to the Cosgrove hotspot (Davies et al., 2015). This mantle plume extends from northern Queensland to southern Victoria and Tasmania, producing lava field provinces composed of exclusive basaltic lavas (Wellman & McDougall, 1974), central volcano provinces with compositions ranging from early basaltic lavas to late felsic flows and intrusions (Davies et al., 2015) and leucitite suites consisting of K-rich basaltic lavas (Wellman & McDougall, 1974).The first eruption of the Cosgrove mantle plume occurred at ca 90 Ma and continued to until < 1 Ma (Wellman & McDougall, 1974; Vasconcelos et al., 2008).

Thickness of the overlying lithosphere attributed to the surface expression of mantle plume volcanism with central volcanoes occurring over thinner lithosphere, and leucitite suites over thicker. Eastern Australia's lithosphere thickens in an abrupt step-like pattern, beginning at ~50-100km in central NSW and southern QLD, further increasing towards the west (~15-20 km at 145°E, and then ~200km+ near the SA and NT border for NSW and QLD respectively) (Figure 2.1) (Davies et al., 2015; Fishwick et al., 2008). Though some eastern Australian lava field provinces fit into a hotspot model, spatial and temporal distribution of them do not if they were expected to be related to a stationary model. Further details into alternative

methods of magmagenesis is briefly described along with a more detailed summary of the Cenozoic intraplate volcanism of eastern Australia by Chandler (2018) (Chapter 3.2).

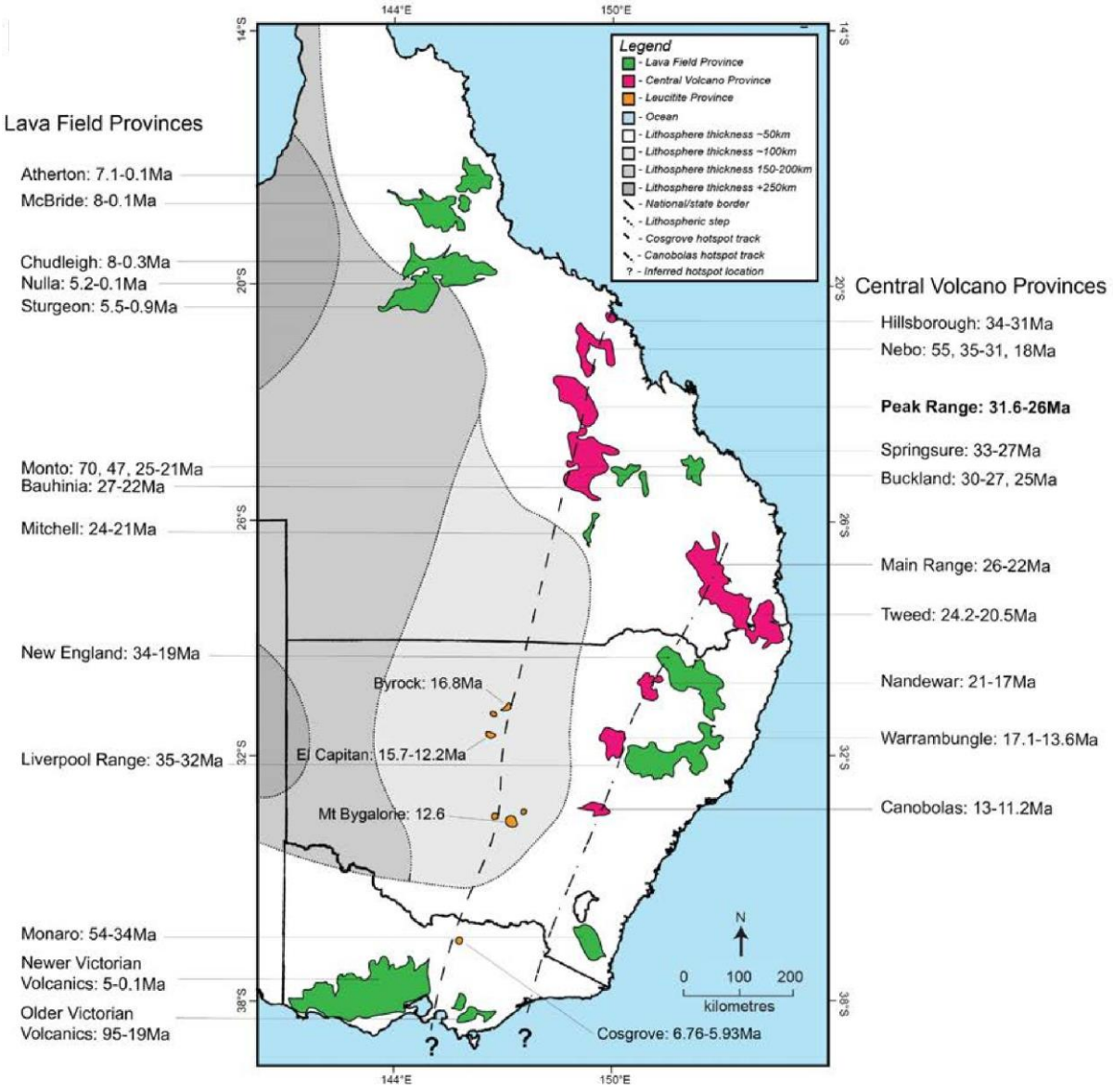

Figure 2.1: Spatial distribution of the three types of Cenozoic volcanism in eastern Australia (central volcanic provinces (pink), lava field provinces (green), & leucitite suites (orange). Age of volcanism is oldest in Queensland (Nebo) progressively becoming younger towards Victoria (Newer Victorian Volcanics). Figure by Chandler (2018), modified from Jones et al (2017).

The Tasmanides of eastern Australia are a result of the break-up of Rodinia followed by the development of orogenic belts along the eastern margin of Gondwana when it collided with Laurussia to form Pangea (Veevers, 2000), through the late Devonian-Cretaceous west-dipping subduction system (Waschbusch et al., 2009). Based on age, structure, and geophysical patterns, the Tasmanides are divided into the Delamerian, Thomson, Lachlan, Mossman (North Queensland) and New England orogenies with an internal Permian-Triassic rift-foreland basin system. These orogenies record the multiple cycles of collision and extension during the Late Neoproterozoic to Middle Cambrian (Glen, 2005; Rosenbaum, 2018).

The locality of the Peak Range is near the border of the Thomson Orogen and the New England Orogen (Withnall et al., 2013) (Figure 2.2), likely due to crustal weakness of the region assisting the NW-SE trend of the range (Mollan, 1965). Tectonic evolution of the Thomson Orogen (Neoproterozoic-Cambrian) is difficult to unravel as it is concealed by Mesozoic cover. Conclusions made by Spampinato (2015) for the early tectonic evolution of the orogen inferred that it represents the interior extensional structure of eastern Australia during the break-up of Rodinia. The New England Orogen (Devonian-Permian) is characteristic of a convergent margin phase consisting of arc, forearc basin and accreted terranes of the west-dipping subduction zone (Glen, 2005) which later became extensional, resulting in the formation of the foreland Bowen-Gunnedah-Sydney Basin. The substrate of the Bowen Basin lies within the Thomson and New England Orogen (green field in Figure 2.2), which the Peak Range volcanics intrude through.

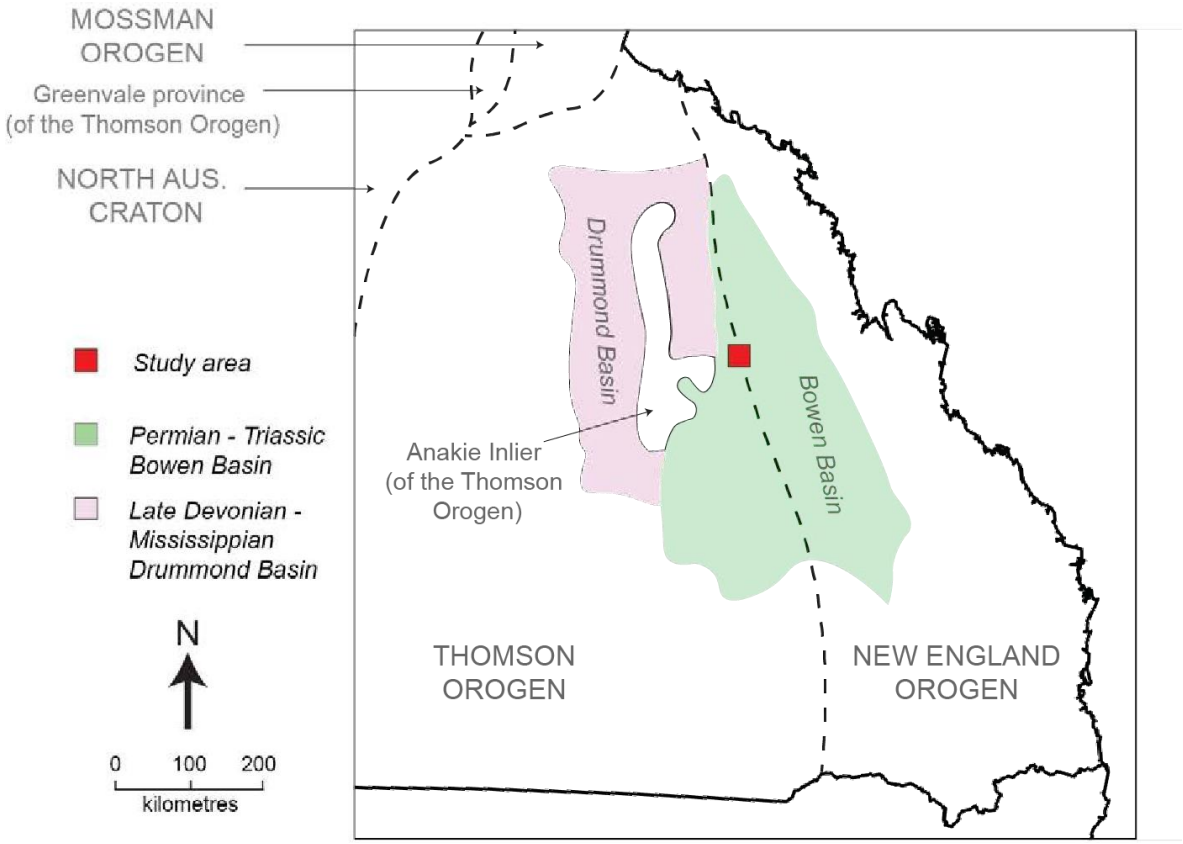

Figure 2.2: Regional setting of the study area (red square). Notice the location of the Peak Range roughly lies on the boundary between the Thomson Orogen (west) and New England Orogen (east) within the Bowen Basin (green). Figure from Chandler (2018).

2.3 PEAK RANGE LOCAL GEOLOGY

The Peak Range consists of two distinct volcanic episodes: early basalt flows and plugs, and later intermediate to felsic intrusions (Withnall, 1995; Mollan, 1965). First, tholeiitic to hawaiite flows, then alkaline olivine basaltic flows erupted through and onto Permian Back Creek Beds of the Bowen Basin during the Late Eocene to Oligocene (Wellman, 1978; Jones et al., 2017; Wellman & McDougall, 1974). The central group of the Peak Range consists of the remnants of basaltic flow piles, forming flat topped mesas and ridges, interpreted as the volcanic centre of the range (Wellman, 1978; Withnall, 1995). Plains covered by volcanic soil contain abundant banded, botryoidal, and vug-filling nodules of quartz, calcite and

zeolite (up to 300mm), interpreted to be amygdaloidal cavities from the eroded flood basalt (Chandler, 2018).

The remainder of the Peak Range consists of rhyolitic and trachytic intrusions located at the northern and southern ends of the range (southern and northern groups), rare mafic intrusions and dykes, and a phonolitic intrusion located 20km NE of the central group (Figure 2.3). The northern group consists of distinct peraluminous pinnacles, domes, and peaks amongst older volcanic units, whereas the southern group are predominantly peralkaline domes, peaks and flows tightly clustered together. The difference in alumina saturation suggests a different petrographic origin for the two groups (Mollan, 1965). For further detail into the surrounding geology and geophysical response of the Peak Range, see (Chandler, 2018).

Chandler (2018) described the petrography and geochemistry of most of the southern Peak Range with a focus on the rare metal enriched bodies. Unmapped sections were sampled and briefly described in this study to update the lithological map of the southern area (Figure 2.4). Table 2.3 summarises the general petrographical characteristics of the newly mapped bodies, and mineral abbreviations used are presented in Table 2.2. Full descriptions are presented in Appendix 5. Geochemical characteristics of these bodies are briefly discussed in Section 4.2 for comparison to Campbell's Peak.

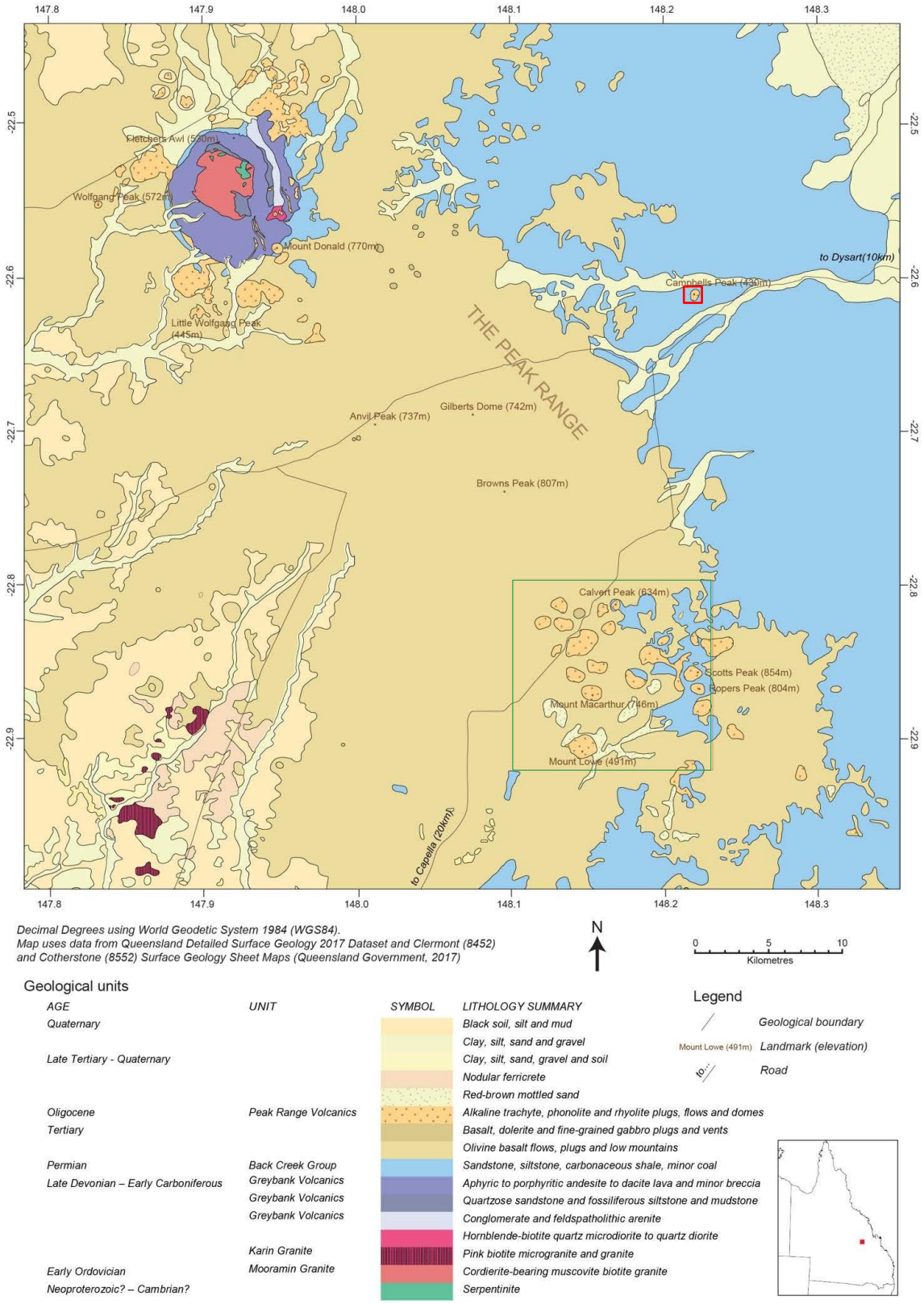

Figure 2.3: Geological map of the Peak Range showing the spatial relationship between the southern Peak Range (green square) and Campbell's Peak (red square). Greater detail of these two areas are show in Figure 2.4 and Figure 4.2 respectively. Figure from Chandler (2018).

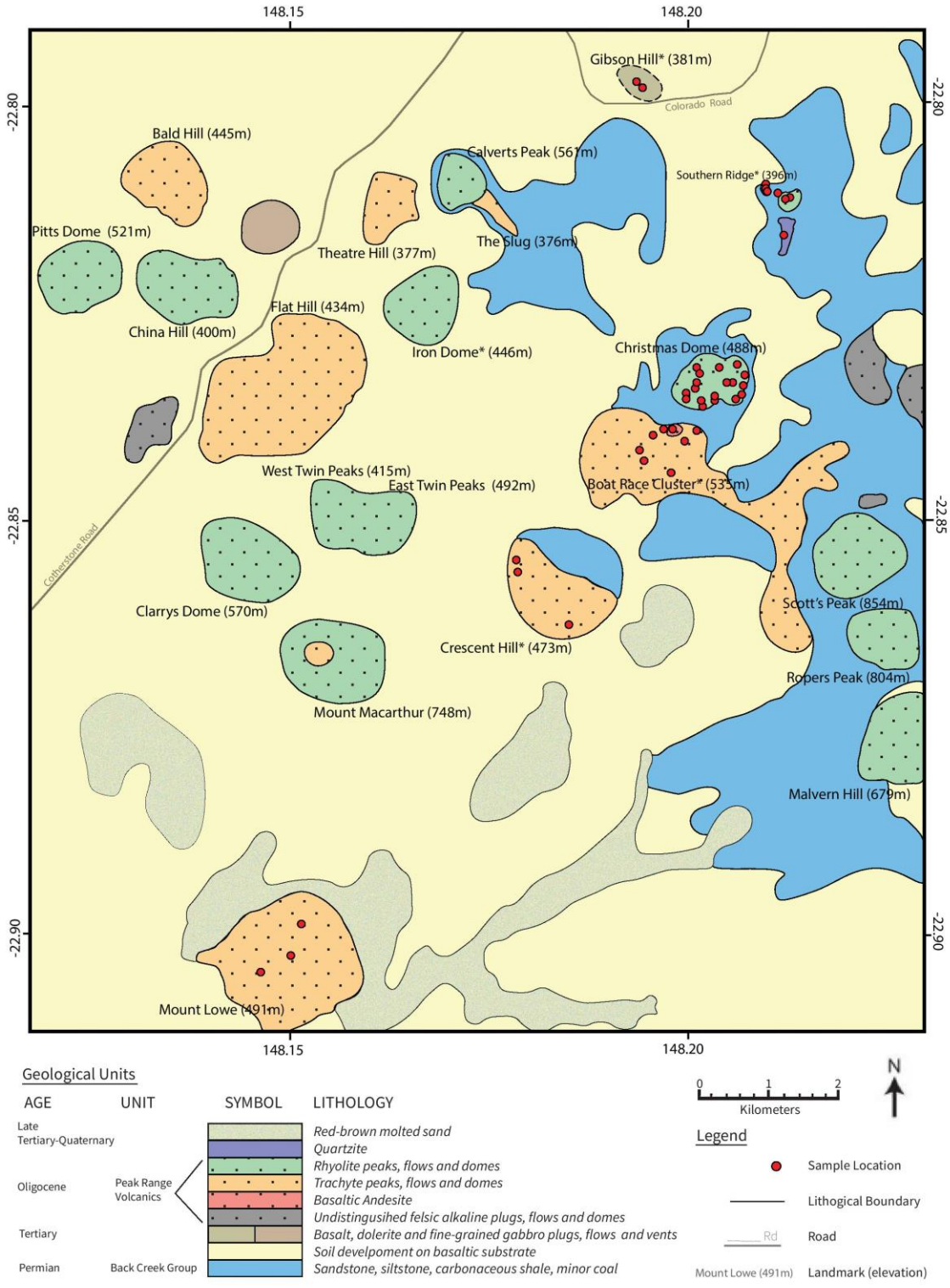

Figure 2.4: Updated lithological map of the southern group of the Peak Range showing sample locations (red dots). Decimal Degrees using World Geodetic System 1984 (WGS84). Map uses data from Queensland Detailed Surface Geology 2017 Dataset and Cotherstone (8552) Surface Geology Sheet Map (Queensland Government, 2017). * denotes unofficial names. Figure modified from Chandler (2018).

Table 2.3: Mineral abbreviations for Table 2.3 and text

Afsp	Alkali Feldspar	Aeg	Aegirine	Opx	Orthopyroxene	Oxi	Opaque Oxides	Qtz	Quartz	Olg	Oligoclase
Alb	Albite	Plg	Plagioclase	Cpx	Clinopyroxene	Amph	Amphibole	Zeo	Zeolite	Spl	Spinel
Pyr	Pyroxene	San	Sanidine	NaA	Na-Amphibole	Mag	Magnetite	Idd	Iddingsite	Olv	Olivine

Table 2.3: General characteristics of the newly mapped bodies of the Peak Range (Figre 2.4). Form based on Mollan (1965), see Appendix 5 for reference. Rock type is based on Figure 4.9.

Body	Elevation (m)	Diameter (km)	Form	Rock Type	Phenocrysts	Groundmass	Defining Features	Hand Sample	Other Features
Boat Race Cluster*	535	0.9	Collapsed Exogenous Dome	Trachyte	Qtz	San+Aeg+sub-opaque matrix	Granoblastic Qtz (PC), Minor Carlsbad twinning (GM)	Blue/green fine groundmass	Barhcan-Shaped, dyke on N flank (see below)
			'Dyke'	Basaltic Andesite	Olv (altered)	Olv+Asfp+Prx+Oxi	Olv altered to Idd (PC)	Fine-grained, dark grey	None Observed
Christmas Dome	488	0.7	Endogenous Dome	Aegirine Rhyolite	Qtz+Afsp+Prx-rimmed Amph	Afsp+Qtz+Aeg+minor NaA	Glomeroporphyritic clusters of Alb+San+Qtz (GM), Prx-rimmed Amph (PC)	Fine-grained, green/blue	Flow banding, brecciated rock
Crescent Hill*	473	1.4	Collapsed Dome	Trachyte	None Observed	San+Oxi+sub-opaque matrix	Carlsbad twinning of Afsp (GM), spherulitic textures (VS)	Fine-grained, blueish	None Observed
Gibson Hill*	381	0.150	Lava Flow	Mugearite	None Observed	Olg+Olv+Oxi	None Observed	Fine-grained, dark grey	None Observed
Mount Lowe	491	1.4	Exogenous Dome	Trachyte	San+Qtz	San+Oxi+sub-opaque matrix	Carlsbad twinning of Afsp (GM), Glomeroporphyritic San (PC), onion-skin weathering	Fine-grained, blue/grey	None Observed
Southern Ridge*	396	0.6	Lava Flow	Aegirine Rhyolite	Qtz+Afsp	San+Qtz	Vesicular pumice at very top	Fine-grained, blueish	Quartzite Dyke on S flank, flow banding

PC = phenocryst Phase VC = vesicle Phase GM = groundmass Phase * = unofficial name

3. METHODS

3.1 FIELD WORK

Seven days were spent in the field collecting samples and mapping individual rock bodies of the southern Peak Range and Campbell's Peak. The field work consisted of examining outcrops, collection of samples for petrological and geochemical analysis, and mapping of mineralogical and textural changes within the examined bodies. The number of samples collected was dependent on the interest of the rock body itself, either collecting along transects or only when seeing an obvious change in fresh outcrop. Christmas Dome received more attention than others as this body is the subject of current exploration work for rare metal mineralisation Chandler (2020). Multiple transects were taken across this body but will be only discussed in brief detail (as well as other rhyolitic and trachytic bodies) as the projects aim changed direction after field work had commenced. Most other bodies only had three or so samples taken as the interest of these were to identify the bulk rock type (with the exemption of the Southern Ridge and the Boat Race Cluster having more samples), and the bodies had experienced high degrees of weathering. Although it was unknown during fieldwork, the mantle xenoliths found in Campbell's Peak became the focus of the project. Enough samples were collected which represent the range of rock types within the peak, but the wet weather prevented detailed mapping of the geological boundaries between rock types due to the steepness of the peak.

Samples were taken from rock outcrops via sledgehammer, and the effort was made to select the least weathered samples and trimming off weathered edges using the sledgehammer or

rock hammer. Descriptions of samples were recorded via notebook and latitude/longitude coordinates were record using GIS Cloud.

Sixty-nine samples were taken in total. For their locations and use in this study refer to Appendix 1.

3.2 PETROGRAPHY

Twenty-nine thin sections were made of the various bodies across the area with at least one for each body. Five of these are of the different rock types from Campbell's Peak. Unfortunately, there is no thin section of the tephriphonolite, and only one small thin section of the mantle xenolith. To overcome this, 1-inch round mounts were made (14 in total) by placing a portion of rock in epoxy resin. Once set, they were then polished, and carbon coated. These mounts were used in a Scanning Electron Microprobe (SEM) to distinguish mineral phases and textures within these rocks. The FEI Quanta 450 FEG Environmental Scanning Electron Microscope (SEM) at the University of Adelaide was used with an accelerating voltage 20kV and a spot intensity of 4.0. Semi-quantitative data via SEM was collected by energy dispersive spectrometry in preparation of using an Electron Microprobe for geochemical data collection, but SEM data will not be presented in this thesis.

3.3 GEOCHEMISTRY

3.3.1 MINERAL GEOCHEMISTRY

Samples from Campbell's Peak were analysed using the Cameca SXFive Electron Microprobe (EMP) at the University of Adelaide. The EMP was used to collect major elements of Si, Al, Ti, Cr, Fe, Mg, Mn, Ca, K, and Na of minerals in each mount. 15 kV acceleration voltage and 40 nA were applied, with a beam size of 5 μm. Points totals for the

mantle xenolith, trachybasalt, trachyandesite, and tephriphonolite were accepted if the ranged between ~98 and 102%. This didn't apply to the amphibole, zeolite, and magnetite due to unmeasured -H_2O and Fe^{3+} content. These totals range between 95-98%, 92-93%, and 92-97% respectively. For a list of major oxide percentages of minerals per rock type, see Appendix 3.

3.3.2 WHOLE ROCK GEOCHEMISTRY

Twenty samples were chosen for whole rock geochemistry. At least one sample was taken from each body examined, with some bodies being more thoroughly sampled due to observed rock change within the body (i.e. Boat Race Cluster), and/or the interest of REE variance over the body i.e. Christmas Dome.

The samples chosen had minimal weathered material and are believed to be representative of the lithology of each body. A representative piece was cut off each sample and then sent to Bureau Veritas Commodities Canada in Vancouver (BC) where they were crushed and pulverised to 200 mesh size before undergoing analysis. Major and trace elements were determined via lithium borate fusion method coupled with ICP-ES/MS. Further trace elements were determined by a multi-acid digestion coupled with ICP-ES and Aqua Regia digestion coupled with ICP-MS. The returned data was processed in Microsoft Excel and Adobe Illustrator. For the complete whole rock geochemistry, see Appendix 2.

3.4 MAGMA EVOLUTION MODELLING

Magma evolution modelling was executed via easyMELTS using a combination of mineral and whole rock geochemistry. EasyMELTS is a software program that allows the thermodynamic modelling of phase equilibria melting and crystallisation in magmatic systems, structured around the thermodynamic work of Ghiorso & Sack (1995), and Asimow

& Ghiorso (1998). It was used to model the magmatic evolution of the spinel peridotite and rocks of Campbell's Peak. The details of the modelling process and physical parameters used are discussed in Section 4.4.For whole rock compositions used in the modelling process, see Appendix 4.

4. OBSERVATIONS AND RESULTS

The rock types presented in this section are based on the TAS classification diagram given in Figure 4.9. Petrographical descriptions of the southern Peak Range are summarised in Table 2.3, but geochemical characteristics are briefly discussed here in Section 4.2.

4.1 PETROGRAPHY OF CAMPBELL'S PEAK

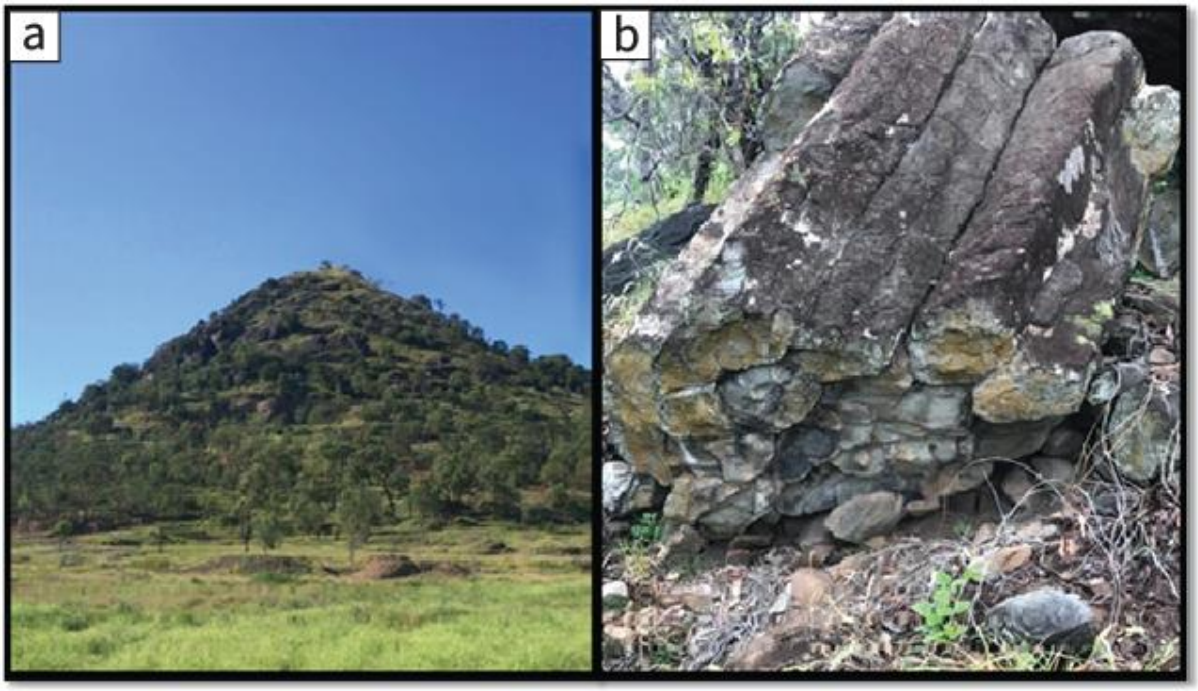

Figure 4.1: Photographs of Campbell's Peak. a) Photograph of the NE side of Campbell's Peak. b) Columnar jointing of trachyandesite, a result of expansion from the development of the thrust dome.

Campbell's Peak is a heterogeneous thrust dome (0.4km in length, Figure 2.4) consisting of an intermediate core, with trachyandesite gradually transitioning into tephriphonolite towards the peak's edge. Trachybasalt appears to rim the tephriphonolite, but this is only visible outcropping in a quarry WNW of the peak (Figure 4.2).

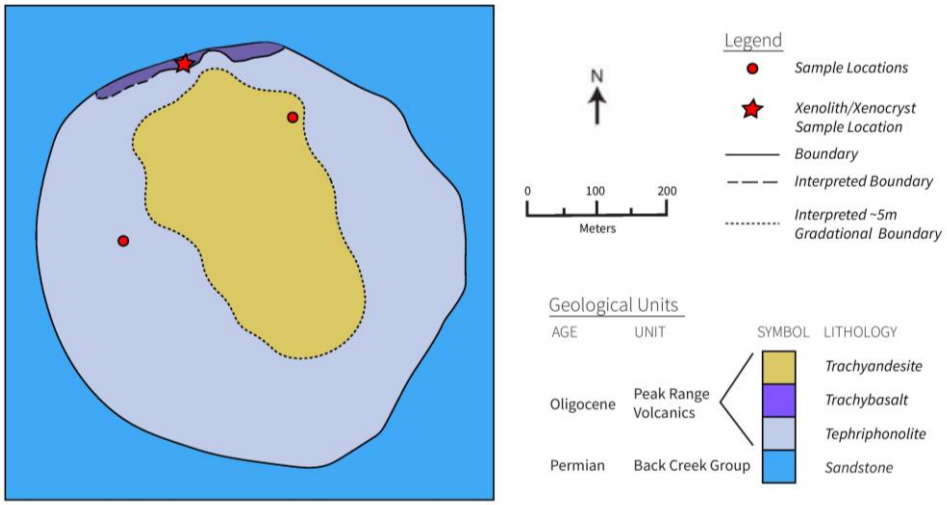

Figure 4.2: Interpreted map of the lithological boundaries of Campbell's Peak. Note the boundary between the trachyandesite and tephriphonolite is a gradational boundary of ~5m.

The trachybasalt contains abundant mantle xenoliths and amphibole megacrysts, which range from 6-75mm and 2-25mm respectively. It should be noted that feldspar megacrysts and Fe-sulphides were also found in the trachybasalt but these are not further discussed in this thesis. Mineralogical and textural differences between the trachyandesite and tephriphonolite is minimal, but both rock types will be discussed separately. Minerals were distinguished via SEM, EMP, and thin section analysis. Nomenclature of spinel and magnetite was classified via the classification of IMA 2018 spinel nomenclature. Zeolite has only been confirmed via comparison of EMP analysis with the Mineralogical Society of America's (MSA) database(see Appendix 7), as thin sections didn't present defined zeolite grains. Total electron microprobe analyses of minerals per rock type are presented in Appendix 3.

4.1.1 TRACHYANDESITE (BENMOREITE)

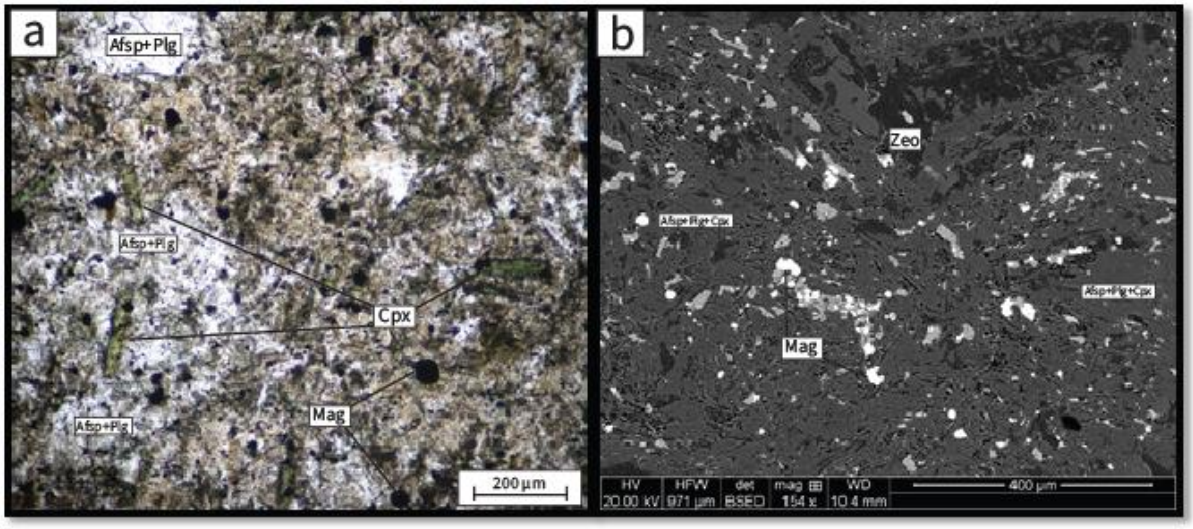

Figure 4.3: Micrographs of trachyandesite from Campbell's Peak. a) Trachyandesite groundmass under PPL. b) Detailed SEM micrograph of trachyandesite groundmass. For mineral abbreviations, see Table 2.2.

Hand sample of trachyandesite is a lighter grey, crystalline, medium to fine grain rock with tabular feldspar phenocrysts that can be seen with the naked eye. Through hand lens, hedenbergite can be recognized as the green minerals amongst the groundmass.

Table 4.1: Representative whole rock data, & microprobe analyses of minerals in Trachyandesite (benmoreite) from Campbell's Peak

	Whole Rock	**Alkali Feldspar**	**Plagioclase**	**Clinopyroxene**	**Magnetite**	**Zeolite**
SiO_2	57.32	63.58	59.48	47.82	0.37	54.79
TiO_2	0.31	0.02	0.01	0.52	9.89	0.00
Al_2O_3	19.53	19.55	24.14	2.15	1.77	25.03
Cr_2O_3	0.00	0.00	0.00	0.00	0.00	0.00
$FeO_{(t)}$	4.89	0.36	0.23	19.63	78.24	0.15
MnO	0.20	0.00	0.02	1.27	1.82	0.00
MgO	0.49	0.01	0.01	5.10	0.11	0.02
CaO	3.04	1.68	5.32	21.37	0.35	0.45
Na_2O	6.86	7.51	7.64	0.89	0.04	11.84
K_2O	3.69	4.65	1.01	0.04	0.02	0.34
NiO	-	0.00	0.00	0.00	0.00	0.00
LOI	3.05	-	-	-	-	-
Total	99.51	97.36	97.87	98.80	92.60	92.63

Table 4.1 shows the representative minerals that compose the trachyandesite. Na_2O 2.0 ≥ K_2O indicates that this rock is the sodic variant; benmoreite, a composition between

mugearite and trachyte. The groundmass consists of primarily alkali feldspar (anorthoclase), plagioclase (oligoclase), clinopyroxene (hedenbergite), and accessory magnetite (with ~10% ulvöspinel) and zeolite (analcime). Euhedral anorthoclase (up to 1.5mm) and oligoclase (up to 1mm) phenocrysts are observed throughout the whole rock.

4.1.2 TEPHRIPHONOLITE

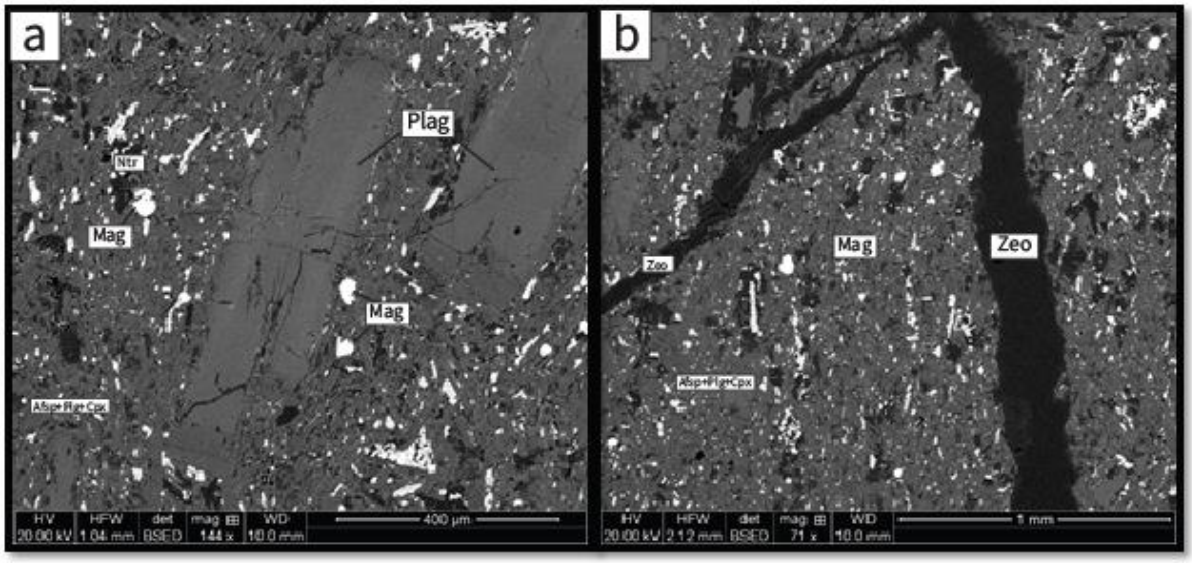

Figure 4.4: Micrographs of tephriphonolite from Campbell's Peak. a) SEM micrograph of plagioclase phenocryst amongst alkali feldspar, plagioclase, clinopyroxene, magnetite and zeolite groundmass. b) SEM micrograph of zeolite vein cutting through tephriphonolite. For mineral abbreviations, see Table 2.2.

As no thin section was prepared for this rock type, only SEM and EMP was used to distinguish the minerals found within the rock. Composition of the tephriphonolite and trachyandesite are very similar, except for the higher whole rock Na_2O, thus why tephriphonolite is classified as a different rock type (see Figure 4.9, Table 4.1 & 4.2). The only mineralogical differences are found within the magnetite and zeolite. Hand sample of the tephriphonolite is also similar to trachyandesite, though it is a darker grey in colour, and finer grained.

Table 4.2: Whole rock data, & representative microprobe analyses of minerals in Tephriphonolite from Campbell's Peak

	Whole Rock	Alkali Feldspar	Plagioclase	Clinopyroxene	Magnetite	Zeolite
SiO_2	56.96	63.87	59.63	48.15	0.31	48.3
TiO_2	0.30	0.02	0.01	0.37	9.58	0.00
Al_2O_3	19.42	20.57	24.23	1.38	1.52	28.74
Cr_2O_3	0.00	0.00	0.00	0.00	0.00	0.00
$FeO_{(t)}$	4.89	0.39	0.23	22.34	79.62	0.12
MnO	0.20	0.01	0.01	1.43	1.98	0.01
MgO	0.32	0.00	0.01	3.73	0.12	0.02
CaO	2.80	1.46	4.99	20.72	0.14	0.37
Na_2O	7.69	8.18	7.67	1.03	0.13	14.89
K_2O	3.82	4.27	1.23	0.02	0.02	0.13
NiO	-	0.00	0.02	0.01	0.00	0.00
LOI	2.90	-	-	-	-	-
Total	99.46	98.78	98.03	99.16	93.44	92.59

The groundmass consists primarily of alkali feldspar (anorthoclase), plagioclase (oligoclase), clinopyroxene (hedenbergite), and accessory magnetite (with ~7-11% ulvöspinel) and zeolite (natrolite). Natrolite veins are observed throughout the tephriphonolite (Figure 4.4b). Only euhedral oligoclase (~0.6mm) phenocrysts are seen in this rock (Figure 4.4a).

4.1.3 TRACHYBASALT (HAWAIITE)

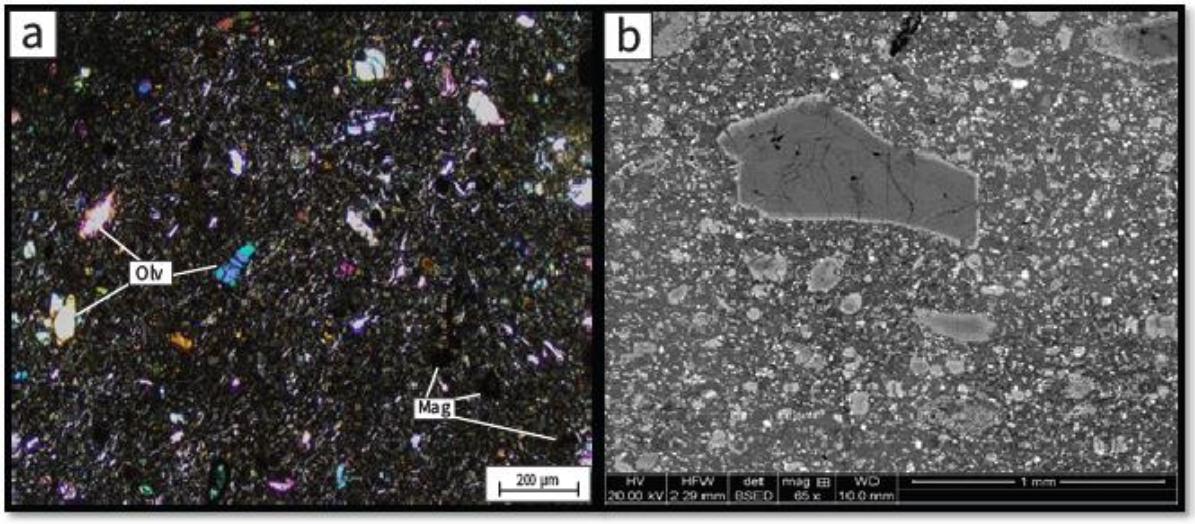

Figure 4.5: Micrographs of trachybasalt from Campbell's Peak. a) Thin section of olivine xenocrysts/phenocrysts amongst orthopyroxene, clinopyroxene, alkali feldspar, plagioclase, spinel, and magnetite under XPL. b) SEM photograph of a large olivine phenocryst exhibiting zoning of higher Fe at the rim and higher Mg at the core (large dark grey grain with light grey rim). Also seen are smaller olivine phenocrysts (grey grains) amongst the orthopyroxene, clinopyroxene, alkali feldspar, plagioclase, spinel, and magnetite groundmass. For mineral abbreviations, see Table 2.2.

Trachybasalt found at Campbell's Peak is a dark grey, crystalline, fine to medium-grained rock with varying sizes of xenoliths/megacrysts mentioned previously. Contact between the trachybasalt and tephriphonolite appeared as a chilled margin, with trachybasalt grain size becoming finer towards the boundary.

Table 4.3: Whole rock data, & representative microprobe analyses of minerals in Trachybasalt from Campbell's Peak

	Whole Rock	**Olivine (core)**	**Olivine (rim)**	**Orthopyroxene**	**Clinopyroxene**	**Alkali Feldspar**	**Plagioclase (1)**	**Plagioclase (2)**	**Spinel**	**Magnetite**
SiO_2	46.65	39.85	38.63	56.60	48.87	64.44	58.40	56.69	0.05	0.45
TiO_2	1.99	0.01	0.05	0.07	1.41	0.00	0.04	0.14	0.12	18.82
Al_2O_3	15.10	0.05	0.18	2.98	6.39	19.98	25.53	25.95	47.40	2.08
Cr_2O_3	0.04	0.01	0.00	0.45	0.36	0.00	0.00	0.00	19.59	1.34
$FeO_{(t)}$	11.19	12.35	19.12	6.00	6.28	0.16	0.57	0.63	14.29	68.59
MnO	0.19	0.18	0.41	0.15	0.16	0.00	0.01	0.00	0.26	0.95
MgO	8.44	47.33	40.69	34.19	13.98	0.01	0.04	0.25	17.28	2.69
CaO	7.82	0.10	0.44	0.56	20.86	1.34	7.01	4.96	0.05	0.37
Na_2O	3.93	0.01	0.02	0.05	0.93	7.06	6.84	8.93	0.01	0.08
K_2O	1.90	0.00	0.01	0.00	0.05	5.67	0.72	1.96	0.00	0.03
NiO	-	0.31	0.19	0.07	0.02	0.00	0.00	0.00	0.25	0.03
LOI	1.80	-	-	-	-	-	-	-	-	-
Total	99.59	100.24	99.80	101.12	99.31	98.78	99.35	99.70	99.41	94.90

Na_2O 2.0 ≥ K_2O of the whole rock compositions indicates that this rock is the sodic variant; hawaiite, an olivine basalt that represents a composition between alkali basalt and mugearite (Table 4.3). The groundmass consists of orthopyroxene (enstatite), clinopyroxene (diopside), alkali feldspar (anorthoclase), plagioclase (oligoclase (1) & andesine (2)), and accessory Cr-spinel and magnetite (with ~12-21% ulvöspinel). Subhedral oligoclase phenocrysts (~0.6mm) are found rarely throughout the hawaiite. Anhedral olivine ($Fo_{79\text{-}87}$ $Fa_{13\text{-}21}$) xenocrysts/phenocrysts found range from ~0.2-0.5mm, the xenocrysts exhibit zoning of higher Fe at the rims and higher Mg at the cores (see Table 4.3, Figure 4.5b), as well as reaction rims from interaction with the melt.

4.1.3.1 MANTLE XENOLITHS (SPINEL PERIDOTITE)

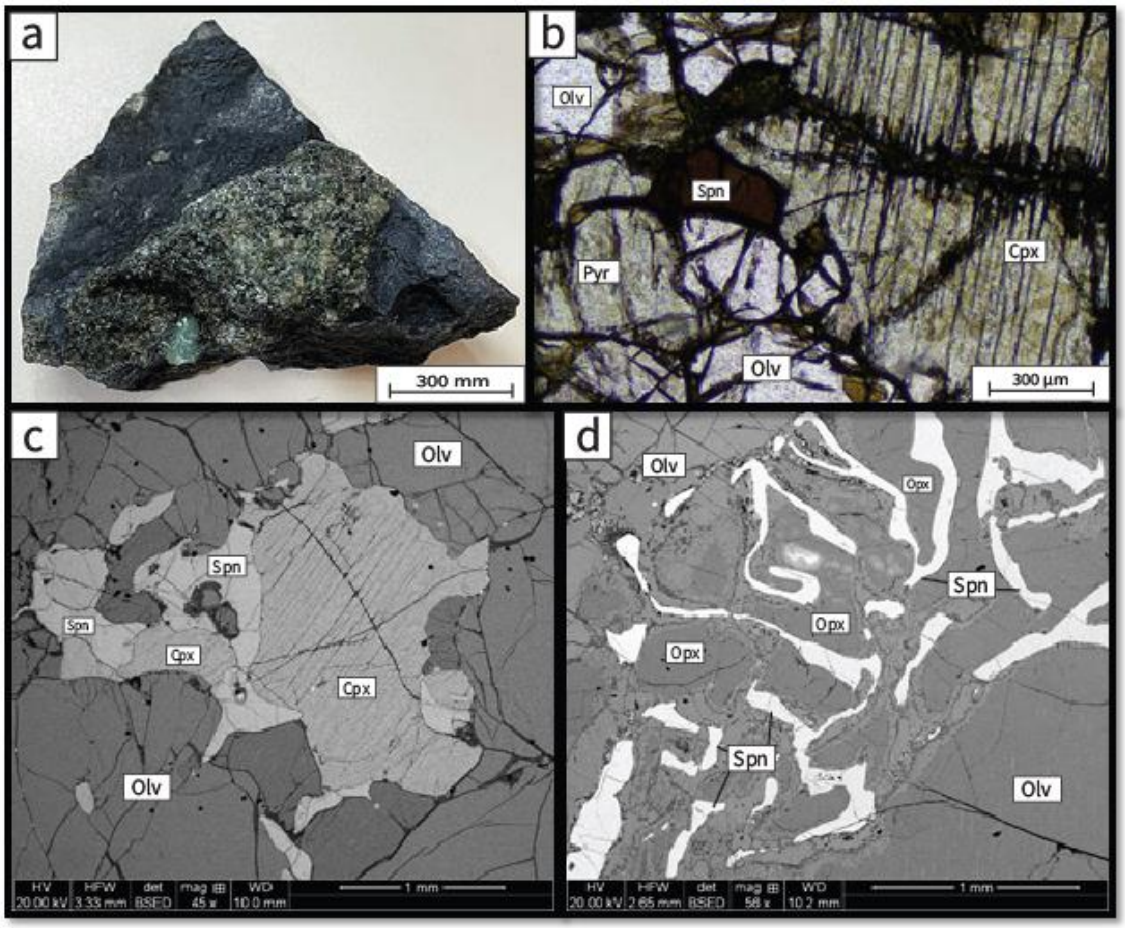

Figure 4.6: Sample photo and micrographs of peridotite xenolith found within the trachybasalt at Campbell's Peak. a) Sample of peridotite (darker green) xenolith in trachybasalt. The lighter green mineral is serpentinised olivine. b) Thin section of peridotite xenolith containing olivine, pyroxene, and spinel (showing exsolution laminae of clinopyroxene). c) SEM photograph of exsolution laminae texture within the peridotite xenolith. d) SEM photograph of vermicular symplectite textures between spinel and orthopyroxene pseudomorphicly replacing olivine. For mineral abbreviations, see Table 2.2.

Mantle xenoliths are classified based on modal proportions of olivine, orthopyroxene, and clinopyroxene, and the primary Al-mineral phase. This mantle xenolith is estimated to be lherzolite (green field in Figure 4.7) but will be referred to as peridotite/spinel peridotite throughout the thesis.

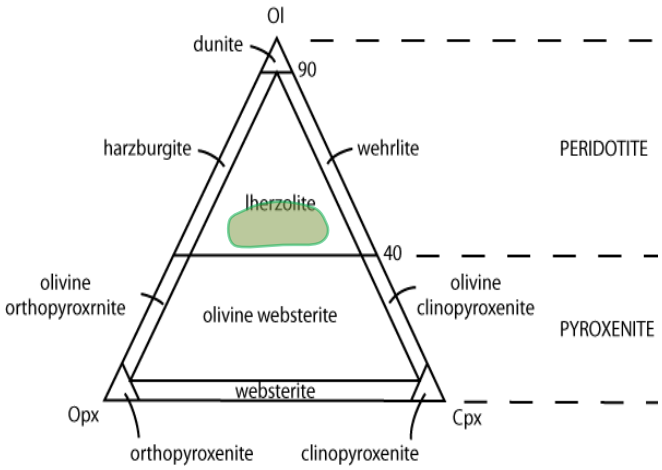

Figure 4.7: Classification of ultramafic rocks based on modal proportions of orthopyroxene (Opx), clinopyroxene (Cpx) and olivine (Ol) after Le Maitre (2002). Green field represents estimated spinel peridotite model proportions.

Varying sizes of spinel peridotite xenoliths (6-75mm) are hosted within the trachybasalt, composed of olivine (Fo_{82-87} Fa_{13-18}), orthopyroxene (enstatite), clinopyroxene (diopside), and accessory Cr-spinel and amphibole (pargasite, refer to Appendix 6) (Table 4.4). The xenoliths sometimes include an apple green, fine-grained mineral identified as serpentinised olivine (Figure 4.6a).

Table 4.4: Whole rock data, & representative microprobe analyses of minerals in peridotite from Campbell's Peak

	Whole Rock	Olivine	Orthopyroxene	Clinopyroxene	Spinel	Amphibole
SiO_2	46.65	40.05	54.41	51.97	0.08	41.67
TiO_2	0.07	0.00	0.06	0.30	0.17	1.32
Al_2O_3	3.26	0.04	3.83	5.23	51.97	14.75
Cr_2O_3	0.394	0.01	0.31	0.70	13.27	1.47
$FeO_{(t)}$	8.96	12.78	7.38	3.17	15.96	6.44
MnO	0.13	0.20	0.17	0.10	0.18	0.11
MgO	37.31	47.18	32.54	16.36	18.25	17.04
CaO	3.02	0.07	1.03	20.93	0.01	10.40
Na_2O	0.21	0.01	0.07	1.08	0.00	3.18
K_2O	0.07	0.36	0.09	0.04	0.36	0.10
NiO	-	0.00	0.00	0.02	0.00	0.69
LOI	0.90	-	-	-	-	-
Total	99.27	100.70	99.90	99.97	100.25	97.17

Na_2O and Al_2O_3 concentrations in clinopyroxene and orthopyroxene respectively are higher than typical mantle pyroxene composition, thus they do not resemble their proposed end member compositions, indicating that this spinel peridotite has experienced mantle enrichment of some sort. The presence of amphibole also supports this suggestion, further discussed in Section 5.3.

Exsolution laminae (Figure 4.6b;c) is common in clinopyroxene in the peridotite, often presented as parallel orientated orthopyroxene exsolving from clinopyroxene controlled by the crystallography, temperature and mineral chemistry of the host pyroxene (Howie et al., 1992). Another common feature in the peridotite is vermicular symplectites between Cr-spinel and orthopyroxene, pseudomorphicly replacing olivine whilst preserving original grain boundaries (Figure 4.6d). The nature of these symplectites likely reflect that they formed as olivine became unstable and reacted with a liquid that had a composition capable of producing orthopyroxene and Cr-spinel (Ambler & Ashley, 2001).

4.1.3.2 AMPHIBOLE MEGACRYSTS (SADANAGAITE)

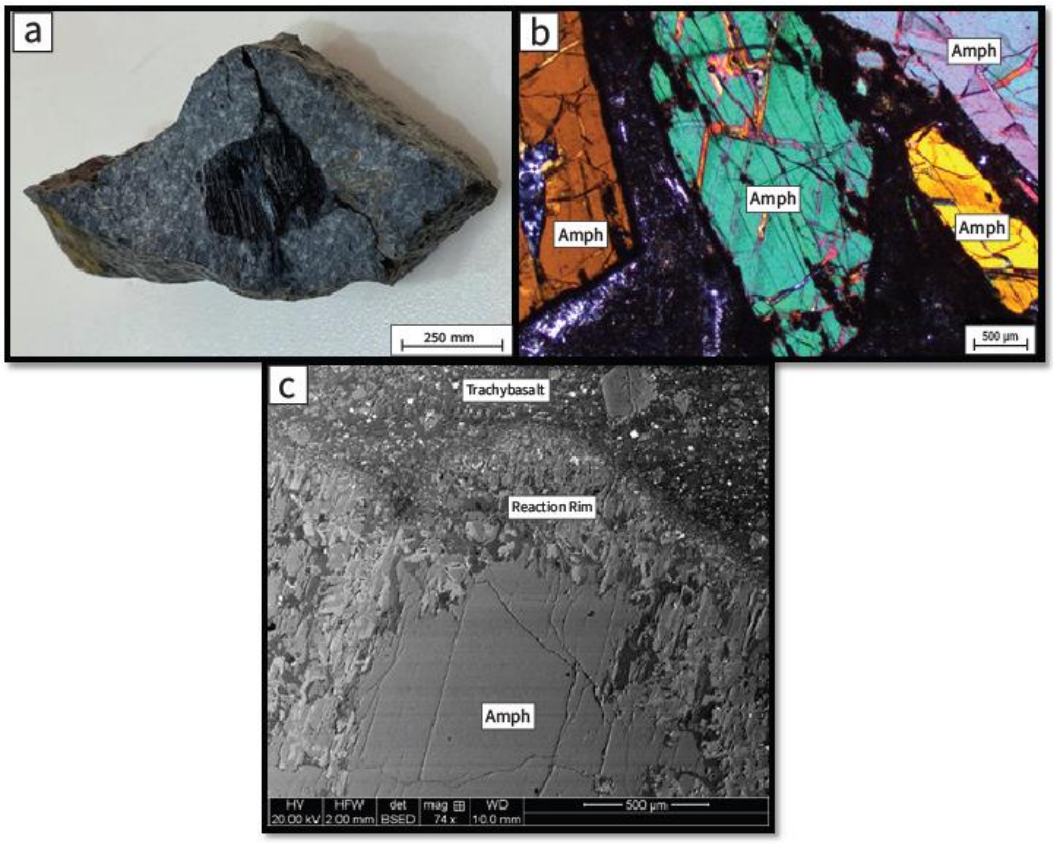

Figure 4.8: Sample photo and micrographs of amphibole (sadanagaite) megacrysts within trachybasalt of Campbell's Peak. a) Sample of amphibole megacryst in trachybasalt. b) Thin section of amphibole showing different orders of birefringence (likely due to thickness of grain and orientation) under XPL. c) SEM photograph of the reaction rim between the amphibole and trachybasalt (host rock). For mineral abbreviations, see Table 2.2.

The trachybasalt also contains abundant coarse amphibole megacrysts (2-25mm) with an average composition presented in Table 4.5. Based on the amphibole supergroup nomenclature of IMA 2012 (refer to Appendix 6), all amphibole megacrysts are defined as Ti-rich sadanagaite with the average empirical formula $(K_{0.36}\,Na_{0.39})(Na_{0.27}\,Ca_{1.73})(Mg_{3.14}\,Fe^{2+}_{0.46}\,Al_{0.37}\,Fe^{3+}_{0.61}\,Ti_{0.40})(Si_{5.72}\,Al_{2.28}\,O_{22})(OH)_2$. Sadanagaite is black, brittle, vitreous, and usually grows in a prismatic manner.

Table 4.5: Representative microprobe analysis of amphibole megacrysts from Campbell's Peak

SiO_2	39.72
TiO_2	3.96
Al_2O_3	15.25
Cr_2O_3	0.03
$FeO_{(t)}$	8.65
MnO	0.09
MgO	14.27
CaO	10.95
Na_2O	2.30
K_2O	1.92
Total	97.14

In thin section, the sadanagaite show birefringence of up to third order (Figure 4.8b), and

reaction rims indicating interaction between the sadanagaite and the melt (Figure 4.8b,c), suggesting they are xenocrysts within the trachybasalt.

4.2 GEOCHEMISTRY OF THE VOLCANIC ROCKS OF THE SOUTHERN PEAK RANGE AND CAMPBELL'S PEAK

4.2.1 TAS CLASSIFICATION

A method of classifying volcanic rocks is plotting SiO_2 against $Na_2O + K_2O$ after Le Maitre (2002) (Figure 4.9). The bodies sampled in this study show a range of rock types from basic through to acidic.

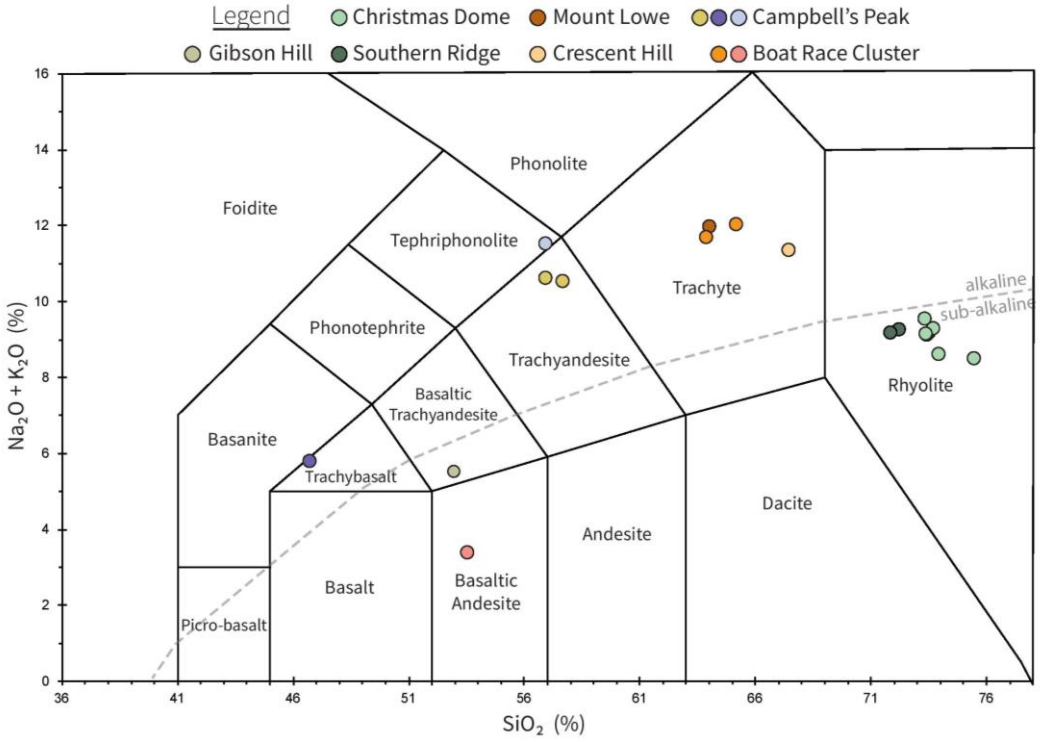

Figure 4.9: TAS classification diagram for the volcanic rocks of the southern Peak Range and Campbell's Peak, after Le Maitre (2002). The dashed line represents the division between alkaline and sub-alkaline rocks, based solely on $Na_2O + K_2O$ vs SiO_2 content.

Most bodies are homogeneous: Christmas Dome and the Southern Ridge are rhyolitic, Crescent Hill and Mount Lowe are trachytic, and Gibson Hill is basaltic trachyandesitic. Two bodies recorded having more than one rock type found: Campbell's Peak; trachybasalt, trachyandesite and tephriphonolite, and the Boat Race Cluster; trachyte and basaltic andesite. Campbell's Peak, Crescent Hill, Mount Lowe, and the trachyte of the Boat Race Cluster are alkaline rocks (not be confused with peralkaline, refer to Section 4.2.2). Christmas Dome, the Southern Ridge, Gibson Hill, and the basaltic trachyandesite of the Boat Race Cluster are sub-alkaline (tholeiitic).

4.2.2 PERALKALINITY INDEX

The Peralkaline Index (PI) is useful to observe the progression of a melt's evolution. This is calculated using the formula:

$$PI = \frac{m.Na_2O + m.K_2O}{m.Al_2O_3}$$

Generally, an increase in PI indicates melt evolution (Marshall et al., 2009). To showcase this, PI was plotted against SiO_2 (Figure 4.10).

An increase in SiO_2 is complemented by slight increases in PI with rocks of the southern Peak Range (excluding Gibson Hill). The rocks of Campbell's Peak exhibit the same trend. Peralkalinity appears to be achieved at a SiO_2 content of ~64 %. Samples with a PI value of 1 or over indicate peralkaline rocks (Crescent Hill, Mount Lowe, Boat Race Cluster, Southern Ridge, and Christmas Dome). Samples below a PI of 1 are metaluminous when $Al_2O_3/(Na_2O+CaO)$ is plotted against $(Na_2O+K_2O)/Al_2O_3$ (Campbell's Peak, Gibson Hill, and Boat Race Cluster), see Appendix 7. Note how all basaltic rocks sampled have the lowest PI of the area, and that the trachytes of Crescent Hill, Mount Lowe, and the Boat Race Cluster are both alkaline and peralkaline.

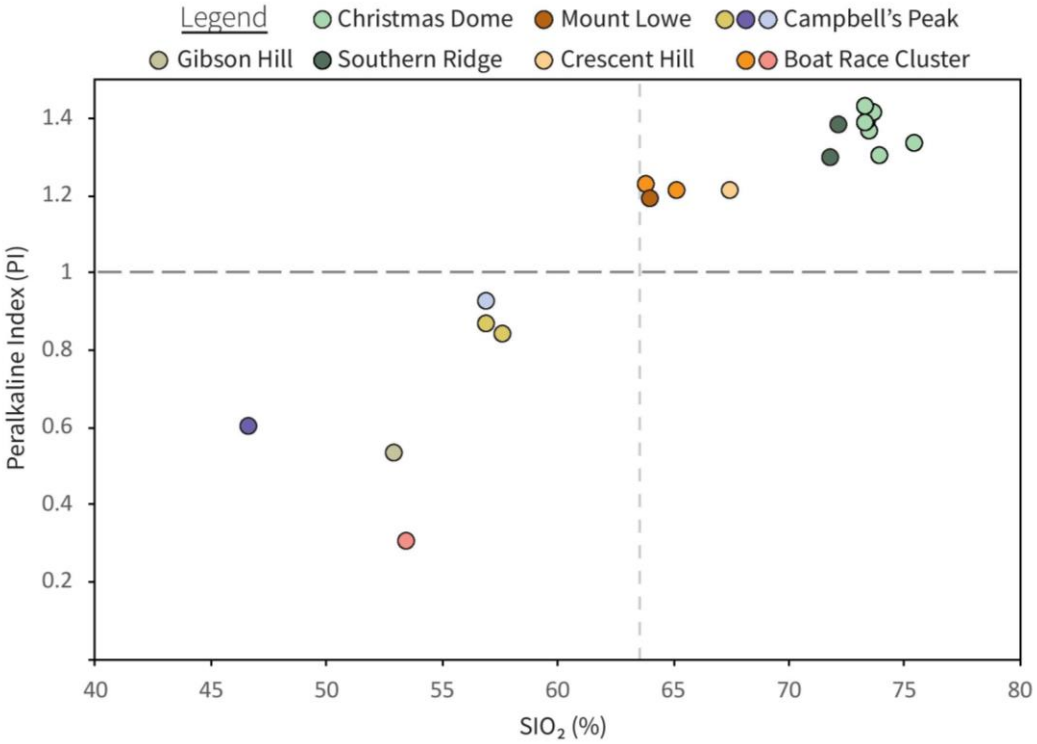

Figure 4.10: Peralkaline Index (PI) against SiO_2 diagram of the southern Peak Range and Campbell's Peak. Peralkalinity (coarse dashed line) is achieved at a SiO_2 content of ~64% (fine dashed line).

4.2.3 MAJOR ELEMENTS

Harker diagrams were produced for eight major elements against SiO_2 (Figure 4.11). Al_2O_3, Na_2O, and K_2O of the southern Peak Range display an initial increase before decreasing at approximately ~64% with increasing SiO_2. MgO, CaO, TiO_2 and P_2O_5 show exponential decreases with increasing SiO2. FeO(t) initially decreases but slightly increases at ~72% SiO2.

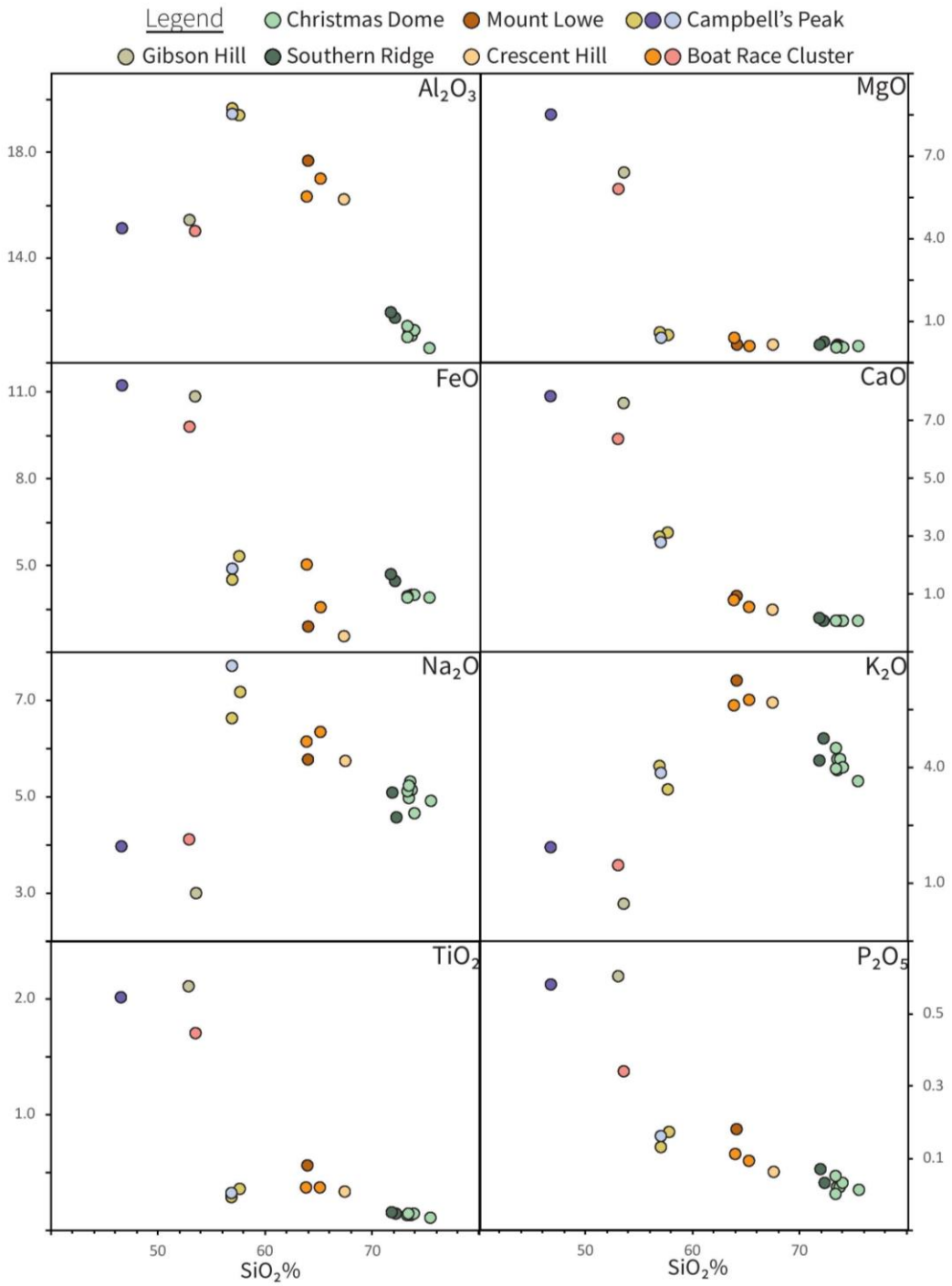

Figure 4.11: Harker diagrams of SiO_2 vs major element oxides of the southern Peak Range and Campbell's Peak. Y axis represents the weight t% of the displayed oxide.

Rocks of Campbell's Peak show an increase of Al_2O_3, Na_2O, and K_2O, and a decrease of MgO, $FeO_{(t)}$, CaO, TiO_2, and P_2O_5 with increasing SiO_2. One feature to note is the slight grouping of the basaltic rock types from Campbell's Peak, Gibson Hill and Boat Race

Cluster, and the slight separation of the trachyandesite and tephriphonolite of Campbell's Peak in most plots (likely a different magma series).

4.2.4 TRACE ELEMENTS

Trace element spiderplots were produced using values normalised against Primitive Mantle of Sun & McDonough (1989) for the different rock types (Figure 4.12a;b;c) of the southern Peak Range and Campbell's Peak (Figure 4.12d).

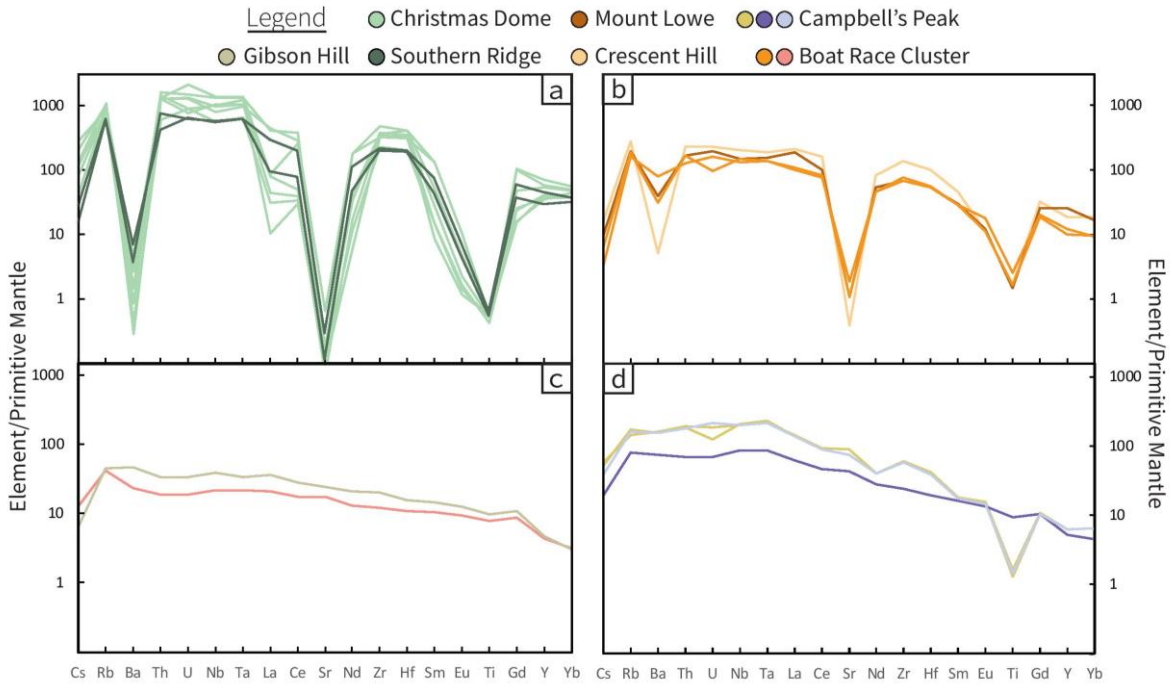

Figure 4.12: Spiderplot of trace element concentrations of the southern Peak Range, divided by rock type (a = rhyolite, b = trachyte, c = basaltic) and rocks of Campbell's Peak (d) Primitive Mantle normalisation values are from Sun & McDonough (1989).

The rhyolites (Christmas Dome and Southern Ridge) and trachytes (Crescent Hill, Boat Race Cluster and Mount Lowe) exhibit overall negative slopes of high-level trace element enrichment with negative anomalies of Ba, Sr, Eu, Ti (rhyolites trends are more variable than trachytes and display the highest enrichments of the area).

Campbell's Peak and the basaltic rocks display overall steady negative slopes, excluding the negative Ti anomaly of trachyandesite and tephriphonolite (Figure 4.12d). The trachyandesite and tephriphonolite slopes are slightly steeper than the rhyolites and trachytes, and the trachybasalt of Campbell's is very similar to the basaltic rocks of the southern area.

The negative anomalies are likely due to Ba^{2+}, Eu^{2+} and Sr^{2+} readily partitioning into alkali feldspar and plagioclase respectively (Tang, 2016), and early fractionation of Ti as they were either crystallised or removed from the remaining melt. Overall low values of Cs are likely a result of alteration features.

4.2.5 ZR VS TIO2

Chandler (2018) plotted Zr against TiO_2 on all his samples from the Peak Range as the use of an immobile incompatible (Zr) and compatible (TiO_2) pair can visualise melt fractionation while attempting to ignore alteration effects (MacLean & Barrett, 1993). To observe suitability of Zr vs TiO_2 as a melt evolution tracker in samples from this study, Zr vs TiO_2 was plotted (Figure 4.13, opposite page) with Chandler (2018) samples as a reference.

Chandler (2018) observed an exponential decrease in TiO_2 with early Zr increase (reasonably linear trend), deeming this as an appropriate measure of melt evolution. Samples from this study plotted along the same trend, confirming the use of Zr vs TiO_2, and the similarity between the samples of both studies.

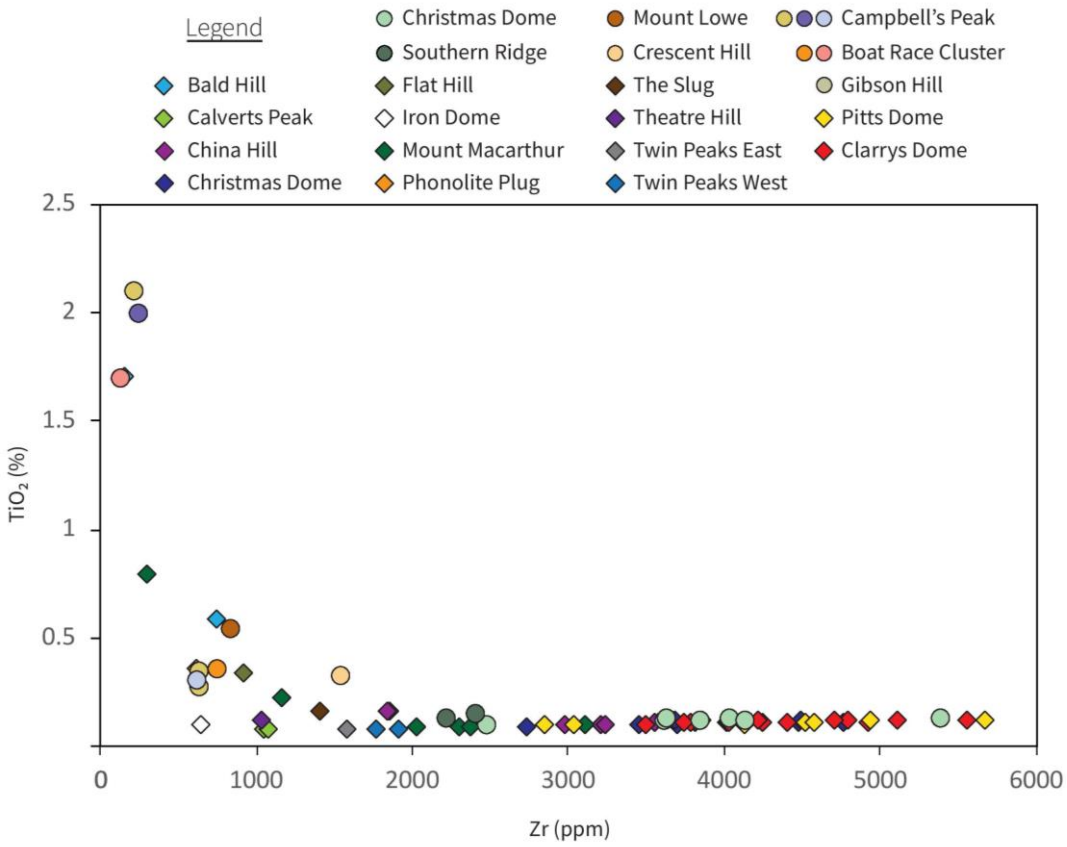

Figure 4.13: Zr vs TiO_2 diagram of the southern Peak Range and Campbell's Peak compared with samples collected in Chandler (2018). Note how both sets of data follow the same trend. For more information and further use of Zr vs TiO_2 on the rocks of the southern Peak Range, see Chandler (2018) Section 6.3.3-5.

4.2.6 RARE EARTH ELEMENTS

Rare earth element spiderplots were produced using values normalised against CI chondrite of McDonough & Sun (1995) for the different rock types (Figure 4.14a;b;c) of the southern Peak Range and Campbell's Peak (Figure 4.14d). All rock types present moderate to strong enrichment in rare earth elements compared to primitive mantle, and most display a general negative slope, indicating most samples are enriched in LREE relative to HREE.

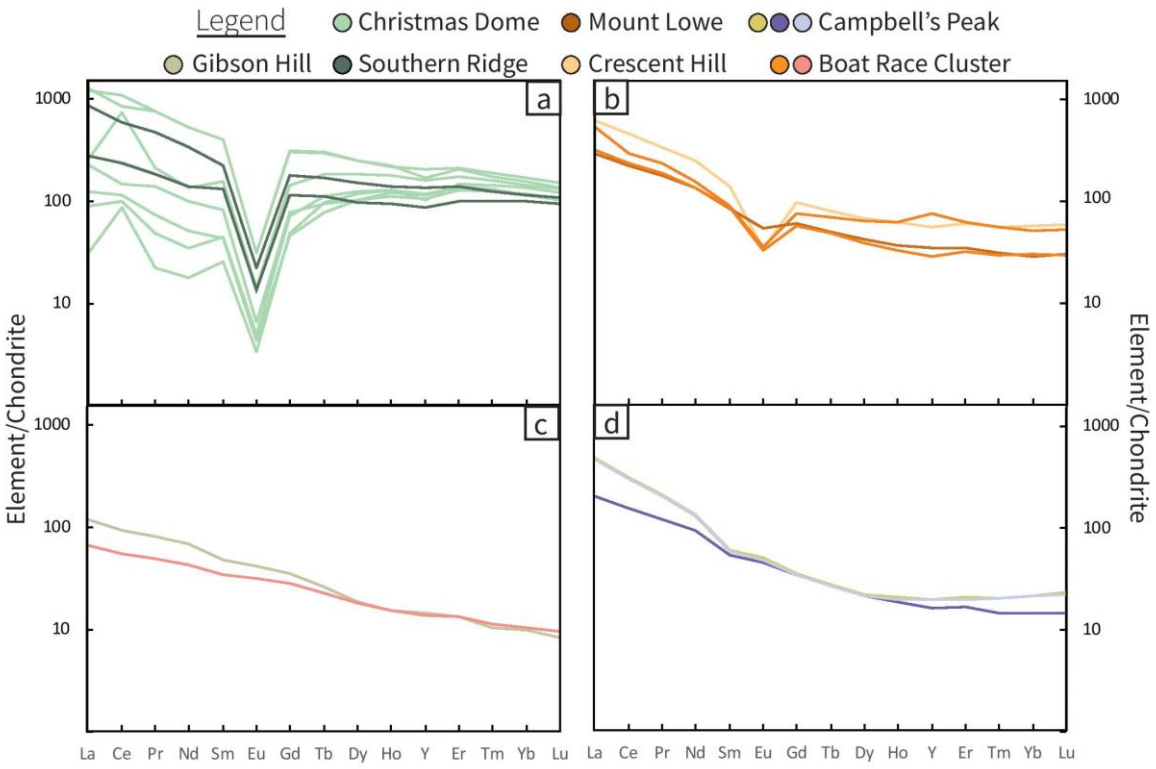

Figure 4.14: Spiderplot of rare earth element concentrations of the southern Peak Range, divided by rock type (a = rhyolite, b = trachyte, c = basaltic) and rocks of Campbell's Peak (d). CI chondrite normalisation values are from McDonough & Sun (1995).

The rhyolites of Christmas Dome exhibit various enrichment of LREE relative to the consistent HREE, some LREE portraying a positive slope and others general flat trends. Two samples are richer in Ce relative to their element neighbours, likely related to weathering aspects. The trachytic rocks are similar to the rhyolites, but slightly less enriched and experience overall slightly steeper negative slopes. Both Eu anomalies are likely due to Eu^{2+} readily partitioning into Ca-plagioclase as it was crystallised or removed from the remaining melt (Weill & Drake, 1973).

REE patterns of the basaltic rocks is similar, although Gibson has slightly higher LREE contents. Campbell's trachyandesite and tephriphonolite patterns are identical, exhibiting a

concave-up shape. The trachybasalt has less enrichment though elements Sm through to Ho are near identical to trachyandesite and tephriphonolite.

4.3 GEOCHEMISTRY OF SPINEL PERIDOTITES

4.3.1 WHOLE ROCK MAJOR ELEMENTS

Al_2O_3, CaO and Na_2O vs Mg# of multiple representative peridotites of different settings were plotted along with the peridotites found at Campbell's Peak to compare bulk composition (Figure 4.15). Representative peridotites from subduction, hotspot, and off-craton settings are plotted as they show evidence of some form of metasomatism seen in trace element concentrations, as well as Primitive Mantle and abyssal peridotites for reference (see Figure 4.15 caption for data reference).

The spinel peridotite (red) is more enriched in Al_2O_3, CaO and Na_2O compared to other peridotite conditions but is significantly lower in MgO and has near TiO_2 values closer to abyssal. Mg# is lower than most, reflecting the influence of melt/fluid enrichment and lower levels of partial melting before being brought to the surface.

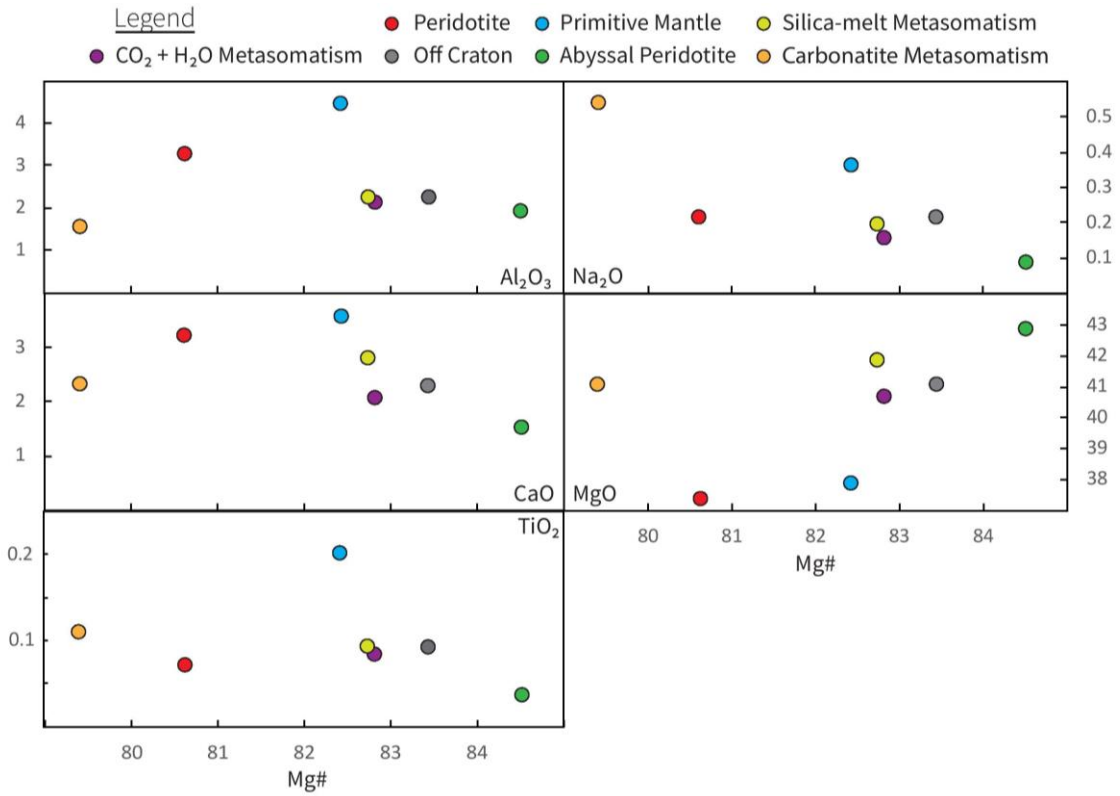

Figure 4.15: Comparison of the peridotite xenolith (red) found at Campbell's Peak with peridotite xenoliths of other settings. Y axis represents the wt% of the displayed oxide. Data for Primitive Mantle and off-craton from McDonough & Rudnick (1999), abyssal (Pacific and Indian transform systems) from Nui (2004), CO_2 + H_2O metasomatism (near craton boundary in China) from Huang (2013), carbonatite metasomatism (southeastern Australian hotspot) from Yaxley (1998), and silica-melt metasomatism (subduction-related) from Downes (2014).

4.3.2 WHOLE ROCK TRACE ELEMENTS

Trace element (Figure 4.3.2a) and rare earth element (Figure 4.3.2b) spiderplots of the spinel peridotite were normalised against Primitive Mantle (McDonough & Sun, 1989), and compared to abyssal peridotites (Nui, 2004).

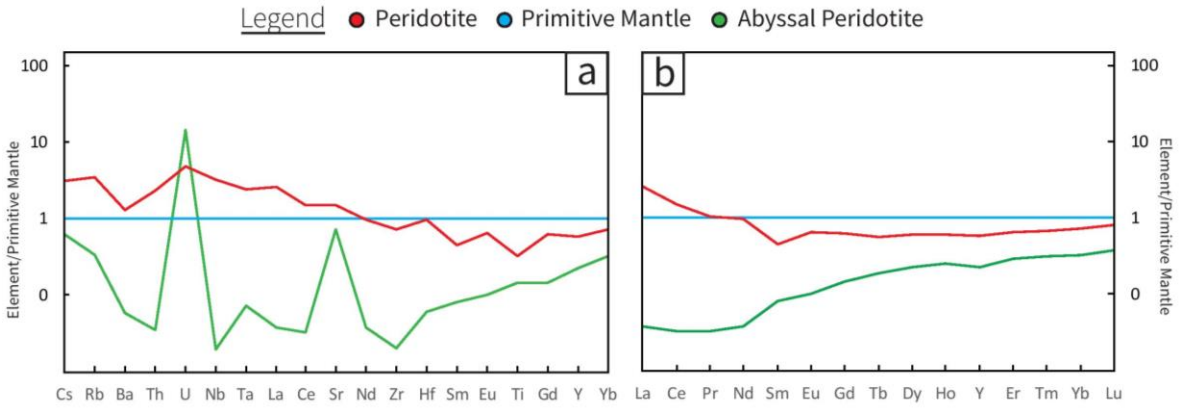

Figure 4.16: Spiderplot of a) trace element and b) rare earth element concentrations of the peridotite xenolith found at Campbell's Peak compared with Primitive Mantle (McDonough & Sun, 1989), and abyssal peridotites (Nui, 2004) Primitive Mantle normalisation values are from Sun & McDonough (1989).

Figure 4.16 shows that the spinel peridotite has an overall negative slope (excluding Ba anomaly) in trace and REE concentrations, with REE displaying a slight concave-up trend. It is enriched in comparison to abyssal peridotites, but only noticeably enriched in Rb, La, Ta, and U compared to Primitive mantle. Otherwise, the spinel peridotite is similar to the Primitive mantle trend, only being slightly less depleted in REE and other HFSE concentrations. Enrichment of U and Sr in the abyssal peridotite is likely due to the infiltration of seawater.

4.3.3 OLIVINE COMPOSITIONS

Figure 4.17 displays how the olivine in the trachybasalt varies in Ca, Ni, and Mn compared to the olivine in the spinel peridotite. Low Ca and Mn, high Ni and Mg# values of some trachybasalt olivines indicate they are peridotite olivine xenocrysts, likely sourced from the peridotite wall rock during trachybasalt ascent. There are observable negative slopes in Ca and Mn content for both rock types, while Ni in trachybasalt phenocryst olivines are distinct from peridotite olivines and fit well against olivine fractionation trends from Sobolev et al. (2007) basaltic compositions.

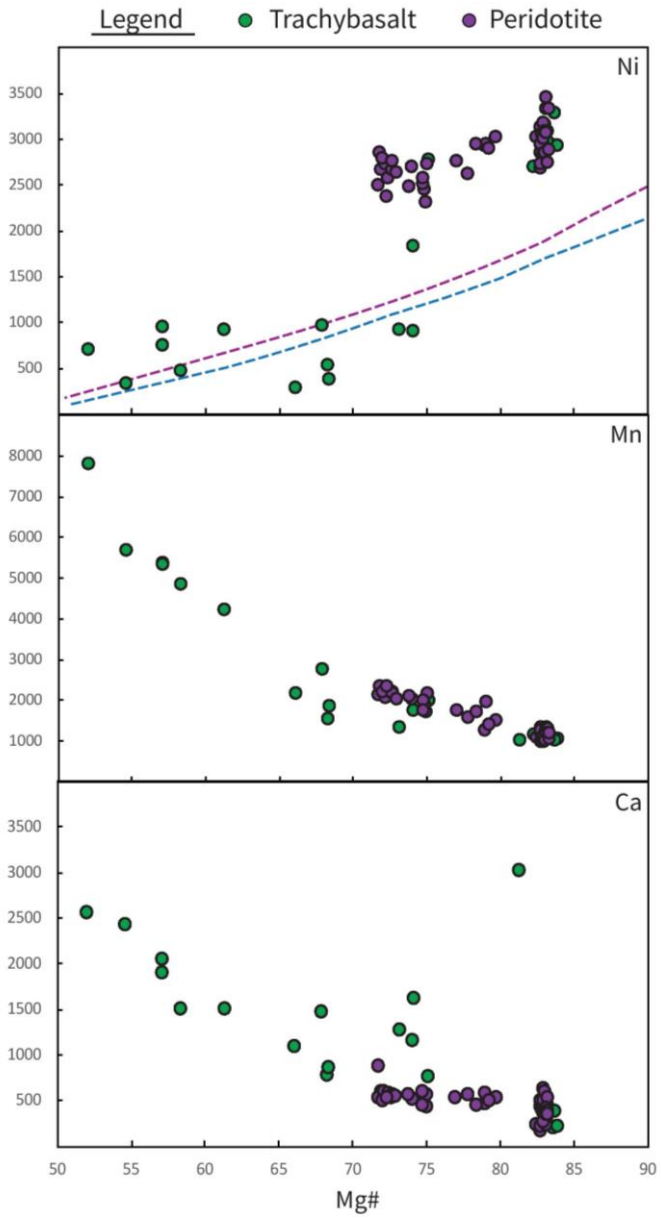

Figure 4.17: Mg# vs Ca, Ni, Mn of olivine phenocrysts in the trachybasalt (green) and olivine within the spinel peridotite xenolith (purple). Y axis represents the ppm of the displayed oxide. Fractionation trends of olivine Ni composition from Sobolev et al (2007) are plotted for comparison.

Traverses of trachybasalt olivine xenocrysts display consistent Mg-Fe elemental zoning with higher Fe rims reflected by lower Mg# (Figure 4.18a). Spinel peridotite olivines are homogeneous except for a lower Mg# rim in one of the olivine grains (Figure 4.18b).

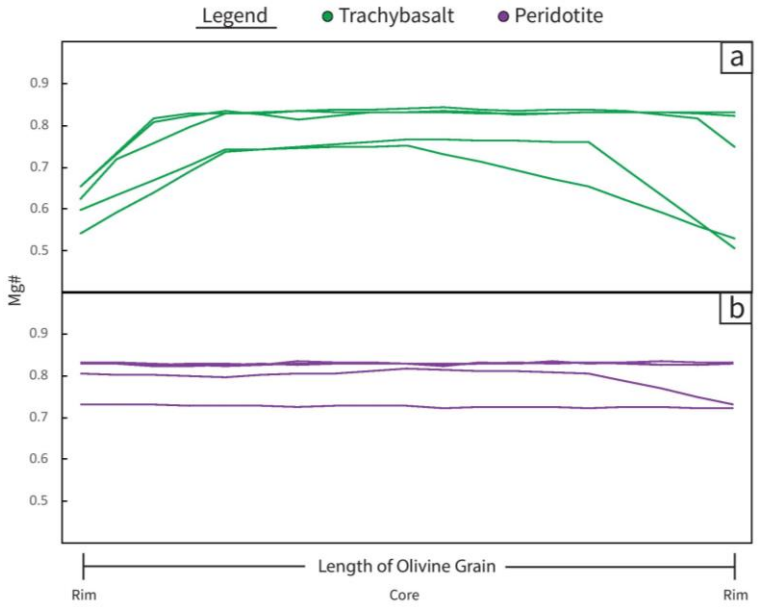

Figure 4.18: Elemental zoning of Mg and Fe reflected by the Mg# of olivine xenocrysts in the a) trachybasalt (green) and b) olivine within the spinel peridotite xenolith (purple).

4.4 MAGMA EVOLUTION MODELLING

EasyMELTS was used to model partial melting of the peridotite and fractionation of the trachybasalt to observe their evolution and relation to each other within Campbell's Peak. Temperature and pressure parameters were based on the solidus/liquidus of the rock, and the QFM buffer was constrained to zero. Compositional parameters for both models are presented in Appendix 4.

4.4.1 MELTING ARRAYS OF SPINEL PERIDOTITE

Melting arrays of the peridotite were made to record the composition of the melt at 1%, 3%, 5%, and 10% melting at different pressures of 5, 10 and 15kbar. Na_2O, Al_2O_3, TiO_2, MgO, CaO, K_2O, and FeO were plotted against SiO_2 to visualise the trends (Figure 4.19). The trachybasalt (purple) and tephriphonolite (light blue) compositions were plotted to see if the peridotite would reach one of their compositions. Also plotted is the composition of the

10kbar 1% melt with 5%, 10%, and 20% of the amphibole composition 'fractionated' (subtracted) and then normalised to 100. For each array, the solidus of the peridotite was found and then the temperature was increased until the percentage of melt was achieved. Compositions used for each array is presented in Appendix 4.

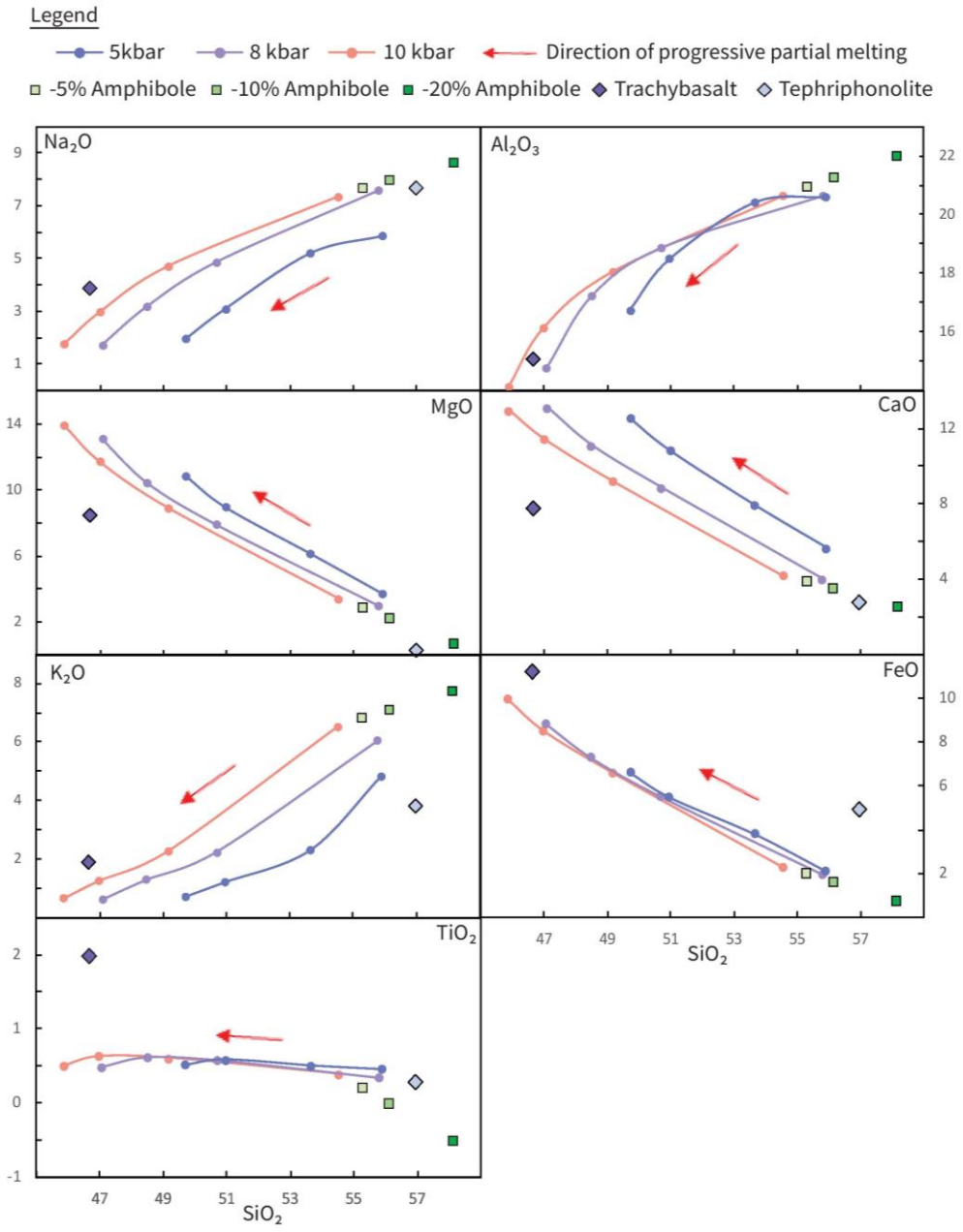

Figure 4.19: Melting arrays of peridotite xenolith found at Campbell's Peak for different pressures (10kbar; pink, 8kbar; purple, 5kbar; blue) using easyMELTS. The red arrow indicates the direction of progressive partial melting, with each dot 1%, 3%, 5%, and 10% (usually from right to left). The 10kbar 1% melt with 5% (light green), 10% (green), and 20% (darker green) amphibole 'fractionation' was plotted to achieve higher levels of SiO_2 for that array. The trachybasalt (purple diamond) and tephriphonolite (light blue diamond) were plotted for comparison.

With progressive partial melting, Na_2O, Al_2O_3, and K_2O decreased with decreasing SiO_2, while MgO, CaO, and FeO increased (TiO_2 remained constant). While the trachybasalt loosely correlates with compositions at ~10kbar, the shift of TiO_2 indicates that this peridotite did not produce this trachybasalt. The tephriphonolite plots closer to the 10kbar 'amphibole fractionated' 1% melt in all plots but $FeO_{(t)}$ and K_2O, possible reasoning due to the extreme incompatibility of Fe^{3+} and K (also K possibly during volatile loss upon eruption), making these elements sensitive to partial melting, thus difficult to model.

4.4.2 FRACTIONATION-DRIVEN EVOLUTION OF TRACHYBASALT

It was in our interest to see if we were able to fractionate the trachybasalt to achieve a similar composition to the tephriphonolite of Campbell's Peak. While keeping a constant pressure of 10kbar, starting at the liquidus, the trachybasalt was fractionated by decreasing the temperature by 50°c, and at each step recording the melt composition until the rock became solid (Figure 4.20). Vertically plotted is the composition of the tephriphonolite (grey line), positioned based on similar SiO2 content of both rock compositions. Total compositions at each temperature are presented in Appendix 4.

Fractionation of the trachybasalt produced a highly evolved, Na_2O-K_2O-Al_2O_3-rich composition with reduced concentrations in FeO, MgO and CaO. The composition of the trachybasalt when fractionated to a comparable SiO_2 concentration of tephriphonolite doesn't produce a similar composition, indicating that this rock didn't fractionate the tephriphonolite that forms Campbell's Peak.

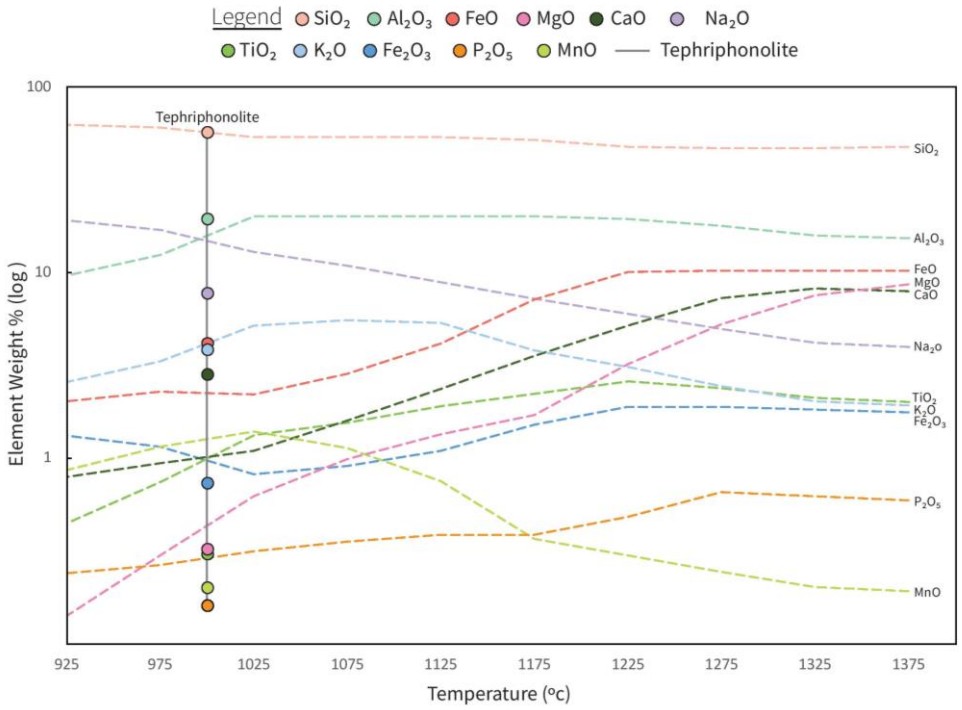

Figure 4.20: Progressive fractionation of the trachybasalt from Campbell's Peak using easyMELTS. Fractionation began at 1375℃ (liquidus), recording each new composition at 50℃ intervals (composition taken from new melt) until 925℃. Vertically plotted is the composition of the tephriphonolite (grey line), positioned based on similar SiO2 content (~57%) of both rock types.

5. DISCUSSION

5.1 ROCK TYPE DIVERSITY AND RARE METAL ENRICHMENT IN THE SOUTHERN PEAK RANGE

The southern Peak Range exhibits a variety of basaltic, trachytic, and rhyolitic domes, flows and peaks. Previous work by Chandler (2018) deemed this was the result of extensive fractionation of an alkali basalt parental melt at a shallow crustal position. Further modelling indicated that the parental melt fractionated from a basanite melt which formed by partial melting of a low fO_2 metasomatised (H_2O, Na_2O, K_2O and TiO_2-enriched) primitive mantle within the stability fields of spinel.

The geochemistry of the newly mapped volcanic bodies documented here are consistent with the model of extensive fractionation of an alkali basalt melt to produce the enriched rhyolitic peaks (Christmas Dome and the Southern Ridge) with high concentrations or Zr (2233-5401 ppm). Trachytic peaks exhibit less enrichment, with concentrations of Zr ranging between 750 and 1549 ppm (Boat Race Cluster and Crescent Hill respectively). This implies that increasing enrichment is consistent with progressive magmatic evolution, as can be seen in Figures 4.10 and Figure 4.13, as PI and Zr/TiO2 increase with SiO2. Though variation between major rock types may be a result of crustal assimilation, Nb/Th and Ta/U ratios indicate a primitive mantle signature (Figure 4.12), suggesting that the contribution of crustal assimilation was minor, if not any at all.

5.2 GEOLOGY OF CAMPBELL'S PEAK

Campbell's Peak consists of an extrusive, sodic, alkaline trachyandesitic core and tephriphonolitic perimeter (Figure 4.2). The mineral assemblage of both rock types consists of anorthoclase, oligoclase, hedenbergite, magnetite (with 7-11% ulvöspinel), and zeolite (analcime and natrolite) groundmasses with phenocrysts of anorthoclase and oligoclase (restricted to only oligoclase in the tephriphonolite). Analcime and natrolite in Campbell's Peak is likely a result of late-stage, low temperature alteration, with analcime forming at higher temperatures than the natrolite, similar to the phonolitic rocks of the Kaiserstuhl Volcanic Complex (Spurgin et al., 2019). The greater occurrence of anorthoclase and oligoclase phenocrysts with the change in zeolite composition in the core implies further fractionation of the trachyandesite melt and that it was hotter during late-stage zeolite alteration i.e., the core is younger.

The later emplacement of the olivine-rich, peridotite- and amphibole-filled trachybasalt is evident in the chilled margin at the contact boundary of the tephriphonolite. Trends of Ni in trachybasalt and peridotite olivine are not linear with increasing Mg# (Figure 4.17), and Ni in the trachybasalt fits well with the projected olivine fractionation trends for basaltic rocks from Sobolev et al., (2007) (blue and purple dashed lines), indicating that the source of the trachybasalt is not consistent with being derived from the spinel peridotites, but rather a normal mantle source. The instability of olivine peridotite xenocrysts (Mg-Fe zoning in Figure 4.18b) also support the lack of direct relationship between the trachybasalt and peridotite, and that the peridotite was there before the eruption of the trachybasalt.

Although there is no field relationship between the peridotite xenoliths and phonolitic rocks, modelling shows that low degree melting of the spinel peridotite, as little as 1%, drastically alters the composition of the melt, and produces a similar tephriphonolitic composition, distinctly different from the trachybasaltic host rock (Figure 4.19). Evidently, fractionation modelling of the trachybasalt (Figure 4.20) revealed that it has no direct relationship to the tephriphonolite, implying the trachybasalt is unrelated to the phonolitic rocks of Campbell's Peak and possibly relates to later flood basalt events.

5.3 SPINEL PERIDOTITES AND THE SCLM

Spinel peridotites from Campbell's Peak have near primitive mantle values of HFSE and HREE (Figure 4.16) illustrating little melting of the peridotite, and the presence of spinel in these peridotites indicate they originate from no deeper than ~60km, where garnet has disappeared and spinel is stable (Robinson et al., 1998). Relatively high Al_2O_3, CaO, and Na_2O concentrations compared to abyssal peridotites (Figure 4.15), and relatively high concentrations of Ni for comparative Mg# in olivine (Figure 4.17), are indicative of an enriched primitive mantle. High concentrations of Rb, La, Ta, U (Figure 4.16), and the presence of sodium-bearing pyroxenes and pargasitic amphibole reveal the existence of cryptic and modal metasomatism of the SCLM beneath the Peak Range (O'Reilly & Griffin, 2013; Yaxley et al., 1991). These spinel peridotites are practically pieces of the SCLM brought to the surface during the quick ascent of the trachybasalt host rock.

Mantle xenoliths in western Victoria have reported multiple episodes of metasomatism, evident in their petrographic (amphibole ± mica, apatite) and geochemical (enriched LREE,

Zr, Ta, K, Rb) signatures (Yaxley et al.,1998; O'Reilly & Griffin, 1988). Enrichment within these xenoliths is interpreted to be a result of cryptic, amphibole ± mica, and apatite metasomatism, likely related to CO_2-rich fluids, CO_2-H_2O fluids with various levels of K, and CO_2 + H_2O fluids respectively (O'Reilly & Griffin, 1988). The lack of mica and apatite phases in the spinel peridotite dictates that the metasomatic fluids that infiltrated the SCLM beneath the Peak Range were likely CO_2-rich with low amounts of K and sodic, based on sodium-bearing clinopyroxene (Dalton & Wood, 1993).

5.4 AMPHIBOLE COMPARISON AND POSSIBLE ORIGIN

Sadanagaite is a relatively new approved Ca-amphibole., now defined by cites A, C^{2+}, and C^{3+} being dominant in Na, Mg, and Al respectively. Sadanagaites were first discovered within skarns of the amphibolite facies in the Ryoke metamorphic belt in Japan, significant for their Si-poor, and Al-Ti- rich compositions (Shimazaki et al. 1984). Due to their wider range of Si, definition of sadanagaite as a calcic amphibole ($(Ca + Na) \geq 1.34$, $Na_B < 0.67$) with $Si < 5.5$, $(Na + K)_A \geq 0.5$, $Al^{VI} \geq Fe3+$ and $Ti < 0.50$ per unit cell formula) required an extension to the silica-poor side of the edenite-pargasite series after Leake (1978) (Shimazaki et al. 1984). Sadanagaite is also found within skarns in Cornwall (van Marcke de Lumen & Verkaeren, 1985), thermally metamorphosed rocks in the Nogo-Hakusan area (Sawaki, 1989) and Caledonian metamorphic rocks in the Western Baikal region (Savel'eva & Korikovskii, 1998). It is possible that with the new 2012 IMA amphibole nomenclature scheme that sadanagaites in the settings above are now redefined according to changes in classification of the dominant species (see Appendix 6).

The presence of megacrystic amphibole is a characteristic feature for some intraplate alkaline magmatic settings, but their petrogenic nature remains a debated subject. For example, Serre et al. (2020), Ellis (1976), and Demény et al. (2005) determined the origin of magnesio-hastingsite-pargasite-kaersutite megacrysts in southern New Zealand, the Newer Volcanics (Victoria), and the Carpathian-Pannonian region (central Europe) respectively to have originated from either: amphibole fractionation of the resulting alkaline melt, or amphibole cumulate phases within the mantle from metasomatic processes (based on specific mineral, geochemical and redox characteristics, and O-Sr-Nd isotopes). Although they are not sadanagaites, they represent possible origins for the amphibole xenocrysts found within Campbell's Peak.

In the Newer Volcanics, the role of amphibole fractionation from the parental melt played a dominant role in controlling the evolution of alkaline rocks, evidently decreasing TiO2, An/(Ab+An), Mg/Fe and normative olivine without significantly altering the K_2O/Na_2O ratio of the melt (Ellis, 1976). If this is true for Campbell's Peak, fractionation of Ti-rich sadanagaite from the spinel peridotite melt could explain the lower levels of TiO_2 in the peridotite, and the correlation between the 10kbar 1% melt with ~15% amphibole 'fractionation' and tephriphonolite (Figure 4.19). The interpretation that sadanagaite could represent cumulate phases beneath Campbell's Peak as a result of metasomatism in the SCLM is possible and would explain the disassociation between the sadanagaites and their host rock, but would require further comprehensive research to understand their petrographic nature and oxygen isotope analysis to determine if they are in accordance with a mantle origin (Demény et al., 2005).

5.5 BROAD GEODYNAMIC SETTING OF THE PEAK RANGE

Model-ages constrained from Sm/Nd isotopes of basaltic rocks in Dubbo, eastern Australia reveal the initial enrichment of the lithosphere to have occurred during the Neoproterozoic, 640-890 Ma (Zhang & O'Reilly, 1997), with enriching components brought in by the repetitive collision and extension preceding the breakup of Rodinia. The onset of the subduction from the collision of Gondwana and Laurussia during the Late Devonian to Cretaceous (Waschbush et al., 2009) subducted the enriched lithosphere prompting the dehydration and transportation of enriched fluids from the enriched subducting slab, metasomatising the overlying SCLM. As the northward-migration of the Australian plate travelled over the upwelling mantle plume, the heating effect of the plume induced partial melting of the SCLM as a result of decompression (Manglik & Christensen, 1997), generating a diverse range of intermediate to felsic volcanic intrusions in the Peak Range related to the distance from the plume centre.

The spatial relationship of Campbell's Peak to the Peak Range suggests that it has experienced a different evolutional pathway compared to the southern area, based on different degrees of partial melting, a result of their distance from the plume centre. Ernst & Bell (2010) suggests the spatial and temporal location of carbonatite intrusions with large igneous provinces (LIPs) are linked to each other, associated by a single magmatic system exhibiting different evolutional pathways. Localities of carbonatitic intrusions are spatially associated with low temperature, low degree partial mantle melting connected to further distances from the magmatic centre, while higher degrees of partial melting occur closer to the magmatic centre generating flood basalts and alkaline magmatism with further melting/ fractionation (Ernst & Bell, 2010). The plume model of Bell & Rukhlov (2004) suggests that

carbonatitic intrusions are generated earlier in respect to their basaltic magmatism (e.g. Bushveld Complex; Keweenawan LIP), but precise age constraints are vague on this topic.

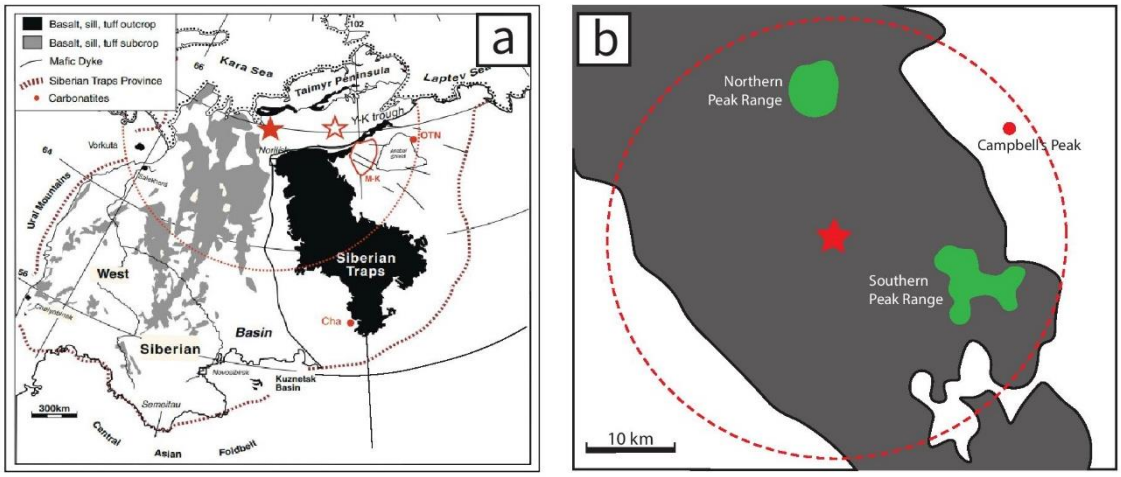

Figure 5.1: Comparison of the distribution of the a) Siberian trap LIP, with the distribution of the b) Peak Range (dark grey = flood basalt event; green = intermediate to felsic volcanics).Inferred 1000km radius of underlying mantle plume (red dashed circle) and plume centre (red star) are plotted for both. The assumption of the Peak Range mantle plume radius and position is based on the central group thought to be the volcanic centre of the Peak Range, and the position of the alkaline volcanism in relation to the centre. The figure of Siberian trap LIP is taken from Ernst & Bell (2010). Abbreviations used in their figure are presented in Fig. 6 caption of their paper.

Figure 5.1 compares the spatial relationship of the Siberian taps LIP and its carbonatitic intrusions with the interpreted spatial relationship of the Peak Range and Campbell's Peak, which shows a similar relationship to Ernst & Bell (2010) proposed model. Low degree melting of the spinel peridotite was likely the result of low temperature magmatism at the outer edge of the mantle plume, producing Campbell's Peak, ~20km NE of the central group (assumed plume centre). The succession of the trachybasalt eruption relates to the temporal model of carbonatitic and LIP magmatism, which coincidentally took the same eruption path as the phonolitic intrusion. Formation of the alkali basalt parental melt for the southern Peak Range is interpreted to have experienced higher degrees of partial melting which is connected to being relatively closer to the plume centre (Figure 5.1), then extensive fractionation to produce felsic volcanism (Chandler, 2018).

6. CONCLUSIONS

6.1 SUMMARY OF FINDINGS

The mantle xenoliths of Campbell's Peak offer intriguing insight into the geodynamic setting diversity of the Peak Range. Fieldwork, petrographic and geochemical analysis, and magma evolution modelling supports the following conclusions:

1. Further petrographical mapping and geochemical analysis of the southern Peak Range and comparison with previously studied volcanic bodies show that the newly mapped bodies also underwent extensive fractionation of an alkali basalt melt to achieve their rare earth enrichment and high peralkalinity.

2. The spinel peridotites represent enriched sub continental lithospheric mantle (SCLM) which has been modally (amphibole phases) and cryptically (enriched Rb, La, Ta, U, and sodium-bearing pyroxenes) metasomatised, likely by a CO_2-rich, sodic fluid in comparison to other metasomatised mantle xenoliths found in eastern Australia. The enrichment of the SCLM beneath the Peak Range is interpreted to be a result of the dehydration of the subducting slab in the west-dipping subduction system during the Late Devonian to Cretaceous, which was initially enriched during the Neoproterozoic (640-890 Ma).

3. Melting models of the peridotite demonstrate a lack of correlation between the basaltic host rock (especially in TiO_2 levels), but a stronger correlation with the phonolitic intrusion when partially melted (<1%) at ~10kbar and if fractionation of

~15% sadanagaite was considered. The fractionation of Ti-rich sadanagaite would explain lower levels of TiO_2 in the peridotite, but further research needs to be completed in order conclude this. It is possible that the sadanagaite is a cumulative phase as a result of metasomatism in the SCLM.

4. The assumption of Campbell's Peak as its own distinct magma series stems from the spatial and temporal relationship of Campbell's Peak to the Peak Range, a result of low degree melting at the outer edge of the mantle plume before the eruption of flood basalts, whereas the Peak Range volcanics are interpreted to have experienced higher degrees of melting due to being closer to the plume centre (central group) after the intrusion of Campbell's Peak.

6.2 FURTHER STUDY

Understanding the early magmatic history could provide information on how the unique occurrence of the southern Peak Range formed and prompt the closer inspection of similar suites across the world. Results of this thesis would benefit from further analysis to achieve a greater understanding of what prompted the enrichment in the peralkaline rock. Further analysis could include:

1. Additional collection and whole rock analysis of peridotite xenoliths: analysing a range of peridotite samples would test the homogeneity of the mantle beneath Campbell's Peak, and likely the Peak Range.

2. Trace and rare earth element analysis on individual minerals: specifically, clinopyroxene in peridotites can contain measurable amounts of LREE and trace element concentrations that reflect specific metasomatic enrichment processes within the mantle.

3. Radiogenic isotope data analysis: Sm-Nd isotope analysis to assist the evaluation of the sources and processes responsible for the diversity of magmatic rocks at Campbell's Peak.

4. Amphibole thermobarometry analysis: pressure and temperature estimates to aid in understanding the crystallising origin of the amphibole megacrysts.

ACKNOWLEDGMENTS

I would like to thank my supervisor Dr Carl Spandler for his continuous guidance, support, and patience throughout my honours year. Also I am grateful for the Geological Survey of Queensland, Australian Linkage Project, and University of Adelaide for their financial assistance that assisted me in completing this project. And lastly, a huge thank you to the honours cohort for providing unconditional support and endless laughs.

REFERENCES

AMBLER E. P. & ASHLEY P. M. 1977 Vermicular orthopyroxene-magnetite symplectites from the Wateranga layered mafic intrusion, Queensland, Australia, Lithos, vol. 10, no. 3, pp. 163-172.

ASIMOW P. D. & GHIORSO M. S. 1998 Algorithmic modifications extending MELTS to calculate subsolidus phase relations, The American mineralogist, vol. 83, no. 9-10, pp. 1127-1132.

BANNO Y., et al. 2004 Magnesiosadanagaite, a new member of the amphibole group from Kasuga-mura, Gifu Prefecture, central Japan, European journal of mineralogy (Stuttgart), vol. 16, no. 1, pp. 177-183.

BELL K. & RUKHLOV A. 2004 Carbonatites from the Kola Alkaline Province: origin, evolution and source characteristics, Phoscorites and carbonatites from mantle to mine: the key example of the Kola Alkaline Province, vol. 10, pp. 421-455.

CHANDLER R. & SPANDLER C. 2020 The igneous petrogenesis and rare metal potential of the peralkaline volcanic complex of the southern Peak Range, Central Queensland, Australia, Lithos, vol. 358-359, p. 105386.

CHANDLER R. 2018 The magmatic evolution and rare metal potential of the Peak Range Volcanics, central Queensland. Earth Sciences. Queensland: James Cook University.

CHANDLER, RB 2018, 'The magmatic evolution and rare metal potential of the Peak Range Volcanics, central Queensland', Earth Sciences, Bachelor of Geology (Honours) thesis, James Cook University.

CREAGER K. C. & JORDAN T. H. 1984 Slab penetration into the lower mantle, Journal of Geophysical Research: Solid Earth, vol. 89, no. B5, pp. 3031-3049.

DALTON J. A. & WOOD B. J. 1993 The compositions of primary carbonate melts and their evolution through wallrock reaction in the mantle, Earth and Planetary Science Letters, vol. 119, no. 4, pp. 511-525.

DAVIES D. R., et al. 2015 Lithospheric controls on magma composition along Earth's longest continental hotspot track, Nature (London), vol. 525, no. 7570, pp. 511-514.

DEMÉNY A., et al. 2005 Origin of amphibole megacrysts in the Pliocene-Pleistocene basalts of the Carpathian-Pannonian region, Geologica Carpathica, vol. 56, no. 2, pp. 179-189.

DOWNES H. 2001 Formation and modification of the shallow sub-continental lithospheric mantle: a review of geochemical evidence from ultramafic xenolith suites and tectonically emplaced ultramafic massifs of western and central Europe, Journal of petrology, vol. 42, no. 1, pp. 233-250.

ELLIS D. 1976 High pressure cognate inclusions in the Newer Volcanics of Victoria, Contributions to Mineralogy and Petrology, vol. 58, no. 2, pp. 149-180.

ERNST R. E. & BELL K. 2010 Large igneous provinces (LIPs) and carbonatites, Mineralogy and Petrology, vol. 98, no. 1, pp. 55-76.

FISHWICK S., et al. 2008 Steps in lithospheric thickness within eastern Australia, evidence from surface wave tomography, Tectonics (Washington, D.C.), vol. 27, no. 4, pp. TC4009-n/a.

GHIORSO M. S. & SACK R. O. 1995 Chemical mass transfer in magmatic processes IV. A revised and internally consistent thermodynamic model for the interpolation and extrapolation of liquid-solid equilibria in magmatic systems at elevated temperatures and pressures, Contributions to mineralogy and petrology, vol. 119, no. 2-3, pp. 197-212.

GLEN R. 2005 The Tasmanides of eastern Australia, Special Publication-Geological Society of London, vol. 246, p. 23.

GRIFFIN W. & O'REILLY S. Y. 2007 The earliest subcontinental lithospheric mantle, Developments in Precambrian Geology, vol. 15, pp. 1013-1035.

HUANG S.-W., et al. 2013 Geochemistry of ultramafic xenoliths in Cenozoic alkali basalts from Jiangsu province, eastern China and their geological implication, Journal of Earth System Science, vol. 122, no. 3, pp. 777-793.

HOWIE, R. A., ZUSSMAN, J., & DEER, W. (1992). An introduction to the rock-forming minerals (p. 696). Longman.

JONES I., et al. 2017 Animated reconstructions of the Late Cretaceous to Cenozoic northward migration of Australia, and implications for the generation of east Australian mafic magmatism, Geosphere (Boulder, Colo.), vol. 13, no. 2, pp. 460-481.

KESSON S. E. & FITZ GERALD J. D. 1992 Partitioning of MgO, FeO, NiO, MnO and Cr 2O 3 between magnesian silicate perovskite and magnesiowüstite: implications for the origin of inclusions in diamond and the composition of the lower mantle, Earth and planetary science letters, vol. 111, no. 2, pp. 229-240.

LE MAITRE R. W., et al. 2005 Igneous rocks: a classification and glossary of terms: recommendations of the International Union of Geological Sciences Subcommission on the Systematics of Igneous Rocks. Cambridge University Press.

MACLEAN W. H. & BARRETT T. J. 1993 Lithogeochemical techniques using immobile elements, Journal of geochemical exploration, vol. 48, no. 2, pp. 109-133.

MANGLIK A. & CHRISTENSEN U. 1997 Mantle plumes, convection and decompression melting, *Current Science*, pp. 1078-1083.

MARSHALL A. S., et al. 2009 Fractionation of Peralkaline Silicic Magmas: the Greater Olkaria Volcanic Complex, Kenya Rift Valley, Journal of petrology, vol. 50, no. 2, pp. 323-359.

MCCALL G. 2005 EARTH| Mantle.

MCDONOUGH W. F. & RUDNICK R. L. 2018 Mineralogy and composition of the upper mantle, Ultrahigh Pressure Mineralogy, pp. 139-164.

MCDONOUGH W. F. & SUN S.-S. 1995 The composition of the Earth, Chemical geology, vol. 120, no. 3-4, pp. 223-253.

MOLLAN R. G. 1965 Tertiary volcanics in the Peak Range, central Queensland. The Australian National University (Australia).

NIU Y. 2004 Bulk-rock major and trace element compositions of abyssal peridotites: implications for mantle melting, melt extraction and post-melting processes beneath mid-ocean ridges, Journal of Petrology, vol. 45, no. 12, pp. 2423-2458.

O'REILLY S. Y. & GRIFFIN W. 2013 Mantle metasomatism. Metasomatism and the chemical transformation of rock. pp. 471-533. Springer.

O'REILLY S. Y. & GRIFFIN W. L. 1988 Mantle metasomatism beneath western Victoria, Australia: I. Metasomatic processes in Cr-diopside lherzolites, Geochimica et cosmochimica acta, vol. 52, no. 2, pp. 433-447.

PALME H. & O'NEILL H. S. C. 2003 Cosmochemical estimates of mantle composition, Treatise on geochemistry, vol. 2, p. 568.

PILET S., BAKER M. B. & STOLPER E. M. 2008 Metasomatized Lithosphere and the Origin of Alkaline Lavas, Science, vol. 320, no. 5878, pp. 916-919.

POUDJOM DJOMANI Y. H., et al. 2001 The density structure of subcontinental lithosphere through time, Earth and planetary science letters, vol. 184, no. 3, pp. 605-621.

POWELL W., et al. 2004 Mantle amphibole trace-element and isotopic signatures trace multiple metasomatic episodes in lithospheric mantle, western Victoria, Australia, Lithos, vol. 75, no. 1, pp. 141-171.

ROBINSON J. A. C. & WOOD B. J. 1998 The depth of the spinel to garnet transition at the peridotite solidus, Earth and Planetary Science Letters, vol. 164, no. 1-2, pp. 277-284.

ROSENBAUM G. 2018 The Tasmanides: Phanerozoic Tectonic Evolution of Eastern Australia, Annual review of earth and planetary sciences, vol. 46, no. 1, pp. 291-325.

SAVEL'EVA V. & KORIKOVSKII S. 1998 Sadanagaite from biotite-corundum-margarite-spinel-anorthite schists of the Western Baikal region. Doklady earth sciences. pp. 477-479. Springer.

SAWAKI T. 1989 Sadanagaite and subsilicic ferroan pargasite from thermally metamorphosed rocks in the Nōgō-Hakusan area, central Japan, Mineralogical Magazine, vol. 53, no. 369, pp. 99-106.

SERRE S. H., et al. 2020 Petrogenesis of amphibole megacrysts in lamprophyric intraplate magmatism in southern New Zealand, New Zealand Journal of Geology and Geophysics, vol. 63, no. 4, pp. 489-509.

SERRE S. H., et al. 2020 Petrogenesis of amphibole megacrysts in lamprophyric intraplate magmatism in southern New Zealand, New Zealand journal of geology and geophysics, vol. 63, no. 4, pp. 489-509.

SHIMAZAKI H., BUNNO M. & OZAWA T. 1984 Sadanagaite and magnesio-sadanagaite, new silica-poor members of calcic amphibole from Japan, The American mineralogist, vol. 69, no. 5-6, pp. 465-471.

SOBOLEV A. V., et al. 2007 The amount of recycled crust in sources of mantle-derived melts, Science (American Association for the Advancement of Science), vol. 316, no. 5823, pp. 412-417.

SPAMPINATO G. P. T., et al. 2015 Early tectonic evolution of the Thomson Orogen in Queensland inferred from constrained magnetic and gravity data, Tectonophysics, vol. 651-652, pp. 99-120.

SPÜRGIN S., WEISENBERGER T. B. & MARKOVIC M. 2019 Zeolite-group minerals in phonolite-hosted deposits of the Kaiserstuhl volcanic complex, Germany, The American mineralogist, vol. 104, no. 5, pp. 659-670.

SUN S.-S. & MCDONOUGH W. F. 1989 Chemical and isotopic systematics of oceanic basalts: implications for mantle composition and processes, Geological Society, London, Special Publications, vol. 42, no. 1, pp. 313-345.

TANG Z., et al. 2016 Novel zirconium silicate phosphor K 2 ZrSi 2 O 7: Eu 2+ for white light-emitting diodes and field emission displays, Journal of Materials Chemistry C, vol. 4, no. 23, pp. 5307-5313.

VAN DER HILST R. D., WIDIYANTORO S. & ENGDAHL E. 1997 Evidence for deep mantle circulation from global tomography, Nature, vol. 386, no. 6625, pp. 578-584.

VASCONCELOS P. M., et al. 2008 Geochronology of the Australian Cenozoic: a history of tectonic and igneous activity, weathering, erosion, and sedimentation, Australian journal of earth sciences, vol. 55, no. 6-7, pp. 865-914.

VEEVERS J. 2000 Impact on Australia and Antarctica of the collisional merging of Gondwanaland and Laurussia in Pangea. Billion-year earth history of Australia and neighbours in Gondwanaland. pp. 283-291. GEMOC Press.

WASCHBUSH, P., KORSCH, R. J., & BEAUMONT, C. 2009, Geodynamic modelling of aspects of the Bowen, Gunnedah, Surat and Eromanga Basins from the perspective of convergent margin processes. Australian Journal of Earth Sciences: An International Geoscience Journal of the Geological Society of Australia, 56(3), 309-334.

WEILL D. F. & DRAKE M. J. 1973 Europium Anomaly in Plagioclase Feldspar: Experimental Results and Semiquantitative Model, Science (American Association for the Advancement of Science), vol. 180, no. 4090, pp. 1059-1060.

WELLMAN P. & MCDOUGALL I. 1974 Cainozoic igneous activity in eastern australia, Tectonophysics, vol. 23, no. 1, pp. 49-65.

WELLMAN P. 1974 Potassium-argon ages on the Cainozoic Volcanic rocks of Eastern Victoria, Australia, Journal of the Geological Society of Australia, vol. 21, no. 4, pp. 359-376.

WITHNALL, I. W. 1995, 'Geology of the southern part of the Anakie Inlier, central Queensland', Brisbane: Department of Minerals and Energy.

WITHNALL, I. W., .HENDERSON, R. A., CHAMPION, D. C., & JELL, P. A. 2013, Chapter 1: Introduction. In P. A. Jell (Ed.), Geology Of Queensland: Geological Survey of Queensland.

YAXLEY G. 1998 Carbonatite Metasomatism in the Southeastern Australian Lithosphere, Journal of petrology, vol. 39, no. 11, pp. 1917-1930.

YAXLEY G. M., CRAWFORD A. J. & GREEN D. H. 1991 Evidence for carbonatite metasomatism in spinel peridotite xenoliths from western Victoria, Australia, Earth and Planetary Science Letters, vol. 107, no. 2, pp. 305-317.

ZHANG M. & O'REILLY S. Y. 1997 Multiple sources for basaltic rocks from Dubbo, eastern Australia: geochemical evidence for plume—lithospheric mantle interaction, Chemical Geology, vol. 136, no. 1-2, pp. 33-54.

APPENDIX 1: SAMPLE CATALOGUE

Note: coordinates are in WGS84

Mountain ID	Sample ID	Latitude	Longitude	Whole Rock Chemistry	Thin Section	Electron Microprobe Puck
Boat Race Cluster	SPR-01-04-CDU57	-22.840749	148.199916	X		
Boat Race Cluster	SPR-06-04-E82	-22.8404	148.196695		X	
Boat Race Cluster	SPR-06-04-N83	-22.840548	148.19583	X	X	
Boat Race Cluster	SPR-06-04-E85	-22.841076	148.194526			
Boat Race Cluster	SPR-06-04-E86	-22.841244	148.194353		X	
Boat Race Cluster	SPR-06-04-N87	-22.842965	148.192807		X	
Boat Race Cluster	SPR-06-04-N88	-22.844351	148.193372			
Boat Race Cluster	SPR-06-04-N89	-22.845783	148.19679			
Boat Race Cluster	SPR-06-04-N90	-22.841908	148.198504	X		
Campbell Peak	SPR-31-03-CP26	-22.604089	148.222299			
Campbell Peak	SPR-31-03-CP27	-22.604089	148.222299			
Campbell Peak	SPR-31-03-CP28	-22.604089	148.222299			
Campbell Peak	SPR-31-03-CP29	-22.604089	148.222299		X	X
Campbell Peak	SPR-31-03-CP30	-22.604089	148.222299			
Campbell Peak	SPR-31-03-CP31	-22.604089	148.222299			
Campbell Peak	SPR-31-03-CP32	-22.604089	148.222299	X		X
Campbell Peak	SPR-31-03-CP33	-22.604089	148.222299		X	
Campbell Peak	SPR-31-03-CP34	-22.604089	148.222299			
Campbell Peak	SPR-31-03-CP35	-22.604089	148.222299	X		X
Campbell Peak	SPR-31-03-CP36	-22.604089	148.222299	X		
Campbell Peak	SPR-31-03-CP37	-22.604089	148.222299		X	3

Campbell Peak	SPR-31-03-CP38	-22.604089	148.222299			
Campbell Peak	SPR-31-03-CP39	-22.604089	148.222299	X		
Campbell Peak	SPR-31-03-CP45A	-22.604089	148.222299	X	X	2
Campbell Peak	SPR-31-03-CP45B	-22.604089	148.222299			6
Campbell Peak	SPR-04-04-CP73	-22.604711	148.223666			
Campbell Peak	SPR-04-04-CP74	-22.606162	148.221657		X	
Christmas Dome	SPR-31-03-CD40	-22.836732	148.202289	X		
Christmas Dome	SPR-31-03-CD41	-22.836732	148.202289		X	
Christmas Dome	SPR-31-03-CD42	-22.836732	148.202289		X	
Christmas Dome	SPR-31-03-CD43	-22.836268	148.2022		X	
Christmas Dome	SPR-31-03-CD44	-22.835183	148.199611	X		
Christmas Dome	SPR-01-04-CD55	-22.833884	148.205782	X		
Christmas Dome	SPR-01-04-CD56	-22.833884	148.205782		X	
Christmas Dome	SPR-03-04-CD58	-22.8351	148.20547			
Christmas Dome	SPR-03-04-CD59	-22.834595	148.20424		X	
Christmas Dome	SPR-03-04-CD60	-22.834694	148.203556		X	
Christmas Dome	SPR-03-04-CD61	-22.8327	148.202623	X		
Christmas Dome	SPR-03-04-CD62	-22.4988	148.201683			
Christmas Dome	SPR-03-04-CD63	-22.832656	148.199907			
Christmas Dome	SPR-03-04-CD64	-22.83352	148.199993			
Christmas Dome	SPR-03-04-CD65	-22.834611	148.19987			
Christmas Dome	SPR-03-04-CD66	-22.83598	148.198711			
Christmas Dome	SPR-03-04-CD67	-22.836711	148.198706	X		
Christmas Dome	SPR-03-04-CD69	-22.836138	148.205415			

Christmas Dome	SPR-03-04-CD70	-22.836711	148.204703	X	X	
Christmas Dome	SPR-03-04-CD71	-22.832237	148.204994			
Christmas Dome	SPR-03-04-CD72	-22.833708	148.205705		X	
Christmas Dome	SPR-05-04-CD80	-22.837586	148.200495	X		
Christmas Dome	SPR-05-04-CD81	-22.836804	148.200234		X	
Crescent Hill	SPR-07-04-CH92	-22.856711	148.177371	X		
Crescent Hill	SPR-07-04-CH93	-22.858183	148.177412			
Crescent Hill	SPR-07-04-CH94	-22.864702	148.183878		X	
Gibson Hill	SPR-07-04-G95	-22.796972	148.192245	X	X	
Gibson Hill	SPR-07-04-G96	-22.797927	148.19307			
Mount Lowe	SPR-05-04-ML75	-22.908009	148.145414			
Mount Lowe	SPR-05-04-ML76	-22.908009	148.145414	X	X	
Mount Lowe	SPR-05-04-ML77	-22.906157	148.149287			
Mount Lowe	SPR-05-04-ML78	-22.90223	148.150489			
Mount Lowe	SPR-05-04-ML79	-22.90223	148.150489		X	
Southern Ridge	SPR-01-04-SR46	-22.810416	148.208082		X	
Southern Ridge	SPR-01-04-SR47	-22.810416	148.208082			
Southern Ridge	SPR-01-04-SR48	-22.810416	148.208082		X	
Southern Ridge	SPR-01-04-SR49	-22.810632	148.208354	X		
Southern Ridge	SPR-01-04-SR50	-22.810937	148.209867			
Southern Ridge	SPR-01-04-SR51	-22.811481	148.211467	X	3	
Southern Ridge	SPR-01-04-SR52	-22.811532	148.21086		X	
Southern Ridge	SPR-01-04-SR53	-22.809798	148.208117		X	
Southern Ridge	SPR-01-04-SR54	-22.816483	148.210231			

APPENDIX 2: WHOLE ROCK GEOCHEMISTRY DATA

ID	SiO2	Al2O3	Fe2O3	MgO	CaO	Na2O	K2O	TiO2	P2O5	MnO	Cr2O3	Ba	Sc	Sum	Cs
Unit	**%**	**%**	**%**	**%**	**%**	**%**	**%**	**%**	**%**	**%**	**%**	**PPM**	**PPM**	**%**	**PPM**
SPR-01-04-CDU57	65.22	16.98	3.55	0.03	0.54	6.31	5.71	0.35	0.09	0.05	<0.002	267	6	99.74	0.3
SPR-06-04-N83	53.55	14.98	10.82	6.31	7.57	2.96	0.41	1.69	0.34	0.14	0.034	161	19	99.84	0.4
SPR-06-04-N90	63.89	16.28	5.01	0.33	0.79	6.12	5.56	0.35	0.11	0.07	<0.002	211	6	99.76	0.2
SPR-31-03-CP32	57.7	19.39	5.29	0.45	3.11	7.13	3.38	0.34	0.17	0.2	<0.002	1083	1	99.57	1.8
SPR-31-03-CP35	56.96	19.42	4.89	0.32	2.8	7.69	3.82	0.3	0.16	0.2	<0.002	1051	1	99.61	1.2
SPR-31-03-CP36	56.94	19.66	4.48	0.53	2.97	6.59	4	0.27	0.13	0.19	<0.002	1039	1	99.62	1.6
SPR-31-03-CP39	45.33	3.26	8.96	37.31	3.02	0.21	0.07	0.07	0.01	0.13	0.394	9	16	99.92	<0.1
SPR-31-03-CP45A	46.65	15.1	11.19	8.44	7.82	3.93	1.9	1.99	0.58	0.19	0.039	512	21	99.74	0.6
SPR-07-04-CH92	67.49	16.21	2.55	0.1	0.43	5.7	5.62	0.32	0.06	0.02	<0.002	36	4	99.62	0.5
SPR-07-04-G95	52.97	15.41	9.8	5.74	6.35	4.09	1.43	2.09	0.6	0.11	0.027	323	14	99.81	0.2
SPR-05-04-ML76	64.06	17.67	2.89	0.07	0.93	5.74	6.21	0.54	0.18	0.03	<0.002	541	13	99.75	<0.1
SPR-31-03-CD40	75.47	10.54	3.86	0.03	0.05	4.88	3.61	0.09	0.01	0.02	<0.002	3	<1	99.45	4.6
SPR-31-03-CD44	73.54	11.09	3.91	0.02	0.06	5.29	3.88	0.11	0.02	0.04	<0.002	32	<1	99.07	2.7
SPR-01-04-CD55	73.47	11.08	3.93	0.07	0.05	4.93	4.18	0.12	0.02	0.04	<0.002	10	<1	98.99	9.2
SPR-03-04-CD61	73.72	11.02	3.97	0.02	0.07	5.12	4.16	0.11	0.02	0.04	<0.002	6	<1	99.11	6.8
SPR-03-04-CD67	73.97	11.19	3.97	<0.01	0.06	4.62	3.96	0.12	0.03	0.04	<0.002	22	<1	99.22	1.4
SPR-03-04-CD70	73.34	11.35	3.94	0.02	0.05	5.08	4.45	0.11	0.05	0.03	<0.002	2	<1	99.17	4.3
SPR-05-04-CD80	73.39	10.94	3.89	<0.01	0.04	5.2	3.92	0.12	<0.01	0.03	0.002	18	<1	98.77	3.8
SPR-01-04-SR49	72.26	11.7	4.46	0.16	0.07	4.53	4.71	0.12	0.03	0.06	<0.002	49	<1	99.47	0.9
SPR-01-04-SR51	71.87	11.89	4.68	0.09	0.15	5.05	4.12	0.14	0.07	0.04	<0.002	26	1	99.37	0.5

ID	Ga	Hf	Nb	Rb	Sn	Sr	Ta	Th	U	V	W	Zr	Y	La	Ce
Unit	**PPM**	**PPM**	**PPM**	**PPM**	**PPM**	**PPM**	**PPM**	**PPM**	**PPM**	**PPM**	**PPM**	**PPM**	**PPM**	**PPM**	**PPM**
SPR-01-04-CDU57	43.4	16.6	103.6	123	7	22.3	6.2	14	4	<8	1	751.3	116.6	126.5	176.9
SPR-06-04-N83	19.1	3.3	15.4	26.3	1	367.6	0.9	1.6	0.4	125	0.5	136.3	20.2	14.3	30.5
SPR-06-04-N90	41.5	16.7	103	116.1	7	22.9	5.6	14.3	2	<8	1.4	750.1	44.8	75.2	143.2
SPR-31-03-CP32	20.3	12.5	137.6	88.5	3	1826.9	8.5	15.7	3.8	<8	0.9	647.3	27.7	94.4	157.7
SPR-31-03-CP35	22.1	11.7	137.9	100.2	3	1548.3	8.4	14.9	4.3	<8	1.3	631.9	27.8	92.9	155.9
SPR-31-03-CP36	20.2	12.5	142	107	3	1518.7	9.2	15.5	2.5	<8	<0.5	643	27.5	91.7	155.3
SPR-31-03-CP39	2.2	0.3	2.3	2.2	<1	32.2	0.1	<0.2	<0.1	75	1.4	8.2	2.7	1.8	2.7
SPR-31-03-CP45A	17.1	5.8	59.6	49.1	2	872.9	3.4	5.7	1.4	174	0.7	257.8	23.1	41.3	81.3
SPR-07-04-CH92	45.6	31.1	142.8	176.1	7	8.2	7.5	19.4	4.7	<8	8.9	1549.1	85.7	144.2	281.3
SPR-07-04-G95	20.3	4.8	27.4	28.3	2	514.7	1.4	2.9	0.7	98	<0.5	226.7	21	24.9	50.4
SPR-05-04-ML76	37.5	17.3	95	100.2	5	38.6	5.6	10.8	3.3	<8	1.3	839.4	54.6	68.2	136.1
SPR-31-03-CD40	64.7	62.5	403.2	418.4	34	2.7	27	51.6	18.8	<8	1.1	2491.8	182.6	21	59.9
SPR-31-03-CD44	72.3	96.4	574.9	527.6	53	13.3	40.2	107.2	26.5	10	1.9	3624.3	319.5	298.2	511.4
SPR-01-04-CD55	74.3	124	989.9	548.9	63	2.7	55.6	111	44.6	<8	2.4	4049.7	246.6	58.4	443
SPR-03-04-CD61	73.4	107.1	743.8	661.7	57	3.8	43.3	106.8	16	<8	1.2	4143.7	164.8	53.1	89
SPR-03-04-CD67	76	101.4	703.5	555.1	64	2	49.6	119	18.8	<8	<0.5	3640.1	157.3	7	53.1
SPR-03-04-CD70	74.6	97	686.2	697.2	54	1.4	43.2	106.2	27.2	<8	2.4	3852.7	178.5	29.5	69.9
SPR-05-04-CD80	77.2	123.8	954.4	527.6	64	3	53.4	135.9	30.8	<8	<0.5	5400.8	261.4	280.5	660.3
SPR-01-04-SR49	65.1	60.4	389.8	395.6	32	2.4	25.7	36.6	13.5	<8	2.5	2232.7	135.8	64.5	141.1
SPR-01-04-SR51	66.3	62.6	411.9	381.9	31	6.3	25.6	63.5	13	<8	1.5	2421.5	210.3	203.8	357.2

ID	Pr	Nd	Sm	Eu	Gd	Tb	Dy	Ho	Er	Tm	Yb	Lu	Ni	LOI	TOT/C
Unit	**PPM**	**PPM**	**PPM**	**PPM**	**PPM**	**PPM**	**PPM**	**PPM**	**PPM**	**PPM**	**PPM**	**PPM**	**PPM**	**%**	**%**
SPR-01-04-CDU57	21.47	71	13.21	2.01	14.92	2.46	15.52	3.35	9.85	1.35	8.06	1.28	<10	0.9	0.02
SPR-06-04-N83	4.12	17.9	4.57	1.6	5.12	0.74	4.13	0.77	2	0.26	1.56	0.22	140	1	0.05
SPR-06-04-N90	17.12	61.6	12.6	1.84	11.21	1.74	9.51	1.76	5.02	0.72	4.77	0.72	<10	1.2	0.02
SPR-31-03-CP32	16.65	53	7.67	2.53	6.21	0.89	4.88	1.01	2.97	0.45	3.06	0.51	<10	2.3	0.04
SPR-31-03-CP35	16.27	52.3	7.55	2.37	6.04	0.87	4.72	0.97	2.85	0.45	3.12	0.49	<10	2.9	0.01
SPR-31-03-CP36	16.18	51.9	7.57	2.44	6.12	0.85	4.84	0.96	2.97	0.45	3.1	0.5	<10	3.8	0.13
SPR-31-03-CP39	0.29	1.3	0.2	0.11	0.38	0.06	0.45	0.1	0.31	0.05	0.36	0.06	1998	0.9	0.04
SPR-31-03-CP45A	9.72	36.7	6.87	2.23	6.12	0.87	4.7	0.9	2.37	0.32	2.13	0.32	183	1.8	0.04
SPR-07-04-CH92	31.08	111.5	20.11	1.86	18.84	2.88	16.45	3.35	9.45	1.37	9.03	1.42	<10	1.1	0.01
SPR-07-04-G95	6.74	28.1	6.34	2.15	6.41	0.86	4.24	0.78	1.96	0.24	1.47	0.19	127	1.1	0.05
SPR-05-04-ML76	16.39	61.7	12.5	3.01	11.84	1.8	10.16	2	5.46	0.77	4.6	0.73	<10	1.4	0.01
SPR-31-03-CD40	4.48	15.8	6.56	0.28	13.89	4	30.42	6.88	21.26	3.04	18.56	2.55	<10	0.9	0.03
SPR-31-03-CD44	69.75	239.9	57.75	1.74	60.64	10.67	60.9	11.71	33.18	4.58	27.05	3.66	<10	1.1	0.06
SPR-01-04-CD55	19.37	60.4	22.57	0.8	28.21	6.62	44.65	9.7	27.86	3.96	22.99	3.18	<10	1.1	0.02
SPR-03-04-CD61	12.7	45.3	12.02	0.37	15.18	3.4	25.11	6.04	20.09	3.08	18.5	2.55	<10	0.9	0.02
SPR-03-04-CD67	2.02	8	3.73	0.19	9.42	3.47	28.64	6.89	23.42	3.47	21.52	2.95	<10	1.3	0.06
SPR-03-04-CD70	6.82	23.2	6.42	0.24	9.08	2.79	25.05	6.57	21.98	3.25	18.36	2.47	<10	0.8	0.04
SPR-05-04-CD80	68.62	240.1	58.36	1.74	60.04	10.45	60.49	11.98	32.81	4.28	24.72	3.25	<10	1.2	0.04
SPR-01-04-SR49	17.02	63.5	19.26	0.75	22.72	4.03	23.64	5.04	15.63	2.44	15.8	2.31	<10	1.3	0.04
SPR-01-04-SR51	43.8	152.2	32.96	1.24	35.12	6.1	36.54	7.6	21.76	3.06	18.3	2.61	<10	1.3	0.04

ID	TOT/S	Mo	Cu	Pb	Zn	Ag	Ni	Co	Mn	As	Au	Cd	Sb	Bi	Cr
Unit	**%**	**PPM**	**PPM**	**PPM**	**PPM**	**PPB**	**PPM**	**PPM**	**PPM**	**PPM**	**PPB**	**PPM**	**PPM**	**PPM**	**PPM**
SPR-01-04-CDU57	<0.01	5.75	6.22	8.67	109.9	27	0.7	0.4	96	0.3	1.6	0.14	0.05	0.03	3.4
SPR-06-04-N83	<0.01	0.95	40.99	0.36	23.9	12	28.6	6.5	142	0.4	0.6	0.02	<0.02	<0.02	29.3
SPR-06-04-N90	<0.01	1.9	9.3	8.51	120.9	28	5.9	0.5	203	<0.1	0.5	0.07	0.03	0.06	2.5
SPR-31-03-CP32	<0.01	5.68	5.62	6.61	82.4	39	1.8	1.1	621	0.4	1.7	0.06	0.06	<0.02	2.8
SPR-31-03-CP35	<0.01	2.93	6.59	5.58	80.1	33	1.8	1	544	1.6	0.6	0.22	0.06	0.04	3.6
SPR-31-03-CP36	<0.01	1.92	6.32	7.85	84.4	46	1.5	0.9	711	0.6	0.9	0.09	0.04	0.02	2.2
SPR-31-03-CP39	0.02	2.15	27.34	0.23	18.5	8	1808.3	78.7	639	1.1	1.4	0.02	<0.02	<0.02	56.3
SPR-31-03-CP45A	<0.01	3.04	30.77	1.91	92.4	34	160.8	31	1110	1	*	0.11	0.03	<0.02	100.9
SPR-07-04-CH92	<0.01	2.57	2.43	7.46	95.2	41	3.6	0.2	40	<0.1	<0.2	0.03	0.02	<0.02	2.5
SPR-07-04-G95	<0.01	0.55	27.22	0.46	41.4	3	68.7	12.1	229	<0.1	0.8	0.04	<0.02	<0.02	78.6
SPR-05-04-ML76	<0.01	3.16	7.02	5.79	182.1	47	0.8	0.7	136	<0.1	<0.2	0.12	0.03	<0.02	2.3
SPR-31-03-CD40	<0.01	0.26	2.13	39.23	185.3	42	0.7	<0.1	14	0.7	*	0.13	0.09	0.17	2.3
SPR-31-03-CD44	0.01	0.58	6.44	39.29	112.4	99	0.8	<0.1	23	<0.1	2.2	0.31	0.19	0.45	2.8
SPR-01-04-CD55	<0.01	0.27	2.3	115.99	129	157	0.5	0.1	40	0.3	*	0.62	0.25	0.86	1.8
SPR-03-04-CD61	<0.01	0.44	2.44	43.25	130.7	*	0.8	0.2	52	3.8	*	1.36	0.36	0.76	2.9
SPR-03-04-CD67	<0.01	0.3	2.02	36.19	124.5	184	1.2	0.1	17	3.6	*	0.86	0.44	0.61	2
SPR-03-04-CD70	<0.01	0.36	2.09	42.62	86.9	*	0.5	<0.1	17	0.9	*	1.04	0.27	0.19	2
SPR-05-04-CD80	<0.01	0.32	1.89	48.28	54.1	*	0.6	0.2	50	<0.1	*	1.85	0.31	0.43	2
SPR-01-04-SR49	<0.01	0.3	2.2	8.41	116.8	45	1	<0.1	18	0.2	<0.2	0.09	0.04	0.12	1.5
SPR-01-04-SR51	<0.01	0.35	3.13	31.77	227.9	20	0.5	<0.1	88	<0.1	0.5	0.38	0.2	0.22	1.8

ID	B	Tl	Hg	Se	Te	Ge	In	Re	Be	Li	Pd	Pt
Unit	**PPM**	**PPM**	**PPB**	**PPM**	**PPM**	**PPM**	**PPM**	**PPB**	**PPM**	**PPM**	**PPB**	**PPB**
SPR-01-04-CDU57	1	<0.02	<5	0.5	<0.02	0.2	0.15	<1	1	1.8	<10	<2
SPR-06-04-N83	<1	<0.02	<5	<0.1	<0.02	<0.1	<0.02	<1	0.1	1.1	<10	<2
SPR-06-04-N90	<1	<0.02	<5	<0.1	<0.02	<0.1	0.17	<1	1	3.1	<10	<2
SPR-31-03-CP32	2	0.07	<5	<0.1	<0.02	0.1	<0.02	<1	3.9	12.8	<10	<2
SPR-31-03-CP35	3	0.03	8	<0.1	<0.02	<0.1	<0.02	<1	3.8	7.9	<10	<2
SPR-31-03-CP36	<1	0.06	<5	<0.1	<0.02	0.1	<0.02	<1	5.6	9.6	<10	<2
SPR-31-03-CP39	5	<0.02	<5	<0.1	<0.02	0.1	<0.02	<1	<0.1	2.8	<10	9
SPR-31-03-CP45A	3	0.04	<5	0.2	<0.02	0.2	<0.02	<1	1.3	9.1	<10	4
SPR-07-04-CH92	<1	0.03	<5	<0.1	<0.02	0.3	0.09	2	0.4	0.7	<10	7
SPR-07-04-G95	<1	0.02	<5	<0.1	<0.02	<0.1	<0.02	<1	0.2	1.7	<10	<2
SPR-05-04-ML76	<1	<0.02	<5	<0.1	<0.02	0.3	0.15	<1	1.5	2.4	<10	<2
SPR-31-03-CD40	<1	0.1	<5	<0.1	0.05	<0.1	<0.02	<1	1.1	15.9	<10	<2
SPR-31-03-CD44	<1	0.25	<5	1.1	0.02	0.3	<0.02	<1	1.5	17.2	*	14
SPR-01-04-CD55	<1	0.29	<5	0.4	0.06	0.3	<0.02	<1	3.3	29.2	*	56
SPR-03-04-CD61	1	0.14	<5	0.2	0.09	0.1	<0.02	<1	3.2	20.1	*	41
SPR-03-04-CD67	<1	0.14	<5	<0.1	0.05	<0.1	<0.02	<1	1.3	6	*	35
SPR-03-04-CD70	<1	0.07	<5	0.1	0.08	0.1	<0.02	<1	1.5	17.1	*	25
SPR-05-04-CD80	<1	0.26	<5	0.8	0.11	0.6	<0.02	<1	2.9	10.2	*	29
SPR-01-04-SR49	<1	0.04	<5	<0.1	<0.02	0.1	<0.02	<1	0.9	2.4	<10	<2
SPR-01-04-SR51	<1	0.08	<5	0.3	<0.02	0.3	<0.02	<1	1.5	3.4	<10	5

APPENDIX 3: ELECTRON MICROPROBE DATA

Note: Data is sorted via rock type/mineral

Trachyandesite

Samples: SPR-31-03-CP29, SPR-31-03-CP32

Mineral	Cl	CaO	K2O	F	TiO2	P2O5	Na2O	SiO2	MgO	Al2O3	FeO	MnO	Cr2O3	NiO	TOTAL
Analcime	0.023	1.213	0.420	0.000	0.000	0.029	11.367	52.133	0.022	26.385	0.129	0.011	0.000	0.000	91.762
Analcime	0.010	0.051	0.290	0.000	0.000	0.009	11.827	55.656	0.000	23.911	0.119	0.000	0.000	0.000	91.904
Analcime	0.000	0.825	0.312	0.000	0.000	0.029	12.249	52.702	0.028	26.326	0.138	0.012	0.002	0.000	92.662
Analcime	0.000	0.123	0.351	0.000	0.000	0.021	12.077	55.913	0.043	24.601	0.193	0.000	0.000	0.000	93.323
Analcime	0.000	0.032	0.307	0.000	0.000	0.000	11.665	57.548	0.006	23.943	0.195	0.000	0.000	0.000	93.724
Anorthoclase	0.000	1.678	4.647	0.000	0.021	0.277	7.505	63.584	0.014	19.546	0.364	0.002	0.000	0.000	97.763
Oligoclase	0.003	3.635	1.665	0.000	0.023	0.000	8.277	61.962	0.007	22.408	0.247	0.023	0.000	0.004	98.474
Oligoclase	0.000	5.000	0.797	0.000	0.013	0.000	7.946	59.893	0.010	23.954	0.199	0.039	0.000	0.002	98.210
Oligoclase	0.000	5.001	0.801	0.000	0.010	0.005	7.774	59.247	0.021	24.231	0.170	0.037	0.014	0.018	97.737
Oligoclase	0.000	5.078	1.113	0.000	0.017	0.000	7.785	59.746	0.000	24.023	0.286	0.014	0.000	0.004	98.413
Oligoclase	0.011	5.669	1.009	0.000	0.011	0.018	7.416	58.885	0.011	24.251	0.223	0.000	0.015	0.000	97.803
Oligoclase	0.000	5.730	0.904	0.000	0.013	0.000	7.553	59.604	0.016	24.482	0.263	0.020	0.000	0.000	98.780
Oligoclase	0.004	5.874	0.880	0.000	0.022	0.002	7.547	59.011	0.000	24.439	0.223	0.000	0.010	0.001	98.246
Oligoclase	0.000	5.905	0.921	0.000	0.011	0.018	7.326	58.597	0.000	24.586	0.178	0.000	0.000	0.007	97.766
Oligoclase	0.000	6.026	0.983	0.000	0.008	0.006	7.116	58.386	0.023	24.865	0.296	0.013	0.000	0.005	97.977
Hedenbergite	0.000	21.333	0.051	0.009	0.559	0.416	0.941	47.888	5.125	2.296	19.359	1.168	0.000	0.005	99.155
Hedenbergite	0.006	20.884	0.040	0.021	0.382	0.051	0.991	48.431	5.988	1.833	18.181	1.295	0.011	0.005	98.135
Hedenbergite	0.003	20.544	0.040	0.000	0.307	0.015	1.196	48.410	4.490	1.815	20.405	1.526	0.000	0.000	98.754
Hedenbergite	0.015	22.712	0.052	0.000	0.541	2.205	0.970	47.405	5.023	2.266	18.968	1.180	0.000	0.000	101.358
Hedenbergite	0.005	22.266	0.028	0.000	0.728	1.557	0.895	45.854	5.325	2.580	18.920	1.175	0.000	0.000	99.338
Hedenbergite	0.003	21.085	0.043	0.000	0.554	0.035	0.883	48.230	5.153	2.460	19.433	1.192	0.000	0.005	99.077
Hedenbergite	0.006	21.674	0.014	0.000	0.423	0.058	0.659	48.123	5.113	1.381	20.524	1.325	0.016	0.004	99.326

Hedenbergite	0.003	21.218	0.017	0.000	0.759	0.058	0.954	47.060	4.747	2.857	20.449	1.210	0.000	0.002	99.374
Hedenbergite	0.010	21.187	0.032	0.000	0.551	0.594	0.801	46.447	3.791	2.261	21.344	1.398	0.024	0.000	98.458
Hedenbergite	0.006	21.209	0.025	0.000	0.661	0.095	0.902	47.631	4.899	2.765	20.377	1.183	0.000	0.000	99.751
Hedenbergite	0.000	21.436	0.035	0.000	0.362	0.215	0.614	47.924	5.068	1.343	19.781	1.333	0.020	0.010	98.166
Hedenbergite	0.001	21.036	0.020	0.000	0.548	0.008	0.850	47.980	5.432	2.342	19.068	1.217	0.010	0.000	98.546
Hedenbergite	0.000	20.432	0.051	0.000	0.341	0.034	1.114	50.168	5.887	1.897	18.757	1.305	0.000	0.000	100.005
Hedenbergite	0.000	21.016	0.023	0.000	0.664	0.140	0.985	48.846	5.785	2.304	19.155	1.240	0.000	0.000	100.179
Hedenbergite	0.000	21.917	0.022	0.009	0.333	0.230	0.586	48.805	5.453	1.233	19.528	1.350	0.000	0.007	99.475
Hedenbergite	0.000	21.286	0.006	0.000	0.663	0.019	0.849	47.449	4.926	2.783	20.124	1.164	0.000	0.018	99.314
Hedenbergite	0.019	22.077	0.111	0.036	0.475	1.717	0.988	46.289	4.523	2.187	19.331	1.334	0.000	0.009	99.142
Magnetite/Ulvöspinel	0.004	0.050	0.017	0.002	9.705	0.005	0.038	0.272	0.072	1.663	78.922	1.787	0.000	0.000	92.769
Magnetite/Ulvöspinel	0.000	0.167	0.008	0.000	9.715	0.012	0.048	0.329	0.096	1.873	77.904	1.847	0.000	0.000	92.141
Magnetite/Ulvöspinel	0.000	0.146	0.019	0.011	9.744	0.000	0.019	0.442	0.068	1.764	78.446	1.934	0.000	0.014	92.754
Magnetite/Ulvöspinel	0.003	0.834	0.010	0.055	9.747	0.481	0.029	0.321	0.107	1.728	77.510	1.742	0.000	0.000	92.770
Magnetite/Ulvöspinel	0.003	0.409	0.012	0.020	9.817	0.022	0.049	0.344	0.113	1.721	78.905	1.903	0.000	0.010	93.513
Magnetite/Ulvöspinel	0.015	0.961	0.018	0.034	9.818	0.800	0.036	0.557	0.098	1.782	77.448	1.823	0.000	0.000	93.545
Magnetite/Ulvöspinel	0.000	0.194	0.015	0.045	9.818	0.050	0.029	0.458	0.146	1.684	78.707	1.781	0.000	0.015	93.093
Magnetite/Ulvöspinel	0.000	0.122	0.024	0.000	9.823	0.043	0.057	0.367	0.109	1.923	78.374	1.795	0.000	0.000	92.808
Magnetite/Ulvöspinel	0.008	0.833	0.014	0.066	9.852	0.501	0.041	0.350	0.137	1.687	77.227	1.768	0.010	0.000	92.660
Magnetite/Ulvöspinel	0.000	0.183	0.032	0.000	9.882	0.106	0.025	0.384	0.119	1.780	78.352	1.805	0.009	0.000	92.839
Magnetite/Ulvöspinel	0.000	0.317	0.007	0.020	9.967	0.153	0.038	0.362	0.118	1.702	77.779	1.830	0.004	0.000	92.441
Magnetite/Ulvöspinel	0.001	0.397	0.014	0.004	9.987	0.367	0.068	0.614	0.136	1.751	76.876	1.819	0.014	0.000	92.222
Magnetite/Ulvöspinel	0.002	0.481	0.025	0.039	9.995	0.370	0.036	0.401	0.125	1.759	78.852	1.681	0.000	0.000	93.937
Magnetite/Ulvöspinel	0.004	0.044	0.029	0.000	9.995	0.018	0.033	0.326	0.074	1.832	78.149	1.804	0.000	0.000	92.470
Magnetite/Ulvöspinel	0.000	0.396	0.007	0.000	10.009	0.067	0.011	0.343	0.148	1.813	78.337	1.813	0.000	0.000	93.100
Magnetite/Ulvöspinel	0.000	0.107	0.015	0.000	10.018	0.028	0.022	0.327	0.109	1.786	78.409	1.860	0.000	0.000	92.809
Magnetite/Ulvöspinel	0.000	0.033	0.016	0.000	10.018	0.000	0.027	0.178	0.097	1.823	79.630	1.820	0.000	0.000	93.799
Magnetite/Ulvöspinel	0.016	0.677	0.019	0.011	10.057	0.619	0.067	0.361	0.108	1.803	78.414	1.859	0.000	0.005	94.169

Tephriphonolite

Samples: SPR-31-03-CP35

Mineral	Cl	CaO	K2O	F	TiO2	P2O5	Na2O	SiO2	MgO	Al2O3	FeO	MnO	Cr2O3	NiO	TOTAL
Natrolite	0.000	0.573	0.082	0.000	0.000	0.000	14.827	47.221	0.028	29.158	0.030	0.006	0.000	0.000	91.925
Natrolite	0.000	0.597	0.061	0.000	0.000	0.000	15.053	47.069	0.027	29.149	0.034	0.000	0.000	0.000	92.000
Natrolite	0.000	0.459	0.053	0.000	0.000	0.014	14.920	47.607	0.041	28.819	0.097	0.000	0.000	0.000	92.009
Natrolite	0.000	0.176	0.061	0.000	0.000	0.004	15.150	48.103	0.011	28.483	0.056	0.000	0.000	0.000	92.043
Natrolite	0.000	0.233	0.330	0.000	0.000	0.000	14.908	49.013	0.009	28.157	0.126	0.006	0.000	0.000	92.790
Natrolite	0.001	0.405	0.126	0.000	0.000	0.000	14.753	48.535	0.071	28.554	0.483	0.020	0.000	0.000	92.966
Natrolite	0.010	0.362	0.151	0.000	0.000	0.000	14.414	49.679	0.000	28.597	0.091	0.000	0.000	0.000	93.327
Natrolite	0.000	0.144	0.171	0.000	0.000	0.000	15.059	49.278	0.010	29.025	0.061	0.013	0.000	0.000	93.782
Oligoclase	0.000	5.658	0.716	0.000	0.014	0.007	7.492	59.053	0.015	24.691	0.191	0.000	0.000	0.015	98.053
Oligoclase	0.000	4.744	2.416	0.000	0.001	0.006	6.888	58.572	0.015	24.748	0.298	0.033	0.000	0.012	98.068
Oligoclase	0.000	4.787	0.853	0.000	0.016	0.000	8.093	60.562	0.018	23.664	0.223	0.014	0.001	0.029	98.540
Oligoclase	0.000	4.756	0.949	0.000	0.027	0.000	8.209	60.324	0.001	23.807	0.207	0.003	0.000	0.018	98.559
Anorthoclase	0.000	1.914	3.470	0.000	0.028	0.003	8.122	63.522	0.002	20.743	0.347	0.007	0.000	0.000	98.848
Anorthoclase	0.000	1.122	4.911	0.000	0.021	0.012	8.637	62.337	0.008	21.162	0.529	0.016	0.012	0.009	98.914
Anorthoclase	0.000	1.150	4.515	0.000	0.012	0.032	8.116	64.915	0.000	20.072	0.364	0.000	0.000	0.000	99.296
Anorthoclase	0.000	1.645	4.177	0.000	0.028	0.009	7.858	64.710	0.001	20.285	0.338	0.012	0.000	0.000	99.457
Natrolite Vein	0.001	0.226	0.118	0.000	0.000	0.009	15.175	48.058	0.008	28.822	0.017	0.008	0.000	0.000	92.442
Natrolite Vein	0.021	0.811	0.125	0.000	0.000	0.029	13.754	47.785	0.152	29.229	0.020	0.000	0.000	0.000	92.052
Natrolite Vein	0.001	0.207	0.084	0.000	0.000	0.000	15.145	47.672	0.037	28.672	0.005	0.000	0.000	0.000	91.833
Natrolite Vein	0.000	0.284	0.074	0.000	0.000	0.000	14.995	48.139	0.026	28.879	0.036	0.000	0.007	0.000	92.441
Hedenbergite	0.003	20.814	0.058	0.000	0.605	0.043	1.097	47.189	5.471	2.520	18.753	1.256	0.000	0.002	97.823
Hedenbergite	0.002	20.476	0.004	0.000	0.328	0.023	1.009	47.355	2.871	1.493	23.242	1.866	0.000	0.016	98.707
Hedenbergite	0.007	20.573	0.015	0.000	0.296	0.014	0.994	47.972	3.085	1.267	22.908	1.764	0.000	0.000	98.907
Hedenbergite	0.000	20.491	0.050	0.000	0.097	0.028	1.128	48.373	3.013	0.328	24.205	1.192	0.004	0.000	98.932
Hedenbergite	0.000	21.277	0.018	0.000	0.626	0.047	0.748	47.732	5.607	2.345	19.342	1.238	0.008	0.025	99.050
Hedenbergite	0.000	20.332	0.020	0.000	0.270	0.002	1.266	48.191	3.052	1.380	22.877	1.790	0.013	0.008	99.211

Hedenbergite	0.000	21.108	0.041	0.000	0.576	0.029	1.028	48.350	5.826	2.369	18.721	1.224	0.000	0.009	99.291
Hedenbergite	0.000	21.387	0.016	0.000	0.721	0.049	0.956	47.724	5.337	2.859	19.401	1.146	0.000	0.000	99.615
Hedenbergite	0.000	20.619	0.004	0.000	0.129	0.015	0.916	48.891	2.740	0.168	24.883	1.248	0.003	0.011	99.627
Hedenbergite	0.005	20.516	0.005	0.000	0.233	0.013	1.126	48.699	1.698	0.251	25.769	1.702	0.011	0.000	100.028
Hedenbergite	0.011	20.318	0.004	0.000	0.164	0.010	1.066	49.138	2.288	0.201	25.584	1.282	0.000	0.000	100.067
Magnetite/Ulvöspinel	0.001	0.289	0.763	0.080	7.064	0.005	1.831	9.203	0.076	3.941	70.587	1.558	0.000	0.000	95.514
Magnetite/Ulvöspinel	0.000	0.164	0.097	0.023	7.266	0.042	0.404	1.476	0.139	1.838	79.757	1.854	0.000	0.000	93.173
Magnetite/Ulvöspinel	0.000	0.137	0.028	0.008	7.889	0.002	0.254	0.548	0.083	1.291	79.658	2.089	0.000	0.000	92.177
Magnetite/Ulvöspinel	0.006	0.201	0.016	0.121	8.037	0.104	0.064	0.279	0.076	1.351	81.509	1.757	0.000	0.000	93.679
Magnetite/Ulvöspinel	0.004	0.050	0.016	0.000	8.194	0.023	0.034	0.135	0.097	1.511	81.811	1.837	0.000	0.000	93.872
Magnetite/Ulvöspinel	0.000	0.058	0.020	0.005	9.354	0.000	0.089	0.525	0.108	1.631	80.624	2.005	0.000	0.004	94.563
Magnetite/Ulvöspinel	0.000	0.547	0.027	0.033	9.534	0.431	0.070	0.168	0.083	1.609	80.167	2.036	0.000	0.000	94.879
Magnetite/Ulvöspinel	0.000	0.400	0.026	0.000	9.572	0.323	0.290	0.301	0.115	1.470	78.859	1.947	0.000	0.000	93.456
Magnetite/Ulvöspinel	0.002	0.031	0.011	0.000	9.589	0.016	0.063	0.303	0.135	1.590	80.252	1.941	0.000	0.000	94.092
Magnetite/Ulvöspinel	0.000	0.312	0.124	0.027	9.674	0.185	0.266	1.999	0.200	1.925	75.687	2.022	0.000	0.009	92.584
Magnetite/Ulvöspinel	0.008	0.050	0.023	0.042	9.862	0.007	0.078	0.219	0.112	1.468	80.056	1.944	0.006	0.000	94.075
Magnetite/Ulvöspinel	0.004	0.073	0.021	0.010	9.863	0.016	0.065	0.225	0.161	1.630	79.862	2.021	0.007	0.009	94.135
Magnetite/Ulvöspinel	0.009	0.161	0.013	0.000	10.212	0.059	0.123	0.248	0.220	1.509	79.401	2.082	0.000	0.006	94.225
Magnetite/Ulvöspinel	0.000	0.048	0.021	0.000	10.333	0.000	0.201	0.177	0.152	1.679	79.197	2.091	0.000	0.000	94.066
Magnetite/Ulvöspinel	0.000	0.053	0.016	0.000	10.859	0.009	0.155	0.413	0.141	1.551	76.904	2.033	0.011	0.000	92.291
Magnetite/Ulvöspinel	0.000	0.077	0.037	0.015	11.246	0.026	0.157	0.531	0.118	1.506	76.793	1.967	0.000	0.000	92.692

Trachybasalt

Samples: SPR-31-03-CP37, SPR-31-03-CP45A

Mineral	Cl	CaO	K2O	F	TiO2	P2O5	Na2O	SiO2	MgO	Al2O3	FeO	MnO	Cr2O3	NiO	TOTAL
Andesine	0.001	7.217	0.783	0.000	0.040	0.019	6.495	57.542	0.060	25.542	0.572	0.014	0.000	0.000	98.459
Andesine	0.000	6.809	0.648	0.000	0.041	0.008	7.183	59.262	0.020	25.525	0.565	0.000	0.000	0.000	100.248
Anorthoclase	0.006	1.604	5.513	0.000	0.000	0.000	7.045	64.176	0.015	20.162	0.176	0.004	0.000	0.000	98.843
Anorthoclase	0.005	1.078	5.828	0.000	0.006	0.018	7.083	64.699	0.013	19.789	0.147	0.000	0.000	0.000	98.707
Oligoclase	0.000	4.665	2.566	0.000	0.100	0.021	9.658	52.079	0.399	27.494	0.685	0.006	0.000	0.000	97.735
Oligoclase	0.000	5.247	1.360	0.000	0.175	0.042	8.198	61.310	0.091	24.406	0.568	0.000	0.000	0.000	101.662
Cr -Spinel	0.000	0.054	0.002	0.148	0.108	0.000	0.000	0.023	18.014	46.577	11.707	0.157	19.705	0.294	96.803
Cr -Spinel	0.000	0.012	0.000	0.158	0.118	0.011	0.001	0.032	15.936	46.451	16.947	0.330	19.278	0.236	99.511
Cr -Spinel	0.000	0.060	0.000	0.136	0.113	0.000	0.000	0.023	19.215	48.440	11.212	0.186	20.044	0.274	99.704
Cr -Spinel	0.002	0.037	0.008	0.139	0.161	0.004	0.015	0.048	13.547	46.095	20.288	0.410	19.080	0.238	100.072
Cr -Spinel	0.002	0.094	0.007	0.076	0.116	0.000	0.011	0.107	19.695	49.428	11.273	0.197	19.835	0.230	101.103
Diopside	0.002	20.921	0.019	0.058	4.914	0.552	0.689	40.939	9.954	8.989	13.324	0.238	0.016	0.012	100.699
Diopside	0.000	20.018	0.655	0.058	1.016	0.056	1.078	51.486	11.070	4.736	10.010	0.481	0.000	0.000	100.666
Diopside	0.000	21.885	0.001	0.019	0.301	0.017	1.183	53.358	16.051	4.264	2.299	0.090	0.919	0.037	100.423
Diopside	0.000	22.003	0.000	0.011	0.294	0.020	1.137	53.439	16.200	4.284	2.319	0.087	0.815	0.052	100.671
Diopside	0.000	22.111	0.001	0.031	0.296	0.006	1.141	53.475	16.206	4.254	2.400	0.079	0.821	0.053	100.874
Diopside	0.000	20.199	0.004	0.000	1.203	0.003	0.765	47.678	14.941	7.765	5.404	0.123	0.538	0.027	98.695
Diopside	0.000	19.872	0.000	0.000	1.619	0.015	0.868	46.785	14.209	8.696	5.506	0.117	0.329	0.020	98.053
Diopside	0.005	21.430	0.025	0.000	1.139	0.023	1.009	47.454	12.469	8.217	7.071	0.143	0.083	0.000	99.092
Diopside	0.000	21.829	0.000	0.000	1.953	0.042	0.542	47.150	13.628	6.003	7.243	0.148	0.331	0.000	98.921
Diopside	0.000	21.547	0.000	0.000	1.321	0.057	1.101	47.445	12.092	7.613	7.189	0.197	0.038	0.033	98.634
Diopside	0.000	21.883	0.000	0.000	1.647	0.013	0.680	47.675	13.572	6.278	6.981	0.137	0.453	0.000	99.371
Diopside	0.000	20.561	0.000	0.000	1.355	0.044	0.729	47.325	14.378	8.241	5.458	0.104	0.686	0.026	98.927
Diopside	0.000	19.111	0.102	0.000	0.675	0.025	0.718	50.465	16.825	5.228	5.191	0.122	0.608	0.006	99.076
Diopside	0.000	18.136	0.003	0.000	0.652	0.023	0.921	51.012	17.685	4.928	5.344	0.105	0.417	0.041	99.284

Diopside	0.000	21.879	0.000	0.000	2.084	0.101	0.450	47.261	13.480	5.744	7.596	0.139	0.154	0.000	98.914
Diopside	0.000	21.024	0.007	0.000	3.875	0.022	0.689	43.738	12.743	12.096	5.172	0.057	0.033	0.028	99.544
Diopside	0.000	19.911	0.012	0.000	1.188	0.033	0.722	48.272	14.853	7.285	5.345	0.117	0.651	0.002	98.428
Diopside	0.004	21.817	0.019	0.000	2.035	0.057	0.576	47.283	12.829	5.579	8.992	0.241	0.000	0.000	99.448
Diopside	0.000	20.951	0.040	0.000	0.410	0.028	1.524	52.101	11.760	2.441	9.193	0.276	0.026	0.018	98.767
Diopside	0.002	21.319	0.008	0.000	0.265	0.014	0.960	50.897	16.362	5.406	3.051	0.114	0.697	0.039	99.164
Diopside	0.004	19.679	0.080	0.000	1.374	0.028	2.062	51.067	12.311	6.065	6.764	0.215	0.014	0.002	99.693
Enstatite	0.000	0.557	0.004	0.063	0.072	0.012	0.050	56.597	34.188	2.980	5.997	0.154	0.448	0.069	101.198
Magnetite/Ulvöspinel	0.007	0.131	0.009	0.274	12.304	0.005	0.039	0.160	1.583	1.802	76.363	1.187	0.021	0.013	94.053
Magnetite/Ulvöspinel	0.000	0.036	0.004	0.364	12.359	0.000	0.027	0.053	1.386	1.983	77.207	1.319	0.018	0.013	94.938
Magnetite/Ulvöspinel	0.006	0.397	0.012	0.324	12.407	0.000	0.032	0.089	1.573	1.890	75.384	1.239	0.049	0.000	93.558
Magnetite/Ulvöspinel	0.000	0.107	0.034	0.324	12.836	0.012	0.037	0.226	1.432	1.737	75.151	1.168	0.057	0.102	93.497
Magnetite/Ulvöspinel	0.009	0.056	0.119	0.000	17.106	0.042	0.468	1.365	3.425	3.765	63.852	0.763	6.209	0.048	97.527
Magnetite/Ulvöspinel	0.000	0.122	0.022	0.000	17.579	0.040	0.028	0.973	3.106	1.713	70.960	0.901	0.051	0.019	95.827
Magnetite/Ulvöspinel	0.000	0.139	0.008	0.343	17.918	0.011	0.051	0.070	2.168	1.666	71.636	1.112	0.050	0.041	95.477
Magnetite/Ulvöspinel	0.011	0.128	0.102	0.028	17.997	0.000	0.202	1.177	3.281	3.102	63.516	0.804	4.611	0.032	95.341
Magnetite/Ulvöspinel	0.011	0.061	0.066	0.000	18.278	0.000	0.161	0.707	3.292	2.827	64.902	0.744	5.486	0.021	96.853
Magnetite/Ulvöspinel	0.006	1.107	0.017	0.167	18.411	0.797	0.010	0.250	2.543	2.104	65.274	0.847	3.255	0.010	95.096
Magnetite/Ulvöspinel	0.000	0.071	0.000	0.350	18.524	0.000	0.032	0.061	3.251	2.051	69.696	0.773	0.137	0.025	95.230
Magnetite/Ulvöspinel	0.002	0.171	0.014	0.000	19.954	0.018	0.033	0.090	2.903	1.871	68.441	0.912	1.880	0.013	96.647
Magnetite/Ulvöspinel	0.000	0.165	0.028	0.000	20.269	0.003	0.076	0.451	2.860	1.690	67.858	0.920	0.244	0.053	95.024
Magnetite/Ulvöspinel	0.018	1.515	0.043	0.094	20.395	1.180	0.073	0.908	2.914	2.050	63.764	0.889	0.888	0.039	95.103
Magnetite/Ulvöspinel	0.003	0.097	0.081	0.021	20.462	0.017	0.246	1.111	3.817	2.583	63.702	0.838	3.725	0.027	97.059
Magnetite/Ulvöspinel	0.000	0.296	0.010	0.000	20.715	0.012	0.066	0.518	3.134	1.955	67.170	0.947	0.042	0.010	95.210
Magnetite/Ulvöspinel	0.018	2.405	0.026	0.387	20.992	1.847	0.032	0.716	2.221	1.708	63.469	0.988	0.115	0.036	95.263
Magnetite/Ulvöspinel	0.006	0.090	0.024	0.000	21.056	0.000	0.016	0.262	3.264	2.017	67.929	0.863	0.911	0.015	96.843
Magnetite/Ulvöspinel	0.001	0.175	0.055	0.328	21.082	0.012	0.032	0.104	2.470	1.524	67.346	0.910	0.273	0.040	94.644
Magnetite/Ulvöspinel	0.000	0.333	0.010	0.000	21.431	0.138	0.033	0.164	3.096	1.811	68.037	0.954	0.101	0.030	96.530
Magnetite/Ulvöspinel	0.003	0.155	0.014	0.000	21.745	0.062	0.008	0.073	2.756	1.887	68.652	0.945	0.080	0.098	96.888

Olivine	0.005	2.128	0.072	0.199	0.085	1.265	0.036	36.047	28.489	1.698	28.917	0.915	0.001	0.022	99.878
Olivine	0.002	0.356	0.011	0.158	0.055	0.035	0.000	37.041	32.069	0.074	29.476	1.004	0.000	0.088	100.370
Olivine	0.000	0.338	0.003	0.003	0.047	0.062	0.030	37.221	33.611	0.180	27.859	0.732	0.000	0.042	100.130
Olivine	0.000	0.264	0.012	0.116	0.040	0.039	0.009	38.230	34.828	0.222	26.139	0.693	0.007	0.095	100.696
Olivine	0.000	0.210	0.008	0.112	0.034	0.017	0.009	38.051	35.902	0.039	25.533	0.622	0.004	0.059	100.599
Olivine	0.000	0.209	0.000	0.011	0.017	0.033	0.017	37.120	37.865	0.020	23.841	0.542	0.003	0.115	99.809
Olivine	0.007	0.152	0.000	0.000	0.015	0.008	0.005	37.435	40.382	0.045	20.665	0.279	0.018	0.036	99.089
Olivine	0.001	0.205	0.004	0.109	0.023	0.002	0.010	39.432	41.575	0.032	19.583	0.352	0.016	0.122	101.470
Olivine	0.000	0.107	0.002	0.016	0.026	0.024	0.000	38.278	41.591	0.044	19.288	0.199	0.014	0.067	99.673
Olivine	0.002	0.119	0.000	0.003	0.025	0.011	0.007	38.740	41.712	0.017	19.208	0.238	0.019	0.047	100.155
Olivine	0.000	0.178	0.000	0.012	0.013	0.042	0.010	39.240	44.076	0.049	16.096	0.168	0.014	0.115	100.024
Olivine	0.003	0.106	0.000	0.000	0.023	0.017	0.012	38.304	44.898	0.074	14.821	0.255	0.010	0.351	98.876
Olivine	0.000	0.027	0.009	0.072	0.005	0.014	0.003	41.175	49.667	0.002	9.666	0.136	0.000	0.372	101.153
Olivine	0.000	0.030	0.000	0.064	0.000	0.022	0.000	41.533	49.984	0.007	9.558	0.135	0.010	0.372	101.714
Olivine Traverse 1	0.000	0.242	0.008	0.132	0.042	0.020	0.012	38.401	36.196	0.039	24.457	0.615	0.000	0.097	100.263
Olivine Traverse 1	0.000	0.161	0.000	0.071	0.033	0.072	0.012	40.052	44.568	0.044	15.521	0.223	0.016	0.232	101.024
Olivine Traverse 1	0.000	0.155	0.004	0.066	0.016	0.049	0.025	40.183	44.898	0.040	14.814	0.217	0.011	0.224	100.702
Olivine Traverse 1	0.000	0.220	0.025	0.149	0.048	0.001	0.015	38.908	38.896	0.243	20.677	0.429	0.007	0.150	99.809
Olivine Traverse 1	0.001	0.396	0.008	0.155	0.236	0.042	0.022	37.295	32.148	0.746	28.574	0.798	0.000	0.035	100.470
Olivine Traverse 1	0.009	2.701	0.590	0.012	0.170	0.307	1.046	39.135	24.671	4.526	22.443	0.658	0.005	0.016	96.370
Olivine Traverse 1	0.008	0.172	0.000	0.007	0.035	0.019	0.014	37.965	37.973	0.026	23.292	0.465	0.000	0.075	100.083
Olivine Traverse 1	0.000	0.150	0.000	0.000	0.029	0.006	0.002	38.112	39.343	0.015	21.829	0.362	0.000	0.011	99.877
Olivine Traverse 1	0.000	0.181	0.000	0.004	0.034	0.027	0.000	38.584	40.378	0.021	20.854	0.265	0.000	0.078	100.426
Olivine Traverse 1	0.009	0.157	0.000	0.009	0.028	0.002	0.000	38.599	40.627	0.032	20.512	0.248	0.015	0.074	100.322
Olivine Traverse 1	0.000	0.142	0.008	0.000	0.022	0.000	0.000	38.801	41.044	0.018	20.342	0.228	0.002	0.058	100.663
Olivine Traverse 1	0.000	0.138	0.000	0.025	0.005	0.000	0.000	38.578	40.772	0.023	20.308	0.279	0.000	0.062	100.196
Olivine Traverse 1	0.000	0.289	0.000	0.000	0.014	0.020	0.002	38.510	40.933	0.038	20.042	0.313	0.023	0.078	100.262
Olivine Traverse 1	0.000	0.225	0.008	0.000	0.021	0.014	0.000	38.289	40.832	0.030	20.503	0.271	0.000	0.046	100.238
Olivine Traverse 1	0.000	0.231	0.004	0.000	0.034	0.010	0.002	37.631	39.155	0.030	20.902	0.368	0.000	0.065	98.447

Olivine Traverse 2	0.000	0.265	0.008	0.147	0.030	0.014	0.006	37.396	33.473	0.038	28.183	0.828	0.005	0.078	100.471
Olivine Traverse 2	0.000	0.175	0.002	0.064	0.017	0.016	0.021	40.096	44.347	0.063	15.758	0.258	0.035	0.209	101.078
Olivine Traverse 2	0.000	0.163	0.000	0.096	0.017	0.044	0.011	40.169	46.002	0.065	13.920	0.175	0.053	0.230	100.946
Olivine Traverse 2	0.000	0.185	0.000	0.076	0.008	0.041	0.016	40.176	45.569	0.061	14.366	0.172	0.054	0.230	100.956
Olivine Traverse 2	0.000	5.619	0.061	0.142	0.233	0.034	0.218	41.297	25.060	0.962	24.352	0.847	0.002	0.066	98.920
Olivine Traverse 2	0.000	0.268	0.003	0.000	0.027	0.020	0.018	37.657	38.044	0.041	22.697	0.520	0.004	0.106	99.404
Olivine Traverse 2	0.000	0.127	0.000	0.008	0.004	0.016	0.021	39.311	45.667	0.042	14.265	0.162	0.000	0.236	99.897
Olivine Traverse 2	0.002	0.114	0.002	0.008	0.009	0.025	0.013	38.670	45.270	0.021	14.030	0.185	0.003	0.229	98.603
Olivine Traverse 2	0.000	0.128	0.000	0.000	0.007	0.012	0.024	39.778	46.271	0.042	13.835	0.176	0.000	0.271	100.544
Olivine Traverse 2	0.006	0.123	0.000	0.032	0.011	0.011	0.008	39.524	45.329	0.040	13.962	0.207	0.010	0.221	99.498
Olivine Traverse 2	0.000	0.325	0.135	0.000	0.017	0.004	0.014	41.103	39.220	2.141	14.844	0.150	0.000	0.214	98.179
Olivine Traverse 2	0.000	0.134	0.000	0.000	0.009	0.020	0.017	39.138	45.051	0.039	13.467	0.184	0.007	0.226	98.311
Olivine Traverse 2	0.009	0.296	0.019	0.000	0.045	0.007	0.012	39.468	39.260	0.657	20.171	0.428	0.027	0.127	100.526
Olivine Traverse 3	0.000	0.065	0.000	0.106	0.003	0.001	0.000	39.421	41.502	0.017	19.044	0.387	0.000	0.262	100.808
Olivine Traverse 3	0.004	0.047	0.004	0.046	0.000	0.000	0.000	41.228	49.216	0.031	10.001	0.142	0.002	0.377	101.111
Olivine Traverse 3	0.000	0.046	0.004	0.042	0.005	0.005	0.000	41.330	49.160	0.020	10.047	0.126	0.015	0.412	101.214
Olivine Traverse 3	0.000	0.046	0.003	0.026	0.004	0.000	0.007	41.456	49.435	0.019	9.947	0.151	0.019	0.391	101.514
Olivine Traverse 3	0.000	0.060	0.000	0.040	0.007	0.006	0.000	42.192	50.040	0.031	9.993	0.138	0.000	0.355	102.862
Olivine Traverse 3	0.000	22.369	0.002	0.000	0.205	0.006	0.683	53.195	16.820	4.463	2.750	0.060	0.567	0.062	101.182
Olivine Traverse 3	0.000	22.572	0.000	0.003	0.261	0.017	0.666	52.987	16.619	4.687	2.858	0.114	0.561	0.040	101.384
Olivine Traverse 3.1	0.000	0.096	0.004	0.000	0.005	0.006	0.000	38.349	42.161	0.024	16.892	0.341	0.000	0.323	98.201
Olivine Traverse 3.1	0.000	0.050	0.003	0.000	0.000	0.009	0.000	40.161	49.636	0.009	9.521	0.158	0.015	0.352	99.926
Olivine Traverse 3.1	0.003	0.046	0.000	0.000	0.000	0.010	0.000	40.462	48.823	0.000	9.203	0.151	0.000	0.411	99.110
Olivine Traverse 3.1	0.007	0.088	0.000	0.000	0.000	0.000	0.012	39.791	48.554	0.075	9.563	0.138	0.002	0.381	98.611
Olivine Traverse 3.1	0.000	0.066	0.001	0.000	0.000	0.007	0.021	41.371	50.357	0.041	9.608	0.126	0.000	0.360	101.980
Olivine Traverse 3.1	0.000	0.071	0.010	0.000	0.000	0.006	0.007	40.376	48.822	0.059	10.427	0.142	0.000	0.369	100.289
Olivine Traverse 3.2	0.000	0.116	0.012	0.000	0.014	0.014	0.025	37.994	38.753	0.055	21.796	0.510	0.000	0.174	99.484
Olivine Traverse 3.2	0.000	0.074	0.010	0.000	0.002	0.016	0.008	40.109	48.021	0.035	11.187	0.176	0.002	0.346	99.987
Olivine Traverse 3.2	0.000	0.067	0.000	0.000	0.003	0.020	0.021	40.348	48.791	0.057	9.482	0.148	0.000	0.378	99.318

Olivine Traverse 3.2	0.000	0.060	0.007	0.000	0.016	0.000	0.023	40.692	49.392	0.030	9.597	0.159	0.017	0.336	100.329
Olivine Traverse 3.2	0.000	0.055	0.002	0.000	0.006	0.000	0.010	40.952	49.690	0.049	9.720	0.133	0.000	0.333	100.949
Olivine Traverse 3.2	0.000	0.062	0.006	0.000	0.000	0.000	0.002	39.974	49.297	0.029	9.539	0.164	0.000	0.375	99.475
Olivine Traverse 3.2	0.003	0.088	0.000	0.000	0.007	0.012	0.006	40.518	49.575	0.033	9.465	0.143	0.005	0.405	100.267
Olivine Traverse 3.2	0.000	0.099	0.000	0.000	0.022	0.030	0.023	39.804	49.134	0.107	9.578	0.151	0.003	0.380	99.354
Olivine Traverse 3.2	0.003	5.941	0.030	0.000	0.509	0.111	0.153	40.621	30.736	0.954	20.448	0.547	0.000	0.109	100.163
Olivine Traverse 4	0.000	0.391	0.004	0.015	0.069	0.069	0.093	36.548	32.939	0.232	28.446	0.774	0.000	0.037	99.642
Olivine Traverse 4	0.004	0.059	0.006	0.000	0.002	0.009	0.012	38.818	46.194	0.031	12.527	0.176	0.011	0.350	98.205
Olivine Traverse 4	0.002	0.122	0.015	0.000	0.017	0.018	0.016	39.250	45.802	0.101	12.921	0.275	0.010	0.429	99.108
Olivine Traverse 4	0.000	0.286	0.008	0.038	0.045	0.032	0.002	36.524	34.706	0.050	26.029	0.687	0.007	0.119	98.562
Olivine Traverse 5	0.000	0.117	0.000	0.017	0.033	0.000	0.008	37.987	39.871	0.007	21.195	0.496	0.003	0.166	99.900
Olivine Traverse 5	0.001	0.053	0.000	0.000	0.000	0.000	0.011	40.133	48.781	0.016	10.864	0.146	0.022	0.371	100.439
Olivine Traverse 5	0.000	0.061	0.009	0.000	0.016	0.010	0.016	40.484	49.503	0.076	10.273	0.152	0.018	0.389	101.030
Olivine Traverse 5	0.000	0.051	0.000	0.000	0.009	0.000	0.017	40.619	49.410	0.009	10.247	0.146	0.003	0.395	100.951
Olivine Traverse 5	0.000	0.054	0.000	0.000	0.000	0.012	0.009	40.887	50.014	0.028	9.971	0.146	0.000	0.360	101.479
Olivine Traverse 5	0.000	0.049	0.002	0.003	0.000	0.003	0.003	40.247	48.941	0.010	9.968	0.156	0.000	0.341	99.728
Olivine Traverse 5	0.001	0.046	0.001	0.000	0.000	0.000	0.004	40.490	49.154	0.013	10.015	0.162	0.021	0.356	100.277
Olivine Traverse 5	0.000	0.057	0.006	0.000	0.000	0.002	0.004	40.621	49.450	0.013	10.095	0.126	0.000	0.333	100.711
Olivine Traverse 5	0.000	0.044	0.002	0.000	0.000	0.008	0.000	40.384	49.026	0.008	10.089	0.122	0.002	0.376	100.084
Olivine Traverse 5	0.000	0.062	0.000	0.018	0.000	0.000	0.000	40.735	49.197	0.005	10.132	0.172	0.004	0.356	100.698
Olivine Traverse 5	0.000	0.052	0.000	0.000	0.006	0.001	0.000	40.422	49.435	0.006	9.987	0.174	0.001	0.415	100.531
Olivine Traverse 5	0.000	0.064	0.000	0.000	0.013	0.008	0.008	40.478	49.589	0.006	10.011	0.132	0.000	0.394	100.716
Olivine Traverse 5	0.000	0.087	0.003	0.000	0.006	0.005	0.040	41.183	49.514	0.066	10.002	0.138	0.000	0.362	101.418
Olivine Traverse 6	0.000	0.214	0.004	0.004	0.030	0.009	0.000	38.598	38.518	0.034	23.170	0.580	0.006	0.120	101.297
Olivine Traverse 6	0.000	0.091	0.000	0.000	0.012	0.002	0.005	39.202	43.529	0.039	17.053	0.370	0.007	0.245	100.576
Olivine Traverse 6	0.004	0.048	0.000	0.000	0.020	0.001	0.004	40.056	47.763	0.020	12.242	0.195	0.001	0.388	100.743
Olivine Traverse 6	0.005	0.046	0.000	0.004	0.007	0.000	0.000	40.318	49.159	0.016	10.219	0.183	0.000	0.381	100.352
Olivine Traverse 6	0.005	0.042	0.000	0.000	0.000	0.000	0.014	40.476	49.846	0.007	9.804	0.135	0.000	0.416	100.746
Olivine Traverse 6	0.004	0.043	0.000	0.000	0.008	0.010	0.009	39.634	50.639	0.130	9.805	0.157	0.000	0.404	100.867

Olivine Traverse 6	0.000	0.053	0.000	0.001	0.002	0.010	0.012	38.711	49.918	0.074	9.678	0.132	0.000	0.417	99.020
Olivine Traverse 6	0.003	0.069	0.000	0.000	0.006	0.008	0.033	37.982	50.305	0.082	9.329	0.096	0.000	0.379	98.319
Olivine Traverse 6	0.000	0.071	0.000	0.000	0.006	0.003	0.041	40.385	49.667	0.090	9.623	0.154	0.010	0.372	100.428
Olivine Traverse 6	0.001	0.042	0.000	0.000	0.001	0.000	0.000	40.153	49.502	0.002	9.701	0.166	0.031	0.343	99.953
Olivine Traverse 6	0.000	0.056	0.000	0.000	0.003	0.017	0.002	40.402	49.441	0.001	9.654	0.162	0.000	0.417	100.177
Olivine Traverse 6	0.000	0.043	0.000	0.000	0.009	0.013	0.003	40.040	48.923	0.032	9.641	0.172	0.000	0.384	99.276
Olivine Traverse 6	0.003	0.077	0.002	0.000	0.008	0.016	0.003	40.736	49.151	0.027	10.922	0.186	0.001	0.376	101.515
Olivine Traverse 6	0.000	0.089	0.002	0.000	0.016	0.000	0.006	39.591	45.199	0.025	15.243	0.229	0.000	0.319	100.718
Olivine Traverse 7	0.000	0.064	0.003	0.000	0.009	0.001	0.000	39.452	48.451	0.009	9.856	0.143	0.003	0.373	98.364
Olivine Traverse 7	0.000	0.036	0.007	0.000	0.000	0.000	0.005	40.323	49.422	0.003	9.858	0.149	0.001	0.320	100.124
Olivine Traverse 7	0.000	0.061	0.000	0.000	0.000	0.007	0.007	40.043	48.864	0.034	9.825	0.155	0.012	0.377	99.383
Olivine Traverse 7	0.000	0.039	0.000	0.004	0.013	0.000	0.007	40.364	49.323	0.031	9.753	0.133	0.029	0.379	100.074
Olivine Traverse 7	0.000	0.037	0.007	0.000	0.013	0.000	0.000	39.869	49.219	0.005	9.660	0.163	0.000	0.350	99.322
Olivine Traverse 7	0.000	0.052	0.004	0.000	0.000	0.000	0.010	41.008	50.745	0.005	9.709	0.173	0.007	0.349	102.066
Olivine Traverse 7	0.001	0.164	0.001	0.005	0.009	0.011	0.019	37.682	39.124	0.017	21.631	0.519	0.000	0.172	99.404
Olivine Traverse 8	0.003	0.089	0.000	0.000	0.000	0.003	0.002	40.107	49.002	0.042	9.877	0.148	0.000	0.381	99.659
Olivine Traverse 8	0.000	0.091	0.000	0.010	0.002	0.001	0.011	39.328	48.050	0.038	10.073	0.159	0.000	0.407	98.198
Olivine Traverse 8	0.000	0.100	0.000	0.000	0.002	0.000	0.014	40.323	48.792	0.027	10.014	0.165	0.000	0.382	99.825
Olivine Traverse 8	0.000	0.085	0.004	0.000	0.005	0.030	0.010	40.495	49.696	0.062	9.868	0.146	0.014	0.425	100.857
Olivine Traverse 8	0.000	0.116	0.008	0.000	0.007	0.002	0.023	41.079	50.209	0.074	9.896	0.144	0.009	0.353	101.938
Olivine Traverse 8	0.000	0.955	0.001	0.000	0.012	0.021	0.017	39.240	47.145	0.073	10.114	0.146	0.000	0.341	98.111
Olivine Traverse 8	0.002	0.082	0.003	0.000	0.023	0.000	0.000	39.309	46.494	0.039	13.664	0.208	0.000	0.298	100.130
Olivine Traverse 8	0.009	0.241	0.007	0.018	0.035	0.043	0.031	37.276	36.863	0.122	23.725	0.548	0.000	0.117	99.078
Olivine Traverse 9	0.000	0.205	0.006	0.033	0.027	0.000	0.011	39.158	41.463	0.083	20.248	0.331	0.009	0.065	101.661
Olivine Traverse 9	0.000	0.180	0.000	0.000	0.022	0.000	0.012	38.567	42.411	0.084	18.237	0.197	0.000	0.096	99.805
Olivine Traverse 9	0.001	0.170	0.002	0.000	0.019	0.000	0.023	38.347	41.834	0.084	18.175	0.217	0.000	0.039	98.911
Olivine Traverse 9	0.005	0.185	0.003	0.003	0.015	0.004	0.023	38.152	41.303	0.086	18.258	0.243	0.000	0.044	98.329
Olivine Traverse 9	0.000	0.197	0.000	0.000	0.023	0.000	0.026	39.716	43.810	0.079	17.857	0.227	0.000	0.065	102.022
Olivine Traverse 9	0.000	0.210	0.004	0.000	0.026	0.025	0.022	38.998	43.155	0.082	17.316	0.256	0.028	0.083	100.228

Olivine Traverse 9	0.000	0.226	0.010	0.000	0.009	0.024	0.029	38.976	44.345	0.067	15.416	0.225	0.042	0.114	99.497
Olivine Traverse 9	0.000	0.216	0.000	0.000	0.037	0.007	0.002	38.560	43.260	0.050	16.195	0.227	0.028	0.103	98.713
Olivine Traverse 9	0.002	0.363	0.058	0.000	0.060	0.029	0.025	37.975	35.900	1.359	22.970	0.512	0.000	0.066	99.359
Olivine Traverse 10	0.000	0.188	0.000	0.000	0.023	0.025	0.011	37.909	39.755	0.064	21.030	0.490	0.000	0.188	99.698
Olivine Traverse 10	0.000	0.171	0.036	0.000	0.060	0.035	0.021	42.662	45.507	0.639	10.832	0.124	0.023	0.331	100.456
Olivine Traverse 10	0.000	0.034	0.000	0.000	0.000	0.000	0.006	39.736	49.831	0.002	9.811	0.141	0.000	0.419	99.984
Olivine Traverse 10	0.014	0.422	0.033	0.000	0.357	0.025	0.054	40.584	45.220	1.076	10.340	0.130	0.000	0.865	99.418
Olivine Traverse 10	0.000	0.026	0.000	0.000	0.005	0.000	0.000	39.610	49.201	0.001	9.988	0.119	0.000	0.402	99.398
Olivine Traverse 10	0.000	0.055	0.002	0.000	0.004	0.000	0.012	40.096	49.385	0.050	9.840	0.152	0.000	0.390	100.012
Olivine Traverse 10	0.004	0.069	0.000	0.016	0.003	0.032	0.006	39.277	48.256	0.005	10.092	0.140	0.006	0.377	98.308
Olivine Traverse 10	0.000	0.041	0.004	0.000	0.000	0.000	0.009	39.815	49.972	0.008	10.004	0.146	0.005	0.367	100.392
Olivine Traverse 10	0.000	0.050	0.000	0.000	0.000	0.000	0.000	40.734	50.012	0.013	10.014	0.142	0.000	0.347	101.315
Olivine Traverse 10	0.000	0.079	0.000	0.000	0.000	0.000	0.001	39.909	48.987	0.002	10.605	0.160	0.000	0.420	100.163

Peridotite

Samples: SPR-31-03-CP45A

Mineral	Cl	CaO	K2O	F	TiO2	P2O5	Na2O	SiO2	MgO	Al2O3	FeO	MnO	Cr2O3	NiO	TOTAL
Olivine	0.005	0.081	0.000	0.090	0.001	0.000	0.014	39.994	43.436	0.025	16.927	0.280	0.013	0.338	101.207
Olivine	0.000	0.074	0.000	0.092	0.000	0.003	0.006	39.853	43.498	0.023	17.078	0.271	0.007	0.316	101.232
Olivine	0.000	0.082	0.003	0.107	0.003	0.014	0.008	39.887	43.752	0.037	16.827	0.264	0.019	0.346	101.361
Olivine	0.000	0.079	0.001	0.084	0.002	0.021	0.003	39.937	43.756	0.026	16.644	0.291	0.004	0.325	101.184
Olivine	0.005	0.121	0.000	0.108	0.026	0.011	0.002	39.034	43.827	0.020	17.173	0.301	0.018	0.362	101.031
Olivine	0.005	0.069	0.000	0.069	0.000	0.021	0.012	39.069	43.858	0.025	16.966	0.282	0.000	0.355	100.732
Olivine	0.000	0.078	0.003	0.076	0.000	0.007	0.008	40.168	43.879	0.030	16.440	0.283	0.011	0.339	101.332
Olivine	0.001	0.073	0.000	0.116	0.000	0.000	0.014	40.084	44.044	0.026	16.551	0.277	0.020	0.350	101.556
Olivine	0.001	0.075	0.000	0.075	0.002	0.000	0.022	40.346	44.175	0.028	16.363	0.260	0.004	0.334	101.685
Olivine	0.000	0.073	0.000	0.077	0.000	0.019	0.008	39.280	44.377	0.012	16.959	0.302	0.018	0.301	101.430
Olivine	0.000	0.070	0.003	0.072	0.000	0.000	0.000	40.078	44.612	0.026	15.606	0.260	0.010	0.342	101.094
Olivine	0.000	0.077	0.000	0.092	0.010	0.004	0.004	40.490	44.760	0.022	15.825	0.268	0.000	0.315	101.871

Olivine	0.003	0.078	0.000	0.116	0.000	0.000	0.018	39.387	45.075	0.037	15.088	0.242	0.014	0.310	100.368
Olivine	0.004	0.058	0.002	0.078	0.000	0.027	0.018	39.467	45.124	0.022	15.002	0.218	0.013	0.293	100.325
Olivine	0.000	0.079	0.000	0.080	0.000	0.015	0.000	39.627	45.313	0.018	15.030	0.276	0.020	0.347	100.804
Olivine	0.000	0.081	0.000	0.096	0.000	0.025	0.013	39.708	45.321	0.032	15.270	0.256	0.012	0.319	101.153
Olivine	0.000	0.062	0.000	0.078	0.006	0.012	0.000	39.443	45.578	0.033	15.316	0.223	0.005	0.327	101.086
Olivine	0.005	0.072	0.002	0.094	0.004	0.012	0.002	39.650	46.651	0.020	13.887	0.225	0.000	0.350	100.972
Olivine	0.000	0.078	0.000	0.065	0.000	0.006	0.008	39.863	46.892	0.024	13.345	0.202	0.001	0.331	100.816
Olivine	0.000	0.063	0.000	0.063	0.020	0.015	0.011	39.939	47.195	0.024	12.539	0.163	0.009	0.371	100.414
Olivine	0.000	0.080	0.000	0.066	0.006	0.000	0.007	40.090	47.319	0.029	12.524	0.250	0.004	0.373	100.747
Olivine	0.007	0.061	0.006	0.069	0.000	0.013	0.006	39.839	47.478	0.018	13.047	0.221	0.002	0.374	101.140
Olivine	0.000	0.031	0.000	0.035	0.004	0.004	0.009	39.254	47.824	0.025	10.163	0.138	0.000	0.383	97.870
Olivine	0.004	0.074	0.000	0.059	0.000	0.000	0.000	39.829	47.866	0.032	12.113	0.193	0.000	0.384	100.572
Olivine	0.005	0.068	0.000	0.074	0.003	0.000	0.027	39.740	47.936	0.027	12.517	0.178	0.000	0.368	100.944
Olivine	0.006	0.060	0.002	0.026	0.005	0.024	0.006	40.054	48.765	0.019	10.139	0.167	0.010	0.341	99.634
Olivine	0.009	0.086	0.002	0.055	0.009	0.004	0.043	39.786	48.766	0.036	9.972	0.144	0.000	0.372	99.300
Olivine	0.000	0.058	0.022	0.040	0.001	0.009	0.092	40.385	48.846	0.220	10.133	0.151	0.000	0.362	100.325
Olivine	0.003	0.051	0.012	0.058	0.001	0.004	0.017	40.079	48.898	0.018	10.056	0.162	0.026	0.360	99.753
Olivine	0.001	0.067	0.018	0.070	0.000	0.004	0.054	39.847	49.136	0.049	10.217	0.171	0.002	0.398	100.032
Olivine	0.006	0.022	0.000	0.070	0.000	0.000	0.001	40.425	49.192	0.038	10.199	0.125	0.001	0.346	100.429
Olivine	0.001	0.055	0.014	0.045	0.003	0.000	0.010	40.321	49.263	0.041	10.146	0.126	0.000	0.388	100.412
Olivine	0.005	0.058	0.005	0.055	0.003	0.000	0.007	40.236	49.270	0.035	10.115	0.127	0.002	0.373	100.295
Olivine	0.000	0.028	0.000	0.035	0.000	0.007	0.000	40.276	49.433	0.036	10.265	0.160	0.000	0.374	100.614
Olivine	0.004	0.038	0.000	0.076	0.001	0.000	0.004	40.433	49.509	0.019	10.110	0.143	0.006	0.400	100.743
Olivine	0.000	0.032	0.000	0.068	0.000	0.000	0.004	40.257	49.513	0.018	10.029	0.169	0.000	0.439	100.530
Olivine	0.000	0.053	0.000	0.075	0.000	0.009	0.004	40.602	49.563	0.021	10.091	0.151	0.005	0.362	100.954
Olivine	0.000	0.035	0.002	0.041	0.006	0.000	0.015	40.499	49.632	0.028	10.171	0.124	0.000	0.381	100.947
Olivine	0.003	0.048	0.000	0.051	0.002	0.000	0.000	40.527	49.643	0.030	10.070	0.155	0.000	0.422	100.951
Olivine	0.000	0.069	0.001	0.045	0.004	0.002	0.014	40.506	49.659	0.031	10.165	0.144	0.000	0.403	101.049
Olivine	0.016	0.082	0.002	0.054	0.000	0.011	0.018	40.832	49.708	0.042	10.088	0.127	0.000	0.391	101.392

Olivine	0.008	0.073	0.004	0.017	0.000	0.000	0.024	40.462	49.777	0.078	10.024	0.165	0.009	0.347	101.004
Olivine	0.008	0.056	0.001	0.088	0.000	0.000	0.013	40.525	50.137	0.023	10.157	0.150	0.000	0.390	101.549
Olivine	0.001	0.053	0.000	0.076	0.000	0.014	0.012	40.911	50.155	0.026	10.038	0.132	0.000	0.422	101.839
Olivine	0.000	0.047	0.000	0.068	0.000	0.000	0.008	41.036	50.364	0.029	10.078	0.152	0.026	0.366	102.195
Cr-Spinel	0.000	0.000	0.000	0.103	0.063	0.000	0.001	0.089	19.895	57.691	11.087	0.130	10.519	0.355	99.941
Cr-Spinel	0.000	0.000	0.000	0.087	0.047	0.000	0.000	0.070	20.803	58.583	10.820	0.091	10.652	0.376	101.535
Cr-Spinel	0.000	0.000	0.000	0.080	0.054	0.000	0.000	0.082	21.110	59.181	10.480	0.112	10.671	0.393	102.162
Cr-Spinel	0.000	0.000	0.000	0.094	0.056	0.001	0.002	0.110	20.543	57.900	10.855	0.124	10.942	0.402	101.029
Cr-Spinel	0.002	0.000	0.000	0.091	0.041	0.000	0.000	0.089	20.305	57.448	10.817	0.127	11.030	0.356	100.329
Cr-Spinel	0.000	0.007	0.000	0.054	0.050	0.000	0.005	0.119	20.240	56.846	10.860	0.125	11.074	0.361	99.741
Cr-Spinel	0.003	0.000	0.000	0.126	0.050	0.019	0.009	0.140	20.527	56.509	10.654	0.133	11.608	0.351	100.136
Cr-Spinel	0.007	0.000	0.000	0.136	0.263	0.008	0.000	0.066	15.239	46.267	23.089	0.256	14.242	0.358	99.931
Cr-Spinel	0.000	0.000	0.004	0.169	0.261	0.000	0.000	0.056	15.229	46.335	23.270	0.252	14.293	0.362	100.231
Cr-Spinel	0.002	0.000	0.000	0.145	0.247	0.007	0.006	0.074	15.085	46.059	23.495	0.253	14.297	0.338	100.007
Cr-Spinel	0.010	0.013	0.000	0.159	0.320	0.010	0.000	0.049	16.349	46.233	19.697	0.199	16.392	0.336	99.766
Cr-Spinel	0.000	0.049	0.000	0.134	0.324	0.008	0.000	0.054	17.315	46.505	19.288	0.232	16.505	0.372	100.787
Cr-Spinel	0.000	0.019	0.001	0.158	0.303	0.004	0.000	0.039	16.555	46.432	19.704	0.224	16.793	0.333	100.566
Cr-Spinel	0.001	0.023	0.000	0.154	0.296	0.012	0.005	0.051	16.342	45.564	19.336	0.273	16.801	0.368	99.235
Diopside	0.000	19.440	0.006	0.024	0.246	0.032	1.111	51.944	17.111	4.870	4.098	0.154	0.764	0.041	99.842
Diopside	0.005	19.729	0.000	0.014	0.179	0.010	0.693	47.449	17.259	10.903	3.601	0.086	1.915	0.096	101.939
Diopside	0.000	20.010	0.003	0.024	0.261	0.018	1.244	51.933	16.222	4.720	4.323	0.142	0.751	0.046	99.697
Diopside	0.000	20.063	0.006	0.009	0.260	0.028	1.220	51.500	16.141	4.958	4.194	0.148	0.645	0.033	99.227
Diopside	0.000	20.084	0.030	0.075	0.338	0.027	1.173	51.838	16.189	5.350	4.163	0.160	0.666	0.069	100.160
Diopside	0.006	20.159	0.000	0.046	0.323	0.017	1.122	51.990	16.442	4.973	3.838	0.143	0.482	0.028	99.573
Diopside	0.000	20.236	0.000	0.026	0.271	0.040	1.159	51.959	16.142	4.981	4.000	0.130	0.618	0.039	99.609
Diopside	0.000	20.312	0.003	0.023	0.279	0.017	1.169	51.813	16.429	4.797	3.862	0.106	0.454	0.058	99.330
Diopside	0.004	20.489	0.001	0.020	0.278	0.027	1.217	52.338	16.487	4.900	3.779	0.109	0.701	0.022	100.377
Diopside	0.000	21.480	0.011	0.000	0.290	0.007	1.177	53.398	16.445	4.926	2.414	0.070	0.599	0.041	100.865
Diopside	0.000	21.599	0.012	0.000	0.255	0.012	1.115	52.459	16.251	4.728	2.411	0.090	0.540	0.046	99.519

Diopside	0.000	21.636	0.006	0.005	0.282	0.038	1.213	53.020	16.374	4.945	2.494	0.072	0.533	0.048	100.675
Diopside	0.000	21.699	0.000	0.027	0.282	0.005	1.092	51.361	15.413	4.679	2.403	0.063	0.597	0.070	97.718
Diopside	0.000	21.723	0.008	0.068	0.282	0.018	1.090	51.791	16.057	4.734	2.376	0.103	0.578	0.046	98.874
Diopside	0.003	21.730	0.000	0.037	0.271	0.012	1.114	52.991	16.398	4.782	2.489	0.091	0.578	0.009	100.506
Diopside	0.000	21.749	0.024	0.020	0.254	0.015	1.150	52.712	16.280	4.742	2.505	0.075	0.553	0.048	100.126
Diopside	0.000	21.750	0.001	0.006	0.265	0.002	1.083	52.582	16.118	4.680	2.386	0.105	0.565	0.049	99.592
Diopside	0.000	21.798	0.012	0.000	0.224	0.024	0.830	52.866	16.923	4.612	2.539	0.091	0.502	0.031	100.451
Diopside	0.000	21.825	0.003	0.017	0.254	0.020	1.029	52.291	16.240	4.789	2.362	0.107	0.577	0.039	99.561
Diopside	0.004	21.852	0.000	0.000	0.286	0.014	1.159	52.835	16.375	4.852	2.444	0.074	0.595	0.030	100.518
Diopside	0.000	21.977	0.000	0.000	0.258	0.032	1.065	53.091	16.637	4.882	2.472	0.066	0.583	0.048	101.113
Diopside	0.004	22.160	0.000	0.021	0.214	0.015	0.747	52.125	16.418	4.582	2.553	0.063	0.567	0.056	99.541
Diopside	0.007	17.107	0.040	0.115	0.681	0.000	0.758	46.231	15.843	6.418	6.598	0.119	1.334	0.240	95.651
Diopside	0.000	17.593	0.018	0.042	0.237	0.013	0.857	50.553	18.342	4.426	4.225	0.146	0.564	0.034	97.053
Diopside	0.067	19.170	1.204	0.022	0.576	0.082	1.070	52.885	13.195	7.040	3.999	0.127	0.649	0.026	100.111
Diopside	0.000	20.351	0.004	0.010	0.303	0.020	1.174	52.674	15.773	4.939	4.547	0.152	0.857	0.049	100.854
Diopside	0.000	17.304	0.010	0.041	0.261	0.023	1.038	52.938	18.571	4.760	4.929	0.152	0.852	0.039	100.918
Diopside	0.000	20.407	0.000	0.029	0.270	0.025	1.213	52.969	16.123	4.845	4.373	0.146	0.787	0.052	101.249
Diopside	0.000	20.385	0.000	0.024	0.290	0.018	1.208	53.128	16.072	4.938	4.435	0.142	0.887	0.032	101.564
Enstatite	0.000	0.606	0.000	0.057	0.045	0.002	0.046	54.662	33.722	3.742	6.321	0.146	0.274	0.082	99.705
Enstatite	0.005	0.619	0.000	0.034	0.055	0.014	0.056	55.091	33.858	3.828	6.397	0.129	0.244	0.099	100.431
Enstatite	0.012	0.619	0.005	0.045	0.065	0.004	0.048	54.646	33.539	3.772	6.402	0.139	0.269	0.073	99.646
Enstatite	0.000	0.636	0.000	0.042	0.043	0.012	0.062	54.942	33.677	3.719	6.366	0.165	0.287	0.087	100.041
Enstatite	0.000	0.641	0.012	0.046	0.072	0.009	0.054	54.520	33.728	3.864	6.502	0.157	0.302	0.072	99.983
Enstatite	0.000	0.648	0.000	0.043	0.064	0.000	0.044	54.836	33.561	3.928	6.468	0.164	0.305	0.126	100.189
Enstatite	0.006	0.650	0.010	0.049	0.056	0.002	0.040	53.961	32.999	3.875	6.369	0.149	0.267	0.085	98.526
Enstatite	0.002	0.657	0.006	0.067	0.049	0.000	0.052	55.090	33.783	3.853	6.374	0.183	0.272	0.103	100.495
Enstatite	0.000	0.681	0.020	0.042	0.066	0.000	0.068	54.811	33.512	3.872	6.431	0.133	0.287	0.099	100.028
Enstatite	0.002	0.749	0.011	0.042	0.070	0.000	0.050	54.668	33.240	3.766	6.508	0.174	0.270	0.052	99.627
Enstatite	0.000	0.888	0.000	0.053	0.079	0.003	0.084	54.504	32.042	3.526	8.507	0.194	0.303	0.102	100.284

Enstatite	0.000	0.913	0.000	0.069	0.059	0.000	0.070	53.790	31.133	3.864	9.931	0.248	0.380	0.087	100.553
Enstatite	0.003	0.925	0.002	0.078	0.069	0.000	0.097	53.346	30.645	3.912	9.977	0.300	0.346	0.112	99.820
Enstatite	0.000	0.945	0.000	0.072	0.052	0.000	0.107	53.880	30.692	3.893	10.004	0.246	0.365	0.100	100.355
Enstatite	0.000	0.947	0.000	0.054	0.067	0.000	0.097	53.773	30.578	3.699	10.081	0.226	0.337	0.105	99.963
Enstatite	0.000	0.950	0.000	0.066	0.062	0.010	0.087	53.741	30.618	3.843	10.130	0.204	0.362	0.064	100.138
Enstatite	0.000	1.280	0.003	0.033	0.061	0.002	0.088	54.955	33.327	3.850	6.353	0.144	0.308	0.104	100.509
Enstatite	0.004	1.848	0.015	0.074	0.079	0.007	0.085	54.496	32.475	3.828	6.275	0.097	0.303	0.112	99.699
Enstatite	0.000	2.546	0.000	0.045	0.071	0.028	0.098	54.045	32.002	3.976	6.153	0.144	0.312	0.067	99.487
Enstatite	0.000	2.915	0.000	0.045	0.086	0.000	0.138	54.353	31.631	4.036	6.027	0.151	0.318	0.072	99.773
Pargasite	0.059	11.082	0.689	0.152	1.542	0.047	3.174	43.202	17.652	14.168	5.131	0.087	0.959	0.070	98.035
Pargasite	0.059	10.140	0.676	0.185	1.081	0.047	3.444	42.025	16.842	14.645	6.861	0.149	1.141	0.150	97.445
Pargasite	0.069	10.261	0.712	0.183	1.102	0.012	3.361	42.055	16.884	14.775	6.802	0.121	1.182	0.092	97.655
Pargasite	0.051	10.116	0.709	0.220	1.070	0.022	3.393	42.231	16.945	14.753	6.720	0.100	1.182	0.089	97.618
Pargasite	0.032	10.324	0.440	0.158	1.418	0.024	2.113	37.486	17.384	17.031	8.036	0.111	3.059	0.148	97.788
Pargasite	0.053	10.484	0.768	0.186	1.393	0.048	3.372	42.215	16.923	14.120	5.808	0.097	1.475	0.090	97.047
Pargasite	0.051	10.360	0.756	0.137	1.491	0.026	3.231	42.248	16.999	14.220	6.016	0.099	1.359	0.054	97.069
Pargasite	0.049	10.463	0.749	0.149	1.464	0.025	3.354	41.871	16.727	14.282	6.145	0.099	1.413	0.103	96.892
Pargasite	0.061	10.551	0.590	0.166	1.028	0.030	3.468	42.757	17.173	14.816	5.704	0.104	1.463	0.117	98.038
Pargasite	0.064	10.512	0.600	0.155	0.982	0.023	3.645	43.005	17.129	14.981	5.766	0.103	1.397	0.110	98.484
Symplectite Cr-Spinel	0.001	0.000	0.000	0.085	0.048	0.012	0.012	0.114	21.020	58.975	11.018	0.164	11.019	0.399	102.872
Symplectite Cr-Spinel	0.000	0.000	0.000	0.115	0.102	0.002	0.000	0.051	16.757	50.080	18.980	0.200	13.201	0.357	99.845
Symplectite Cr-Spinel	0.002	0.000	0.000	0.153	0.118	0.008	0.002	0.043	16.700	50.035	18.949	0.230	13.318	0.351	99.917
Symplectite Cr-Spinel	0.000	0.000	0.000	0.119	0.114	0.000	0.006	0.068	16.564	49.951	19.063	0.231	13.400	0.349	99.866
Symplectite Cr-Spinel	0.000	0.000	0.000	0.141	0.106	0.001	0.010	0.060	16.616	49.707	19.200	0.206	13.416	0.359	99.823

Symplectite Cr-Spinel	0.000	0.000	0.003	0.140	0.107	0.003	0.010	0.064	16.475	49.769	19.177	0.216	13.479	0.358	99.803
Symplectite Cr-Spinel	0.000	0.000	0.002	0.115	0.104	0.007	0.000	0.050	17.070	50.396	18.457	0.197	13.560	0.363	100.324
Symplectite Cr-Spinel	0.003	0.000	0.002	0.130	0.106	0.003	0.000	0.046	16.582	49.984	19.327	0.216	13.618	0.346	100.363
Symplectite Cr-Spinel	0.005	0.000	0.000	0.110	0.106	0.000	0.003	0.049	16.445	49.441	19.362	0.206	13.663	0.337	99.739
Symplectite Cr-Spinel	0.000	0.000	0.000	0.113	0.089	0.007	0.000	0.069	16.549	49.755	19.805	0.242	13.692	0.359	100.684
Symplectite Cr-Spinel	0.007	0.000	0.000	0.121	0.108	0.000	0.016	0.163	16.621	49.773	19.766	0.242	13.737	0.333	100.919
Symplectite Cr-Spinel	0.000	0.000	0.000	0.143	0.101	0.005	0.006	0.035	17.532	50.342	17.492	0.207	14.147	0.318	100.330
Symplectite Cr-Spinel	0.000	0.006	0.000	0.129	0.129	0.011	0.026	0.041	16.565	47.653	18.993	0.265	16.401	0.303	100.521
Symplectite Cr-Spinel	0.004	0.000	0.000	0.117	0.117	0.018	0.012	0.032	17.263	48.188	17.633	0.221	16.730	0.345	100.695
Symplectite Cr-Spinel	0.004	0.000	0.000	0.168	0.153	0.000	0.000	0.060	16.753	47.383	18.411	0.215	16.784	0.355	100.298
Symplectite Cr-Spinel	0.000	0.005	0.005	0.117	0.139	0.000	0.012	0.036	16.981	47.835	17.586	0.251	17.042	0.324	100.357
Symplectite Cr-Spinel	0.006	0.000	0.005	0.162	0.137	0.015	0.000	0.038	17.110	47.130	17.710	0.218	17.539	0.322	100.391
Symplectite Cr-Spinel	0.000	0.012	0.000	0.174	0.156	0.001	0.000	0.060	17.185	46.975	17.769	0.193	18.219	0.324	101.090
Symplectite Cr-Spinel	0.000	0.000	0.000	0.163	0.160	0.007	0.003	0.050	16.949	46.286	17.498	0.247	18.449	0.312	100.124
Symplectite Cr-Spinel	0.000	0.000	0.000	0.147	0.147	0.000	0.001	0.048	16.643	47.379	18.284	0.236	16.932	0.343	100.167
Symplectite Cr-Spinel	0.000	0.000	0.000	0.109	0.145	0.005	0.000	0.049	16.708	47.033	18.187	0.221	17.387	0.332	100.176

Symplectite Enstatite	0.000	0.971	0.094	0.127	0.044	0.000	0.086	52.929	30.112	4.292	9.271	0.211	0.329	0.059	98.524
Symplectite Enstatite	0.000	0.888	0.004	0.072	0.052	0.000	0.099	54.456	30.817	4.146	9.251	0.243	0.326	0.094	100.448
Symplectite Enstatite	0.000	0.876	0.000	0.076	0.047	0.000	0.100	54.712	30.680	4.141	9.549	0.237	0.382	0.089	100.900
Symplectite Enstatite	0.000	0.839	0.003	0.047	0.037	0.000	0.090	54.877	30.732	4.086	9.568	0.244	0.361	0.098	100.981
Symplectite Enstatite	0.000	0.882	0.001	0.050	0.037	0.000	0.087	54.620	30.791	4.456	9.499	0.241	0.386	0.085	101.152
Diopside Traverse 1	0.000	21.716	0.000	0.000	0.280	0.017	1.126	52.955	16.305	4.764	2.496	0.070	0.603	0.063	100.395
Diopside Traverse 1	0.006	21.739	0.015	0.000	0.286	0.030	1.110	52.914	16.537	4.843	2.480	0.082	0.582	0.027	100.651
Diopside Traverse 1	0.000	21.775	0.000	0.041	0.307	0.023	1.060	51.175	15.517	4.632	2.428	0.090	0.629	0.049	97.728
Diopside Traverse 1	0.001	21.761	0.016	0.034	0.275	0.028	1.060	50.046	15.032	4.585	2.444	0.058	0.582	0.031	95.951
Diopside Traverse 1	0.001	21.320	0.012	0.000	0.299	0.019	1.118	51.846	15.735	4.782	2.414	0.074	0.536	0.028	98.203
Diopside Traverse 1	0.000	21.238	0.004	0.000	0.291	0.000	1.175	53.252	16.417	4.864	2.450	0.077	0.545	0.038	100.361
Diopside Traverse 1	0.079	20.336	0.051	0.037	0.326	0.140	1.218	51.954	16.340	5.068	2.670	0.062	0.561	0.057	98.967
Diopside Traverse 1	0.002	21.643	0.014	0.000	0.294	0.007	1.197	53.258	16.608	4.853	2.530	0.095	0.559	0.040	101.100
Diopside Traverse 1	0.012	20.781	0.008	0.050	0.273	0.001	1.048	51.767	16.805	4.641	2.613	0.103	0.593	0.041	98.736
Diopside Traverse 1	0.000	21.715	0.000	0.022	0.284	0.009	1.094	52.344	16.369	4.866	2.414	0.064	0.551	0.033	99.768
Diopside Traverse 1	0.000	21.659	0.003	0.000	0.273	0.023	1.032	51.748	16.143	4.760	2.461	0.076	0.535	0.044	98.763
Diopside Traverse 2	0.000	22.699	0.004	0.024	0.461	0.030	0.606	51.036	15.469	4.100	4.170	0.122	0.739	0.046	99.505
Diopside Traverse 2	0.000	20.088	0.000	0.034	0.253	0.021	1.116	52.040	16.160	4.811	4.486	0.114	0.728	0.042	99.893
Diopside Traverse 2	0.004	21.093	0.000	0.043	0.399	0.026	1.022	51.415	15.544	4.936	4.295	0.144	0.808	0.043	99.773
Diopside Traverse 2	0.000	21.107	0.046	0.055	0.341	0.028	0.640	50.796	16.887	4.133	4.254	0.120	0.867	0.007	99.293
Diopside Traverse 2	0.001	19.852	0.057	0.048	0.361	0.035	1.192	51.782	16.011	4.956	4.355	0.139	0.907	0.028	99.725
Diopside Traverse 2	0.002	19.827	0.017	0.035	0.299	0.028	1.283	51.747	16.113	5.137	4.533	0.140	0.949	0.066	100.176
Diopside Traverse 2	0.004	20.036	0.004	0.005	0.282	0.023	1.241	51.985	16.050	4.903	4.445	0.138	0.922	0.015	100.061
Diopside Traverse 2	0.000	19.918	0.006	0.013	0.266	0.044	1.229	51.797	15.969	4.963	4.597	0.148	0.840	0.040	99.847
Diopside Traverse 2	0.001	19.924	0.020	0.071	0.261	0.030	1.165	51.661	15.941	4.972	4.510	0.144	0.902	0.034	99.635

Diopside Traverse 2	0.000	22.041	0.000	0.035	0.489	0.036	0.788	51.158	15.447	4.293	4.182	0.111	0.947	0.044	99.582
Diopside Traverse 2	0.002	22.803	0.015	0.017	0.497	0.014	0.762	51.379	15.828	3.902	3.903	0.094	0.939	0.020	100.193
Diopside Traverse 2	0.000	22.353	0.009	0.073	0.361	0.026	0.698	51.278	15.476	4.632	4.219	0.159	0.857	0.055	100.195
Diopside Traverse 2	0.000	19.369	0.000	0.033	0.285	0.053	1.082	51.131	16.111	4.767	4.748	0.137	0.842	0.021	98.592
Diopside Traverse 2	0.000	22.788	0.000	0.043	0.468	0.022	0.726	50.629	15.000	4.458	4.214	0.110	1.076	0.003	99.537
Diopside Traverse 2	0.004	19.826	0.005	0.021	0.281	0.054	1.188	51.833	15.925	4.946	4.579	0.138	0.772	0.079	99.651
Diopside Traverse 2	0.002	22.332	0.052	0.056	0.779	0.020	0.776	50.333	14.998	5.086	4.388	0.115	0.818	0.041	99.816
Diopside Traverse 2	0.000	19.792	0.000	0.019	0.268	0.044	1.176	51.823	16.075	4.935	4.698	0.131	0.618	0.019	99.638
Diopside Traverse 2	0.000	20.223	0.000	0.022	0.272	0.018	1.112	52.550	16.280	4.374	4.663	0.148	0.552	0.058	100.271
Diopside Traverse 2	0.000	19.865	0.007	0.035	0.274	0.040	1.195	51.762	16.112	4.845	4.699	0.170	0.460	0.036	99.512
Diopside Traverse 2	0.000	21.641	0.011	0.002	0.274	0.050	1.121	52.870	16.390	4.711	2.378	0.061	0.476	0.029	100.016
Diopside Traverse 2	0.000	17.314	0.003	0.043	0.254	0.020	0.875	42.546	16.969	15.212	4.220	0.108	2.824	0.067	100.455
Diopside Traverse 2	0.000	21.865	0.002	0.003	0.268	0.010	1.137	52.111	16.098	4.817	2.440	0.074	0.562	0.081	99.467
Diopside Traverse 2	0.000	21.813	0.005	0.000	0.304	0.029	1.209	52.886	16.448	4.913	2.525	0.077	0.536	0.027	100.788
Diopside Traverse 2	0.000	21.622	0.004	0.011	0.267	0.004	1.154	52.522	16.255	4.887	2.390	0.084	0.573	0.048	99.822
Diopside Traverse 2	0.000	21.638	0.008	0.008	0.283	0.035	1.085	52.706	16.330	4.768	2.458	0.071	0.553	0.035	99.979
Diopside Traverse 2	0.000	21.617	0.029	0.014	0.291	0.037	1.161	52.226	16.214	4.883	2.339	0.095	0.574	0.072	99.550
Diopside Traverse 2	0.006	21.658	0.007	0.000	0.281	0.019	1.160	52.856	16.209	4.954	2.414	0.102	0.574	0.038	100.277
Diopside Traverse 2	0.000	21.845	0.001	0.020	0.293	0.017	1.109	52.928	16.359	5.008	2.468	0.078	0.539	0.045	100.707
Diopside Traverse 2	0.000	21.453	0.000	0.040	0.283	0.015	1.072	52.710	16.427	4.804	2.572	0.083	0.560	0.026	100.042
Diopside Traverse 2	0.000	21.737	0.000	0.000	0.303	0.009	1.092	51.886	16.083	4.726	2.422	0.093	0.554	0.037	98.942
Diopside Traverse 2	0.000	21.601	0.018	0.008	0.273	0.025	1.150	52.742	16.325	4.960	2.460	0.067	0.611	0.050	100.303
Diopside Traverse 2	0.012	21.608	0.000	0.000	0.302	0.009	1.175	52.459	16.427	4.896	2.494	0.112	0.553	0.041	100.086
Diopside Traverse 2	0.001	21.871	0.009	0.006	0.290	0.022	1.117	52.185	16.275	4.885	2.416	0.083	0.611	0.060	99.839
Diopside Traverse 2	0.000	21.692	0.002	0.023	0.306	0.035	1.139	52.312	16.152	4.908	2.552	0.092	0.571	0.041	99.826
Diopside Traverse 2	0.000	21.597	0.004	0.004	0.281	0.002	1.127	52.897	16.329	4.850	2.381	0.113	0.602	0.029	100.235
Diopside Traverse 2	0.000	21.694	0.009	0.027	0.282	0.030	1.181	52.801	16.496	4.915	2.479	0.066	0.541	0.047	100.581
Diopside Traverse 2	0.006	21.775	0.000	0.000	0.300	0.017	1.152	52.788	16.432	4.861	2.524	0.076	0.632	0.033	100.620
Diopside Traverse 2	0.000	21.853	0.003	0.011	0.283	0.010	1.090	52.542	16.102	4.798	2.495	0.064	0.620	0.006	99.900

Diopside Traverse 2	0.002	21.618	0.014	0.024	0.300	0.020	1.166	52.438	16.091	4.725	2.471	0.075	0.556	0.058	99.569
Diopside Traverse 2	0.014	21.136	0.020	0.000	0.251	0.015	0.992	52.218	16.953	4.237	2.418	0.082	0.396	0.031	98.764
Diopside Traverse 2	0.000	21.799	0.005	0.018	0.239	0.014	1.104	52.849	16.511	4.566	2.520	0.077	0.498	0.075	100.277
Diopside Traverse 3	0.000	21.600	0.004	0.015	0.266	0.024	1.090	53.100	16.248	4.859	2.473	0.064	0.530	0.047	100.328
Diopside Traverse 3	0.000	21.690	0.012	0.013	0.290	0.017	1.124	52.303	16.095	4.981	2.429	0.066	0.566	0.082	99.676
Diopside Traverse 3	0.000	21.792	0.009	0.008	0.286	0.012	1.108	52.454	16.197	4.950	2.474	0.106	0.554	0.028	99.984
Diopside Traverse 3	0.003	21.785	0.003	0.012	0.309	0.009	1.135	53.039	16.380	4.930	2.419	0.082	0.574	0.039	100.722
Diopside Traverse 3	0.000	21.774	0.005	0.045	0.286	0.019	1.112	52.592	16.241	4.878	2.426	0.107	0.609	0.025	100.118
Diopside Traverse 3	0.013	19.051	0.026	0.014	0.288	0.000	1.062	49.742	17.524	9.601	3.142	0.091	1.393	0.052	102.025
Diopside Traverse 3	0.003	20.138	0.012	0.019	0.296	0.007	1.055	49.683	16.532	8.518	2.980	0.107	1.271	0.053	100.686
Diopside Traverse 3	0.003	21.889	0.012	0.027	0.274	0.002	0.985	52.098	16.150	4.681	2.512	0.091	0.518	0.023	99.266
Diopside Traverse 3	0.004	21.702	0.007	0.000	0.290	0.019	1.099	52.528	16.266	4.821	2.573	0.071	0.530	0.041	99.969
Diopside Traverse 3	0.000	21.734	0.009	0.019	0.313	0.000	1.144	52.615	16.357	4.966	2.341	0.070	0.571	0.020	100.175
Diopside Traverse 3	0.000	21.768	0.001	0.023	0.323	0.012	1.204	52.553	16.279	4.885	2.390	0.070	0.523	0.009	100.050
Diopside Traverse 3	0.000	18.588	0.006	0.032	0.280	0.001	1.000	49.429	17.898	9.225	3.355	0.109	1.406	0.081	101.421
Diopside Traverse 3	0.000	17.273	0.012	0.012	0.252	0.017	0.896	51.965	19.664	5.602	3.377	0.100	0.730	0.037	99.961
Diopside Traverse 3	0.012	21.236	0.001	0.017	0.295	0.007	1.079	52.453	16.522	4.730	2.543	0.062	0.568	0.044	99.571
Diopside Traverse 3	0.009	21.258	0.025	0.021	0.290	0.004	1.117	51.699	16.171	5.899	2.615	0.086	0.730	0.042	99.993
Diopside Traverse 3	0.000	21.815	0.000	0.000	0.311	0.000	1.171	52.525	16.378	4.856	2.531	0.074	0.528	0.039	100.227
Diopside Traverse 3	0.001	21.897	0.008	0.000	0.301	0.004	1.082	53.054	16.277	4.907	2.442	0.069	0.555	0.037	100.634
Diopside Traverse 3	0.000	21.728	0.000	0.000	0.313	0.011	1.148	52.612	15.946	4.799	2.458	0.039	0.543	0.056	99.652
Diopside Traverse 3	0.001	21.573	0.000	0.026	0.298	0.011	1.082	52.667	16.328	4.842	2.417	0.104	0.522	0.037	99.908
Diopside Traverse 3	0.004	20.482	0.015	0.032	0.279	0.000	1.068	53.070	17.374	4.858	2.698	0.065	0.530	0.032	100.510
Diopside Traverse 3	0.003	21.283	0.010	0.023	0.303	0.009	1.149	51.198	16.165	5.735	2.606	0.069	0.710	0.062	99.324
Diopside Traverse 3	0.001	21.587	0.005	0.031	0.317	0.006	1.123	52.417	16.053	4.846	2.481	0.060	0.544	0.047	99.519
Diopside Traverse 3	0.002	21.802	0.005	0.036	0.288	0.020	1.157	52.605	16.196	4.875	2.472	0.074	0.507	0.055	100.093
Diopside Traverse 3	0.000	20.216	0.017	0.000	0.292	0.016	1.092	52.174	17.409	5.162	2.837	0.060	0.638	0.044	99.955
Enstatite Traverse 1	0.000	0.817	0.000	0.068	0.086	0.000	0.090	54.836	32.373	3.474	8.200	0.229	0.296	0.098	100.566
Enstatite Traverse 1	0.000	0.798	0.000	0.076	0.074	0.013	0.084	54.442	32.107	3.438	8.224	0.215	0.332	0.109	99.911

Enstatite Traverse 1	0.000	0.778	0.003	0.057	0.080	0.000	0.080	54.540	32.193	3.384	8.387	0.175	0.308	0.092	100.095
Enstatite Traverse 1	0.000	0.795	0.000	0.073	0.074	0.000	0.075	54.698	32.243	3.346	8.412	0.187	0.319	0.100	100.326
Enstatite Traverse 1	0.000	0.811	0.000	0.055	0.083	0.006	0.070	54.722	32.085	3.386	8.475	0.185	0.265	0.092	100.236
Enstatite Traverse 1	0.000	0.844	0.000	0.051	0.071	0.000	0.105	54.908	32.013	3.346	8.562	0.194	0.335	0.124	100.555
Enstatite Traverse 1	0.000	0.862	0.000	0.062	0.073	0.016	0.076	54.960	32.129	3.374	8.699	0.197	0.338	0.062	100.849
Enstatite Traverse 1	0.000	0.843	0.000	0.072	0.082	0.000	0.079	54.581	32.024	3.309	8.664	0.237	0.303	0.121	100.316
Enstatite Traverse 1	0.002	0.901	0.000	0.068	0.081	0.000	0.095	54.483	32.001	3.325	8.833	0.196	0.318	0.096	100.417
Enstatite Traverse 1	0.001	0.999	0.000	0.088	0.116	0.001	0.080	54.454	31.822	3.476	8.834	0.193	0.288	0.117	100.469
Enstatite Traverse 2	0.006	0.633	0.005	0.098	0.067	0.012	0.030	54.379	33.432	3.785	6.389	0.134	0.263	0.087	99.334
Enstatite Traverse 2	0.006	0.619	0.000	0.050	0.060	0.000	0.046	54.579	33.588	3.778	6.506	0.168	0.312	0.105	99.816
Enstatite Traverse 2	0.006	0.634	0.000	0.042	0.063	0.000	0.056	54.964	33.642	3.751	6.303	0.155	0.266	0.107	99.992
Enstatite Traverse 2	0.001	0.671	0.001	0.062	0.055	0.000	0.061	55.398	33.870	3.991	6.410	0.163	0.266	0.068	101.030
Enstatite Traverse 2	0.000	1.080	0.000	0.057	0.061	0.000	0.046	55.166	33.475	3.898	6.415	0.181	0.290	0.072	100.741
Enstatite Traverse 2	0.000	0.603	0.003	0.018	0.061	0.004	0.036	54.663	33.841	3.854	6.468	0.149	0.275	0.083	100.088
Enstatite Traverse 2	0.003	0.625	0.001	0.044	0.051	0.004	0.048	54.700	33.621	3.876	6.461	0.174	0.259	0.072	99.962
Enstatite Traverse 2	0.002	0.927	0.000	0.051	0.069	0.002	0.045	54.985	33.358	3.853	6.448	0.162	0.308	0.084	100.313
Enstatite Traverse 2	0.002	0.621	0.000	0.044	0.056	0.000	0.057	55.246	33.910	3.918	6.451	0.149	0.284	0.069	100.806
Enstatite Traverse 2	0.001	0.757	0.000	0.053	0.067	0.014	0.063	54.741	33.752	3.906	6.557	0.187	0.321	0.104	100.522
Enstatite Traverse 2	0.000	0.596	0.000	0.061	0.048	0.000	0.056	55.472	33.962	3.927	6.349	0.173	0.311	0.051	101.006
Enstatite Traverse 2	0.000	0.618	0.004	0.054	0.065	0.002	0.026	54.812	33.443	3.903	6.373	0.138	0.279	0.094	99.813
Enstatite Traverse 2	0.000	0.645	0.010	0.059	0.059	0.009	0.038	54.686	33.382	3.885	6.435	0.152	0.279	0.103	99.741
Enstatite Traverse 2	0.000	0.568	0.000	0.037	0.057	0.003	0.032	51.224	32.991	8.266	6.630	0.191	0.890	0.108	101.049
Enstatite Traverse 2	0.003	0.610	0.002	0.057	0.064	0.000	0.049	54.511	33.374	4.073	6.372	0.160	0.306	0.098	99.680
Enstatite Traverse 2	0.004	0.648	0.000	0.048	0.062	0.000	0.045	54.773	34.060	3.980	6.487	0.141	0.270	0.104	100.626
Enstatite Traverse 2	0.012	1.791	0.010	0.062	0.057	0.019	0.095	54.647	33.066	3.984	6.280	0.162	0.326	0.090	100.609
Enstatite Traverse 2	0.001	0.786	0.006	0.071	0.073	0.016	0.050	55.027	33.584	3.964	6.412	0.137	0.265	0.101	100.492
Enstatite Traverse 2	0.002	0.624	0.006	0.050	0.064	0.000	0.036	54.806	33.621	3.941	6.343	0.154	0.300	0.082	100.040
Enstatite Traverse 2	0.000	0.607	0.000	0.043	0.065	0.002	0.042	55.168	33.975	3.955	6.335	0.177	0.280	0.097	100.747
Enstatite Traverse 2	0.000	0.641	0.003	0.075	0.046	0.000	0.051	54.757	33.286	3.793	6.371	0.143	0.329	0.069	99.578

Enstatite Traverse 2	0.017	4.690	0.011	0.022	0.083	0.019	0.195	54.797	31.089	4.029	5.817	0.124	0.333	0.081	101.315
Enstatite Traverse 2	0.000	0.632	0.000	0.031	0.050	0.002	0.037	55.082	33.695	3.844	6.376	0.135	0.289	0.090	100.281
Enstatite Traverse 2	0.010	2.037	0.006	0.045	0.063	0.000	0.140	55.440	32.952	3.942	6.164	0.154	0.296	0.086	101.354
Olivine Traverse 1	0.003	0.086	0.006	0.096	0.002	0.027	0.017	39.462	44.338	0.034	16.366	0.244	0.010	0.358	101.086
Olivine Traverse 1	0.005	0.079	0.003	0.084	0.005	0.020	0.013	39.518	44.479	0.026	16.406	0.239	0.000	0.325	101.202
Olivine Traverse 1	0.000	0.097	0.000	0.119	0.011	0.000	0.006	39.327	44.185	0.024	16.418	0.297	0.000	0.321	100.804
Olivine Traverse 1	0.000	0.075	0.000	0.088	0.000	0.000	0.000	39.133	44.385	0.020	16.487	0.261	0.000	0.332	100.792
Olivine Traverse 1	0.001	0.082	0.000	0.122	0.011	0.014	0.000	39.158	44.037	0.030	16.663	0.271	0.000	0.329	100.723
Olivine Traverse 1	0.000	0.080	0.000	0.082	0.009	0.018	0.006	39.218	44.123	0.031	16.425	0.262	0.000	0.322	100.575
Olivine Traverse 1	0.000	0.079	0.000	0.102	0.006	0.010	0.006	39.431	44.382	0.026	16.458	0.244	0.000	0.327	101.083
Olivine Traverse 1	0.000	0.081	0.000	0.096	0.000	0.010	0.016	39.102	44.400	0.037	16.617	0.246	0.024	0.287	100.915
Olivine Traverse 1	0.000	0.075	0.000	0.099	0.005	0.011	0.000	38.717	43.501	0.022	16.655	0.276	0.000	0.353	99.727
Olivine Traverse 1	0.000	0.083	0.000	0.054	0.008	0.006	0.017	39.300	44.266	0.040	16.671	0.257	0.027	0.350	101.090
Olivine Traverse 1	0.000	0.067	0.000	0.079	0.002	0.000	0.007	38.934	44.031	0.032	16.750	0.264	0.000	0.350	100.531
Olivine Traverse 1	0.000	0.074	0.000	0.089	0.000	0.006	0.018	39.159	44.164	0.022	16.867	0.290	0.000	0.343	101.032
Olivine Traverse 1	0.000	0.068	0.000	0.105	0.000	0.011	0.010	39.021	43.853	0.032	16.638	0.261	0.007	0.386	100.415
Olivine Traverse 1	0.005	0.064	0.000	0.117	0.010	0.024	0.018	39.021	43.898	0.024	16.766	0.265	0.000	0.342	100.555
Olivine Traverse 1	0.002	0.083	0.000	0.109	0.004	0.000	0.013	39.166	43.967	0.020	16.886	0.279	0.000	0.345	100.873
Olivine Traverse 1	0.001	0.152	0.051	0.094	0.191	0.041	0.366	40.468	47.326	0.801	11.254	0.180	0.000	0.373	101.316
Olivine Traverse 1	0.000	0.104	0.016	0.106	0.004	0.000	0.027	39.127	47.377	0.055	10.403	0.157	0.000	0.376	97.762
Olivine Traverse 1	0.000	0.260	0.005	0.101	0.026	0.036	0.033	38.250	38.121	0.040	24.505	0.620	0.007	0.144	102.158
Olivine Traverse 1	0.012	0.115	0.007	0.029	0.018	0.028	0.040	39.520	47.609	0.100	11.490	0.175	0.000	0.685	100.108
Olivine Traverse 1	0.000	0.127	0.049	0.083	0.017	0.015	0.094	39.953	46.947	0.244	11.995	0.187	0.000	0.358	100.069
Olivine Traverse 1	0.002	0.053	0.000	0.091	0.006	0.000	0.000	39.534	48.086	0.046	10.807	0.159	0.000	0.371	99.170
Olivine Traverse 1	0.013	0.223	0.092	0.112	0.066	0.035	0.195	40.190	46.872	0.535	11.401	0.230	0.003	0.352	100.346
Olivine Traverse 1	0.003	0.193	0.013	0.128	0.008	0.028	0.000	38.962	44.010	0.067	16.122	0.284	0.006	0.247	100.100
Olivine Traverse 2	0.025	0.082	0.025	0.009	0.000	0.005	0.050	40.755	49.421	0.091	10.122	0.139	0.010	0.365	101.108
Olivine Traverse 2	0.008	0.042	0.002	0.042	0.008	0.016	0.000	40.749	49.708	0.021	10.370	0.130	0.000	0.380	101.484
Olivine Traverse 2	0.036	0.075	0.025	0.000	0.003	0.014	0.052	40.247	49.401	0.065	10.184	0.142	0.014	0.354	100.625

Olivine Traverse 2	0.026	0.064	0.011	0.107	0.000	0.014	0.002	39.496	48.004	0.047	10.139	0.150	0.000	0.366	98.441
Olivine Traverse 2	0.013	0.080	0.007	0.078	0.000	0.016	0.021	40.296	49.469	0.019	10.147	0.154	0.000	0.380	100.711
Olivine Traverse 2	0.001	0.036	0.002	0.072	0.008	0.022	0.000	40.322	49.674	0.027	10.236	0.170	0.008	0.366	100.953
Olivine Traverse 2	0.003	0.059	0.011	0.069	0.003	0.005	0.021	39.923	48.542	0.034	10.209	0.141	0.000	0.350	99.392
Olivine Traverse 2	0.000	0.023	0.001	0.054	0.002	0.000	0.006	40.926	50.509	0.027	10.108	0.138	0.011	0.382	102.191
Olivine Traverse 2	0.004	0.033	0.000	0.090	0.000	0.009	0.007	40.410	49.718	0.021	10.054	0.095	0.000	0.385	100.824
Olivine Traverse 2	0.000	0.047	0.010	0.047	0.000	0.014	0.029	41.032	50.192	0.030	10.096	0.171	0.000	0.401	102.079
Olivine Traverse 2	0.005	0.049	0.002	0.068	0.000	0.016	0.005	40.497	49.806	0.028	10.210	0.124	0.000	0.397	101.207
Olivine Traverse 2	0.000	0.065	0.000	0.058	0.000	0.007	0.003	39.870	48.482	0.091	9.900	0.139	0.000	0.383	98.998
Olivine Traverse 2	0.001	0.043	0.008	0.104	0.000	0.010	0.000	39.986	48.634	0.024	10.129	0.155	0.000	0.387	99.495
Olivine Traverse 2	0.000	0.048	0.002	0.054	0.008	0.000	0.007	41.099	50.309	0.033	10.051	0.141	0.003	0.391	102.158
Olivine Traverse 2	0.023	0.044	0.017	0.009	0.011	0.000	0.004	39.384	48.307	0.031	10.066	0.124	0.019	0.348	98.405
Olivine Traverse 2	0.006	0.055	0.006	0.028	0.004	0.023	0.015	42.992	53.271	0.042	9.932	0.139	0.017	0.412	106.950
Olivine Traverse 2	0.006	0.038	0.009	0.045	0.000	0.009	0.009	40.807	49.821	0.043	10.158	0.171	0.009	0.397	101.524
Olivine Traverse 2	0.011	0.159	0.009	0.029	0.000	0.000	0.019	41.097	50.162	0.051	10.002	0.139	0.008	0.399	102.116
Olivine Traverse 2	0.034	0.075	0.029	0.033	0.006	0.011	0.044	39.986	48.976	0.055	9.956	0.130	0.000	0.413	99.746
Olivine Traverse 2	0.000	0.057	0.000	0.060	0.019	0.000	0.006	40.794	50.113	0.040	10.070	0.168	0.011	0.393	101.741
Olivine Traverse 3	0.002	0.041	0.007	0.044	0.001	0.000	0.010	40.833	49.764	0.036	10.017	0.135	0.001	0.384	101.290
Olivine Traverse 3	0.000	0.036	0.006	0.060	0.005	0.004	0.005	40.275	49.209	0.028	10.085	0.147	0.003	0.357	100.221
Olivine Traverse 3	0.010	0.059	0.000	0.078	0.000	0.004	0.000	39.559	48.227	0.032	10.321	0.131	0.000	0.367	98.810
Olivine Traverse 3	0.007	0.046	0.000	0.032	0.000	0.009	0.005	39.928	48.757	0.015	10.076	0.147	0.000	0.370	99.392
Olivine Traverse 3	0.000	0.042	0.000	0.067	0.000	0.009	0.011	40.153	49.182	0.021	10.110	0.168	0.000	0.375	100.137
Olivine Traverse 3	0.012	0.042	0.000	0.084	0.010	0.002	0.023	39.449	48.549	0.025	10.140	0.152	0.006	0.401	98.898
Olivine Traverse 3	0.011	0.048	0.000	0.019	0.000	0.000	0.023	39.637	48.290	0.018	10.048	0.119	0.000	0.374	98.601
Olivine Traverse 3	0.013	0.061	0.000	0.039	0.000	0.000	0.010	40.745	49.989	0.049	10.006	0.192	0.000	0.423	101.549
Olivine Traverse 3	0.002	0.066	0.004	0.046	0.003	0.000	0.007	39.149	47.811	0.033	10.178	0.153	0.000	0.346	97.842
Olivine Traverse 3	0.008	0.055	0.000	0.092	0.000	0.000	0.014	40.399	49.066	0.017	10.150	0.143	0.000	0.367	100.311
Olivine Traverse 4	0.005	0.048	0.002	0.050	0.001	0.026	0.014	40.718	50.127	0.019	10.138	0.141	0.004	0.371	101.664
Olivine Traverse 4	0.010	0.056	0.012	0.051	0.000	0.012	0.022	40.053	48.647	0.031	10.420	0.174	0.000	0.385	99.873

Olivine Traverse 4	0.000	0.039	0.005	0.045	0.000	0.004	0.001	39.742	48.738	0.000	10.025	0.131	0.000	0.370	99.108
Olivine Traverse 4	0.005	0.056	0.002	0.088	0.007	0.000	0.004	40.076	48.778	0.018	10.207	0.150	0.000	0.424	99.823
Olivine Traverse 4	0.000	0.061	0.000	0.031	0.007	0.016	0.020	40.047	49.407	0.026	10.130	0.164	0.000	0.383	100.292
Olivine Traverse 4	0.002	0.055	0.001	0.061	0.000	0.012	0.000	39.026	47.657	0.015	10.301	0.170	0.000	0.406	97.711
Olivine Traverse 4	0.007	0.065	0.000	0.008	0.001	0.006	0.013	40.438	49.423	0.051	10.098	0.160	0.000	0.420	100.705
Olivine Traverse 4	0.009	0.051	0.012	0.064	0.000	0.000	0.004	39.868	49.351	0.025	10.099	0.148	0.000	0.388	100.059
Olivine Traverse 4	0.006	0.062	0.000	0.056	0.008	0.002	0.007	40.289	49.296	0.024	10.166	0.133	0.000	0.360	100.414
Olivine Traverse 4	0.002	0.053	0.005	0.035	0.004	0.000	0.009	40.406	49.760	0.030	10.152	0.128	0.009	0.431	101.037
Olivine Traverse 4	0.019	0.071	0.015	0.026	0.004	0.002	0.017	40.484	49.500	0.055	10.168	0.147	0.000	0.368	100.876
Olivine Traverse 4	0.014	0.033	0.000	0.095	0.000	0.000	0.017	40.770	50.084	0.025	10.050	0.146	0.008	0.426	101.667
Olivine Traverse 4	0.018	0.059	0.004	0.080	0.000	0.024	0.011	40.351	48.914	0.033	10.347	0.150	0.000	0.403	100.396
Olivine Traverse 4	0.014	0.045	0.003	0.071	0.004	0.000	0.020	40.336	48.973	0.034	10.200	0.183	0.000	0.391	100.290

Amphibole

Samples: SPR-31-03-CP37

Mineral	Cl	CaO	K2O	F	TiO2	P2O5	Na2O	SiO2	MgO	Al2O3	FeO	MnO	Cr2O3	NiO	TOTAL
Sadanagaite	0.042	10.956	1.637	0.190	4.347	0.037	2.449	38.593	12.174	15.536	10.715	0.123	0.000	0.000	96.923
Sadanagaite	0.034	11.209	1.665	0.136	4.428	0.029	2.409	38.665	12.199	15.865	10.490	0.096	0.000	0.000	97.391
Sadanagaite	0.033	10.938	1.627	0.179	4.425	0.016	2.381	38.817	12.196	15.619	10.919	0.129	0.000	0.000	97.397
Sadanagaite	0.038	10.871	1.714	0.172	4.324	0.045	2.419	38.681	12.150	15.842	10.909	0.141	0.017	0.000	97.431
Sadanagaite	0.032	10.976	1.590	0.154	4.455	0.035	2.485	38.570	11.814	15.776	11.336	0.118	0.009	0.000	97.442
Sadanagaite	0.036	10.975	1.665	0.169	4.313	0.009	2.471	38.910	12.252	15.754	10.730	0.123	0.000	0.000	97.506
Sadanagaite	0.041	10.977	1.630	0.169	4.470	0.031	2.516	38.741	12.191	15.536	11.055	0.105	0.000	0.000	97.561
Sadanagaite	0.041	11.116	1.627	0.180	4.448	0.014	2.444	39.094	11.987	15.629	10.752	0.122	0.000	0.000	97.585

Sadanagaite	0.034	10.861	1.614	0.134	4.510	0.026	2.453	38.901	12.069	15.623	11.207	0.110	0.000	0.000	97.644
Sadanagaite	0.038	10.915	1.610	0.142	4.394	0.025	2.494	38.822	11.918	15.865	11.261	0.138	0.000	0.000	97.743
Sadanagaite	0.039	10.929	1.633	0.148	4.409	0.005	2.467	38.922	11.996	15.709	11.245	0.105	0.004	0.018	97.752
Sadanagaite	0.036	10.851	1.607	0.146	4.446	0.024	2.463	38.877	12.042	15.775	11.292	0.114	0.000	0.000	97.779
Sadanagaite	0.030	10.866	1.751	0.165	4.055	0.030	2.486	39.858	12.902	14.927	10.595	0.098	0.000	0.000	97.846
Sadanagaite	0.052	10.810	1.677	0.174	4.555	0.042	2.541	38.783	12.167	15.905	11.044	0.114	0.000	0.000	97.945
Sadanagaite	0.047	10.898	1.631	0.160	4.345	0.028	2.550	39.329	12.385	15.412	10.931	0.123	0.000	0.000	97.956
Sadanagaite	0.038	11.020	1.715	0.167	4.354	0.028	2.477	39.124	12.387	15.595	10.832	0.107	0.009	0.000	97.960
Sadanagaite	0.044	10.927	1.601	0.154	4.503	0.027	2.429	38.801	12.002	15.782	11.405	0.144	0.003	0.000	97.973
Sadanagaite	0.048	10.948	1.636	0.135	4.472	0.028	2.426	39.053	11.858	15.923	11.221	0.105	0.003	0.000	97.975
Sadanagaite	0.035	10.755	1.728	0.156	4.356	0.020	2.502	39.111	12.081	15.894	11.137	0.109	0.000	0.000	98.003
Sadanagaite	0.035	10.922	1.613	0.181	4.347	0.023	2.550	39.207	12.406	15.790	10.698	0.140	0.008	0.000	98.005
Sadanagaite	0.041	11.072	1.627	0.138	4.482	0.009	2.462	39.011	11.853	15.674	11.395	0.131	0.000	0.000	98.007
Sadanagaite	0.030	11.063	1.648	0.168	4.348	0.015	2.434	39.205	12.172	15.766	10.935	0.116	0.012	0.002	98.031
Sadanagaite	0.049	11.021	1.638	0.162	4.469	0.007	2.462	39.022	12.041	15.896	11.057	0.122	0.000	0.000	98.063
Sadanagaite	0.023	10.932	1.647	0.161	4.411	0.017	2.519	39.204	12.229	15.650	11.091	0.120	0.006	0.002	98.119
Sadanagaite	0.037	10.995	1.612	0.159	4.498	0.020	2.554	38.696	11.953	15.913	11.455	0.136	0.000	0.000	98.141
Sadanagaite	0.043	10.966	1.592	0.178	4.446	0.025	2.507	39.171	12.295	16.032	11.059	0.125	0.009	0.000	98.572
Sadanagaite	0.017	10.040	1.995	0.154	3.719	0.023	2.371	39.873	14.224	15.332	9.071	0.120	0.000	0.000	97.021
Sadanagaite	0.028	10.602	1.666	0.192	4.006	0.005	2.391	39.502	13.877	14.481	9.339	0.080	0.008	0.000	96.285
Sadanagaite	0.027	10.529	1.654	0.086	3.932	0.008	2.570	40.777	14.553	15.301	9.389	0.099	0.002	0.000	99.005
Sadanagaite	0.046	10.615	1.664	0.117	4.037	0.032	2.599	40.762	14.517	15.126	9.259	0.130	0.000	0.009	99.028
Sadanagaite	0.043	10.449	1.662	0.169	3.980	0.032	2.616	40.022	14.107	14.770	9.388	0.115	0.000	0.006	97.475
Sadanagaite	0.039	10.670	1.672	0.193	3.960	0.055	2.469	39.770	13.827	14.457	9.443	0.115	0.027	0.001	96.801
Sadanagaite	0.037	10.596	1.656	0.188	3.987	0.026	2.615	40.511	14.505	15.012	9.373	0.093	0.000	0.000	98.685
Sadanagaite	0.039	10.637	1.661	0.177	3.925	0.034	2.580	39.844	14.182	14.701	9.282	0.094	0.000	0.000	97.260
Sadanagaite	0.032	10.617	1.599	0.182	3.953	0.031	2.487	40.538	14.308	14.894	9.176	0.087	0.016	0.021	98.021
Sadanagaite	0.031	10.556	1.677	0.231	3.942	0.023	2.476	39.691	13.894	14.550	9.272	0.094	0.021	0.000	96.564
Sadanagaite	0.030	10.894	1.530	0.191	4.107	0.032	2.531	39.572	14.213	14.616	9.243	0.111	0.004	0.013	97.182

Sadanagaite	0.036	10.604	1.725	0.184	3.924	0.055	2.431	39.604	14.076	14.647	9.160	0.096	0.012	0.000	96.689
Sadanagaite	0.038	10.606	1.675	0.124	4.026	0.036	2.546	40.629	14.623	15.326	9.192	0.117	0.000	0.015	99.020
Sadanagaite	0.091	10.188	1.722	0.064	3.606	0.027	2.621	40.929	15.270	15.777	8.469	0.108	0.015	0.000	98.974
Sadanagaite	0.032	10.732	1.713	0.168	3.973	0.039	2.440	39.713	14.060	15.060	9.234	0.095	0.000	0.006	97.342
Sadanagaite	0.032	10.695	1.672	0.192	3.962	0.044	2.445	39.364	13.982	15.052	9.166	0.104	0.006	0.009	96.781
Sadanagaite	0.037	10.623	1.723	0.157	4.034	0.041	2.465	40.313	14.270	15.539	8.990	0.112	0.000	0.000	98.381
Sadanagaite	0.030	10.580	1.693	0.112	3.986	0.029	2.505	39.399	14.061	15.074	9.061	0.085	0.014	0.000	96.715
Sadanagaite	0.031	10.652	1.726	0.169	4.001	0.034	2.585	40.018	14.262	15.365	9.053	0.113	0.000	0.020	98.094
Sadanagaite	0.022	10.711	1.725	0.138	4.054	0.039	2.497	39.650	13.909	15.118	9.006	0.102	0.000	0.000	97.055
Sadanagaite	0.032	10.618	1.828	0.178	4.073	0.029	2.341	39.431	13.812	15.151	9.375	0.072	0.000	0.025	97.087
Sadanagaite	0.028	10.691	1.770	0.111	3.996	0.031	2.524	40.647	14.298	15.406	9.207	0.104	0.006	0.000	98.959
Sadanagaite	0.024	10.735	1.780	0.157	4.039	0.014	2.415	39.669	14.230	15.249	9.290	0.119	0.018	0.007	97.790
Sadanagaite	0.023	10.611	1.778	0.220	3.969	0.031	2.397	39.894	14.017	14.954	9.222	0.082	0.006	0.000	97.263
Sadanagaite	0.024	10.631	1.757	0.194	3.976	0.029	2.391	39.134	13.886	14.904	9.421	0.104	0.010	0.000	96.508
Sadanagaite	0.035	10.701	1.690	0.104	3.514	0.003	2.475	39.415	14.586	15.041	8.615	0.124	0.000	0.000	96.397
Sadanagaite	0.035	10.548	1.631	0.129	4.015	0.023	2.605	40.041	14.549	15.121	9.360	0.116	0.000	0.012	98.250
Sadanagaite	0.024	10.573	1.635	0.148	3.972	0.026	2.512	40.948	14.739	15.047	9.139	0.082	0.003	0.000	98.909
Sadanagaite	0.031	11.007	1.641	0.179	4.039	0.005	2.530	40.116	14.535	15.057	9.390	0.135	0.012	0.037	98.800
Sadanagaite	0.035	10.590	1.639	0.142	3.987	0.020	2.663	40.420	14.258	14.962	9.258	0.105	0.000	0.011	98.139
Sadanagaite	0.031	10.528	1.642	0.167	3.964	0.028	2.526	41.308	14.229	14.954	9.102	0.106	0.015	0.046	98.707
Sadanagaite	0.026	10.464	1.599	0.055	4.003	0.036	2.606	39.717	14.378	14.939	9.248	0.111	0.035	0.018	97.292
Sadanagaite	0.027	10.809	1.880	0.183	3.964	0.034	2.305	39.460	14.183	15.087	8.343	0.100	0.021	0.000	96.465
Sadanagaite	0.035	10.845	1.880	0.165	3.948	0.037	2.339	39.785	14.377	15.450	8.439	0.074	0.037	0.040	97.540
Sadanagaite	0.060	10.796	1.790	0.147	3.937	0.044	2.301	39.077	14.050	14.951	8.476	0.097	0.040	0.000	95.894
Sadanagaite	0.056	11.542	1.563	0.184	4.125	0.048	2.225	38.757	14.773	14.710	8.612	0.075	0.057	0.021	96.836
Sadanagaite	0.043	10.821	1.919	0.151	3.958	0.023	2.309	39.666	14.276	15.252	8.468	0.088	0.026	0.008	97.091
Sadanagaite	0.044	10.880	1.910	0.160	3.988	0.024	2.371	40.074	14.666	15.737	8.389	0.073	0.033	0.033	98.490
Sadanagaite	0.038	11.000	1.956	0.237	4.006	0.039	2.322	39.783	14.306	15.202	8.474	0.078	0.060	0.029	97.590
Sadanagaite	0.031	10.851	1.929	0.197	3.937	0.024	2.298	39.835	14.578	15.508	8.311	0.073	0.056	0.020	97.720

Sadanagaite	0.033	10.882	1.960	0.177	4.018	0.013	2.268	39.589	14.481	15.405	8.315	0.095	0.029	0.045	97.376
Sadanagaite	0.026	10.959	1.941	0.183	3.969	0.023	2.406	39.869	14.653	15.814	8.319	0.058	0.053	0.000	98.318
Sadanagaite	0.029	11.006	1.868	0.195	3.955	0.021	2.282	39.932	14.364	15.388	8.270	0.067	0.026	0.015	97.476
Sadanagaite	0.021	10.993	1.914	0.169	3.956	0.028	2.357	39.939	14.506	15.402	8.416	0.074	0.046	0.011	97.901
Sadanagaite	0.056	10.936	1.985	0.223	3.948	0.050	2.259	39.133	13.887	14.895	8.441	0.086	0.050	0.049	96.078
Sadanagaite	0.054	11.057	1.948	0.190	3.960	0.052	2.350	39.192	14.287	14.809	8.430	0.109	0.049	0.002	96.557
Sadanagaite	0.038	10.887	1.968	0.169	3.995	0.029	2.344	40.200	14.565	15.732	8.462	0.098	0.039	0.001	98.584
Sadanagaite	0.035	11.029	1.984	0.147	3.963	0.011	2.288	39.878	14.587	15.517	8.297	0.051	0.066	0.000	97.889
Sadanagaite	0.042	10.954	2.025	0.192	4.001	0.031	2.269	39.766	14.344	15.415	8.401	0.070	0.035	0.000	97.615
Sadanagaite	0.061	10.965	1.972	0.173	3.931	0.026	2.274	39.520	14.064	15.177	8.436	0.089	0.036	0.030	96.862
Sadanagaite	0.034	10.939	1.969	0.159	3.931	0.037	2.185	39.373	14.388	15.227	8.288	0.071	0.045	0.035	96.779
Sadanagaite	0.043	11.016	1.950	0.125	3.919	0.010	2.318	40.235	14.535	15.325	8.416	0.095	0.066	0.000	98.112
Sadanagaite	0.022	10.999	2.005	0.182	4.011	0.026	2.198	39.721	14.419	15.313	8.549	0.102	0.046	0.024	97.708
Sadanagaite	0.029	10.904	1.951	0.157	3.961	0.021	2.286	39.740	14.464	15.165	8.415	0.104	0.057	0.035	97.360
Sadanagaite	0.036	10.947	2.004	0.135	4.013	0.031	2.220	39.584	14.306	15.289	8.295	0.085	0.078	0.011	97.110
Sadanagaite	0.059	10.993	2.003	0.180	3.968	0.024	2.205	39.288	14.075	15.321	8.479	0.075	0.036	0.005	96.781
Sadanagaite	0.032	11.018	2.032	0.155	4.026	0.036	2.392	40.219	14.730	15.542	8.362	0.060	0.048	0.027	98.746
Sadanagaite	0.041	10.898	2.004	0.156	4.014	0.006	2.307	39.501	14.417	15.384	8.434	0.073	0.023	0.025	97.373
Sadanagaite	0.039	10.944	2.007	0.162	4.006	0.028	2.278	40.090	14.367	15.381	8.458	0.097	0.050	0.000	97.999
Sadanagaite	0.032	10.965	1.979	0.162	4.006	0.049	2.296	39.893	14.261	15.257	8.317	0.093	0.095	0.006	97.481
Sadanagaite	0.019	11.001	1.961	0.197	4.009	0.028	2.273	40.045	14.517	15.487	8.525	0.058	0.033	0.011	98.220
Sadanagaite	0.035	11.219	2.016	0.153	3.996	0.023	2.307	39.626	14.570	15.564	8.481	0.074	0.044	0.009	98.192
Sadanagaite	0.037	10.989	1.986	0.133	3.975	0.072	2.348	40.222	14.553	15.443	8.376	0.091	0.049	0.000	98.401
Sadanagaite	0.068	11.036	1.995	0.112	4.000	0.016	2.219	39.562	14.298	15.504	8.337	0.086	0.022	0.000	97.350
Sadanagaite	0.146	10.452	1.850	0.043	3.939	0.028	2.379	39.422	14.631	15.303	8.218	0.077	0.045	0.009	96.757
Sadanagaite	0.033	10.939	2.020	0.165	3.938	0.033	2.294	40.428	14.744	15.639	8.363	0.082	0.031	0.006	98.776
Sadanagaite	0.035	10.974	2.025	0.179	3.983	0.047	2.329	39.525	14.162	15.263	8.490	0.103	0.046	0.000	97.265
Sadanagaite	0.052	11.172	1.976	0.189	4.020	0.034	2.159	39.404	14.071	14.946	8.094	0.102	0.046	0.021	96.366
Sadanagaite	0.014	10.972	1.983	0.162	3.909	0.000	2.321	39.949	14.552	15.449	8.342	0.097	0.041	0.000	97.855

Sadanagaite	0.038	11.002	1.927	0.180	3.853	0.011	2.256	40.125	14.481	15.274	8.358	0.056	0.062	0.000	97.719
Sadanagaite	0.031	10.771	1.976	0.157	3.955	0.016	2.367	39.658	14.320	15.263	8.451	0.095	0.035	0.025	97.219
Sadanagaite	0.043	10.978	1.971	0.185	3.931	0.021	2.211	39.205	13.975	15.055	8.453	0.079	0.069	0.023	96.272
Sadanagaite	0.042	11.078	2.013	0.181	3.946	0.010	2.353	39.953	14.494	15.340	8.562	0.116	0.049	0.000	98.208
Sadanagaite	0.035	10.650	1.738	0.202	4.226	0.062	2.604	39.971	13.632	15.692	9.708	0.120	0.000	0.000	98.755
Sadanagaite	0.050	10.280	1.657	0.157	4.149	0.044	2.531	39.804	14.043	15.672	9.405	0.113	0.014	0.000	97.985
Sadanagaite	0.043	10.806	1.718	0.221	4.186	0.029	2.531	39.144	13.507	15.456	9.475	0.106	0.000	0.000	97.314
Sadanagaite	0.041	10.719	1.733	0.140	4.231	0.037	2.458	39.604	13.831	15.550	9.539	0.099	0.009	0.009	98.089
Sadanagaite	0.077	10.651	1.779	0.153	4.172	0.034	2.480	39.173	13.397	15.458	9.455	0.111	0.000	0.008	97.024
Sadanagaite	0.057	10.717	1.730	0.122	4.200	0.022	2.448	39.028	13.316	15.255	9.732	0.086	0.009	0.012	96.835
Sadanagaite	0.044	10.677	1.767	0.152	4.231	0.027	2.461	40.020	14.015	15.603	9.588	0.112	0.007	0.023	98.858
Sadanagaite	0.055	10.744	1.727	0.174	4.160	0.020	2.489	38.617	13.352	15.279	9.620	0.076	0.004	0.000	96.408
Sadanagaite	0.044	10.718	1.755	0.138	4.243	0.016	2.538	40.276	13.948	15.644	9.544	0.095	0.000	0.000	99.023
Sadanagaite	0.052	10.801	1.738	0.169	4.270	0.045	2.451	39.586	13.747	15.397	9.420	0.093	0.000	0.000	97.892
Sadanagaite	0.049	10.837	1.711	0.150	4.154	0.035	2.573	39.927	13.928	15.619	9.562	0.113	0.000	0.000	98.729
Sadanagaite	0.052	10.751	1.763	0.149	4.191	0.034	2.421	39.921	13.754	15.619	9.472	0.076	0.007	0.000	98.283
Sadanagaite	0.051	10.718	1.786	0.149	4.250	0.032	2.443	38.897	13.669	15.524	9.680	0.108	0.000	0.000	97.369
Sadanagaite	0.047	10.848	1.636	0.239	4.189	0.045	2.376	38.294	13.328	14.825	10.152	0.092	0.000	0.000	96.154
Sadanagaite	0.061	10.770	1.750	0.189	4.233	0.027	2.512	39.392	13.857	15.607	9.606	0.104	0.015	0.000	98.241
Sadanagaite	0.050	10.903	1.781	0.180	4.220	0.042	2.506	39.828	13.915	15.877	9.548	0.125	0.003	0.015	99.063
Sadanagaite	0.042	10.930	1.970	0.178	3.941	0.020	2.180	39.733	14.381	15.190	8.389	0.073	0.039	0.000	97.139
Sadanagaite	0.036	10.964	2.018	0.106	3.933	0.035	2.112	40.058	14.424	15.408	8.216	0.063	0.027	0.004	97.486
Sadanagaite	0.042	10.906	1.967	0.140	3.844	0.013	2.250	39.914	14.705	15.500	8.191	0.077	0.020	0.006	97.653
Sadanagaite	0.044	11.030	2.016	0.142	3.846	0.028	2.193	39.976	14.549	15.506	8.282	0.121	0.035	0.012	97.878
Sadanagaite	0.035	10.991	2.013	0.138	3.888	0.024	2.271	39.944	14.842	15.343	8.194	0.118	0.033	0.015	97.930
Sadanagaite	0.046	11.000	1.978	0.143	3.894	0.015	2.281	40.047	14.662	15.425	8.359	0.111	0.068	0.006	98.103
Sadanagaite	0.037	10.813	1.937	0.180	3.863	0.003	2.224	39.382	14.113	15.105	8.100	0.106	0.040	0.020	95.994
Sadanagaite	0.035	11.009	2.023	0.160	3.849	0.024	2.136	39.544	14.401	15.298	8.267	0.096	0.019	0.011	96.980
Sadanagaite	0.041	10.984	1.990	0.180	3.883	0.024	2.133	39.942	14.668	15.429	8.413	0.080	0.013	0.009	97.853

Sadanagaite	0.031	10.946	2.031	0.174	3.865	0.011	2.179	39.246	14.203	15.281	8.280	0.116	0.029	0.005	96.521
Sadanagaite	0.037	10.935	2.000	0.168	3.947	0.003	2.188	39.705	14.608	15.329	8.410	0.111	0.013	0.012	97.537
Sadanagaite	0.047	11.118	1.963	0.179	3.898	0.011	2.266	40.025	14.664	15.320	8.198	0.078	0.053	0.000	97.898
Sadanagaite	0.034	10.965	2.046	0.183	3.964	0.018	2.185	39.747	14.558	15.505	8.421	0.094	0.038	0.000	97.884
Sadanagaite	0.047	10.972	1.992	0.143	3.898	0.036	2.150	39.181	14.098	14.960	8.219	0.063	0.014	0.044	95.897
Sadanagaite	0.046	11.002	2.008	0.177	3.843	0.011	2.163	39.396	14.189	15.291	8.295	0.057	0.019	0.000	96.550
Sadanagaite	0.035	11.133	2.015	0.199	3.917	0.047	2.225	39.375	14.242	15.194	8.210	0.101	0.060	0.005	96.831
Sadanagaite	0.037	11.089	2.041	0.148	3.856	0.031	2.157	39.451	14.367	15.027	8.265	0.092	0.023	0.020	96.693
Sadanagaite	0.039	11.062	2.019	0.170	3.915	0.031	2.276	40.344	14.759	15.464	8.306	0.113	0.000	0.006	98.592
Sadanagaite	0.034	11.023	2.053	0.178	3.895	0.016	2.168	39.628	14.448	15.264	8.323	0.087	0.043	0.010	97.252
Sadanagaite	0.029	11.044	2.019	0.136	3.893	0.011	2.233	40.193	14.671	15.445	8.278	0.107	0.059	0.008	98.200
Sadanagaite	0.049	10.981	2.012	0.162	3.935	0.026	2.210	39.828	14.581	15.381	8.369	0.074	0.030	0.004	97.697
Sadanagaite	0.034	10.876	2.015	0.154	3.870	0.026	2.203	40.240	14.765	15.348	8.164	0.089	0.031	0.000	97.924
Sadanagaite	0.030	11.001	2.030	0.164	3.964	0.008	2.229	39.699	14.520	15.191	8.418	0.081	0.037	0.016	97.485
Sadanagaite	0.033	11.054	1.996	0.149	3.943	0.020	2.231	40.306	14.662	15.457	8.260	0.078	0.025	0.024	98.361
Sadanagaite	0.029	10.800	1.988	0.084	3.904	0.028	2.236	39.783	14.787	15.534	8.138	0.082	0.040	0.000	97.538
Sadanagaite	0.043	11.190	2.009	0.169	3.918	0.031	2.237	39.528	14.460	15.211	8.190	0.076	0.040	0.010	97.211
Sadanagaite	0.036	11.156	2.036	0.183	3.954	0.021	2.259	40.204	14.837	15.492	8.197	0.093	0.033	0.051	98.640
Sadanagaite	0.032	11.158	2.025	0.185	3.910	0.029	2.274	40.297	14.784	15.588	8.214	0.119	0.011	0.000	98.692
Sadanagaite	0.027	10.941	2.028	0.184	3.932	0.029	2.125	39.828	14.362	15.344	8.344	0.095	0.039	0.005	97.388
Sadanagaite	0.040	11.114	2.027	0.157	3.853	0.021	2.314	40.124	14.780	15.486	8.228	0.070	0.005	0.000	98.299
Sadanagaite	0.059	11.098	2.022	0.171	3.863	0.021	2.372	39.864	14.653	15.299	8.119	0.054	0.018	0.000	97.681
Sadanagaite	0.047	10.929	1.983	0.178	3.951	0.028	2.299	40.045	14.401	15.589	8.234	0.081	0.044	0.000	97.895
Sadanagaite	0.042	10.947	1.964	0.167	3.922	0.031	2.287	39.713	14.642	15.194	8.397	0.095	0.058	0.000	97.508
Sadanagaite	0.041	10.984	1.987	0.165	3.913	0.018	2.263	39.862	14.573	15.243	8.251	0.091	0.044	0.000	97.553
Sadanagaite	0.022	10.964	1.945	0.211	3.874	0.029	2.245	38.950	14.240	14.919	8.273	0.078	0.055	0.000	95.946
Sadanagaite	0.050	11.036	2.042	0.184	3.872	0.018	2.248	39.707	14.471	15.337	8.211	0.087	0.044	0.010	97.380
Sadanagaite	0.033	11.007	1.986	0.133	3.929	0.031	2.239	39.710	14.519	15.400	8.231	0.092	0.030	0.026	97.491
Sadanagaite	0.034	10.968	2.010	0.160	3.875	0.003	2.171	39.600	14.576	14.916	8.164	0.101	0.030	0.013	96.700

Sadanagaite	0.018	11.327	2.058	0.145	3.691	0.000	2.277	39.233	14.866	15.165	8.091	0.071	0.053	0.018	97.105
Sadanagaite	0.037	11.002	1.987	0.205	3.866	0.034	2.164	39.346	14.382	14.704	8.128	0.088	0.030	0.015	96.070
Sadanagaite	0.033	11.032	2.013	0.181	3.880	0.007	2.284	40.328	14.733	15.080	8.278	0.075	0.020	0.021	98.057
Sadanagaite	0.024	11.004	2.048	0.165	3.826	0.038	2.228	39.630	14.560	14.840	8.281	0.080	0.036	0.021	96.839
Sadanagaite	0.027	10.809	1.983	0.144	3.870	0.025	2.176	39.658	14.643	14.971	8.253	0.102	0.018	0.014	96.753
Sadanagaite	0.045	10.988	1.991	0.177	3.832	0.023	2.139	39.797	14.555	14.886	8.249	0.109	0.021	0.004	96.948
Sadanagaite	0.024	11.020	2.094	0.155	3.824	0.018	2.284	40.320	15.139	15.179	8.173	0.069	0.050	0.001	98.429
Sadanagaite	0.030	11.068	1.997	0.184	3.797	0.038	2.293	40.258	14.832	15.203	8.155	0.094	0.012	0.000	98.046
Sadanagaite	0.030	11.009	2.018	0.130	3.808	0.030	2.158	39.658	14.670	14.843	8.221	0.092	0.025	0.011	96.747
Sadanagaite	0.024	11.162	2.048	0.162	3.881	0.017	2.281	40.604	14.978	15.166	8.120	0.095	0.047	0.000	98.651
Sadanagaite	0.032	10.876	2.051	0.158	3.807	0.034	2.320	40.668	15.115	15.459	8.112	0.078	0.017	0.000	98.798
Sadanagaite	0.038	10.998	2.009	0.171	3.822	0.026	2.141	39.381	14.331	14.899	8.103	0.091	0.007	0.026	96.129
Sadanagaite	0.039	11.046	2.034	0.136	3.805	0.031	2.151	39.787	14.881	15.096	8.108	0.107	0.040	0.038	97.401
Sadanagaite	0.033	10.935	2.032	0.144	3.895	0.020	2.271	40.060	14.785	15.255	8.198	0.094	0.039	0.024	97.881
Sadanagaite	0.020	10.860	1.989	0.159	3.861	0.023	2.228	40.479	14.854	15.268	8.026	0.110	0.022	0.026	98.009
Sadanagaite	0.036	10.935	2.042	0.169	3.826	0.016	2.266	39.758	14.739	14.991	8.178	0.100	0.034	0.026	97.176
Sadanagaite	0.039	10.875	2.010	0.176	3.891	0.018	2.288	40.859	15.236	15.226	8.379	0.092	0.000	0.049	99.192
Sadanagaite	0.037	11.136	1.888	0.189	3.832	0.013	2.415	39.744	14.568	14.342	8.008	0.096	0.039	0.018	96.424
Sadanagaite	0.049	11.001	1.981	0.192	3.827	0.015	2.110	39.720	14.409	14.711	8.210	0.078	0.057	0.054	96.500
Sadanagaite	0.036	10.992	2.037	0.238	3.811	0.024	2.219	39.178	14.570	14.773	8.176	0.082	0.055	0.041	96.363
Sadanagaite	0.031	10.944	1.958	0.135	3.878	0.034	2.124	39.793	14.458	15.240	8.211	0.095	0.018	0.008	97.031
Sadanagaite	0.038	10.936	2.060	0.200	3.932	0.015	2.228	40.209	14.973	15.640	8.224	0.086	0.038	0.023	98.674
Sadanagaite	0.025	10.994	1.989	0.165	3.859	0.010	2.152	39.977	14.586	15.404	8.274	0.093	0.055	0.020	97.682
Sadanagaite	0.024	11.027	2.015	0.175	3.863	0.005	2.206	39.939	14.554	15.210	8.217	0.065	0.016	0.015	97.427
Sadanagaite	0.031	10.962	2.026	0.209	3.915	0.023	2.133	39.450	14.373	15.169	8.309	0.066	0.044	0.000	96.813
Sadanagaite	0.026	10.954	1.991	0.189	3.889	0.028	2.193	39.638	14.331	15.266	8.330	0.080	0.050	0.000	97.022
Sadanagaite	0.028	11.054	2.032	0.122	3.942	0.000	2.326	40.166	14.855	15.666	8.201	0.067	0.070	0.008	98.597
Sadanagaite	0.044	11.047	2.041	0.205	3.903	0.037	2.311	39.940	14.364	15.381	8.271	0.077	0.031	0.004	97.708
Sadanagaite	0.063	11.047	2.033	0.168	3.876	0.019	2.189	39.198	14.300	15.135	8.047	0.090	0.032	0.016	96.459

Sadanagaite	0.049	11.073	1.983	0.191	3.942	0.055	2.189	39.378	14.347	15.150	8.242	0.066	0.048	0.000	96.769
Sadanagaite	0.042	10.989	2.031	0.169	3.911	0.034	2.148	39.762	14.483	15.247	8.297	0.093	0.025	0.024	97.347
Sadanagaite	0.030	10.932	2.037	0.174	3.936	0.011	2.262	40.188	14.600	15.157	8.180	0.099	0.023	0.013	97.718
Sadanagaite	0.022	11.009	2.022	0.179	3.873	0.020	2.103	39.764	14.490	15.249	8.239	0.089	0.044	0.031	97.223
Sadanagaite	0.038	10.986	2.027	0.163	3.945	0.025	2.180	39.287	14.329	15.087	8.197	0.075	0.021	0.014	96.430
Sadanagaite	0.051	11.007	2.016	0.186	3.923	0.021	2.162	39.936	14.537	15.387	8.204	0.126	0.033	0.009	97.704
Sadanagaite	0.030	10.881	1.996	0.110	3.919	0.029	2.208	39.867	14.394	15.418	8.196	0.066	0.031	0.009	97.259
Sadanagaite	0.023	10.962	2.039	0.178	3.839	0.027	2.174	39.343	14.250	15.082	8.348	0.068	0.041	0.032	96.503
Sadanagaite	0.035	11.028	2.093	0.188	3.886	0.021	2.184	39.752	14.432	15.343	8.180	0.067	0.025	0.001	97.310
Sadanagaite	0.033	11.053	2.014	0.194	3.887	0.021	2.163	40.161	14.655	15.464	8.418	0.082	0.052	0.000	98.276
Sadanagaite	0.033	10.967	2.011	0.195	3.898	0.013	2.253	39.771	14.599	15.413	8.306	0.090	0.028	0.039	97.703
Sadanagaite	0.025	11.025	2.060	0.161	3.955	0.028	2.319	39.878	14.527	15.317	8.314	0.090	0.043	0.003	97.822
Sadanagaite	0.042	11.045	2.002	0.180	3.945	0.013	2.307	40.030	14.499	15.429	8.201	0.059	0.060	0.023	97.926
Sadanagaite	0.048	10.879	1.983	0.208	3.921	0.026	2.141	38.903	14.529	15.019	8.252	0.096	0.027	0.006	96.150
Sadanagaite	0.035	10.755	2.014	0.161	3.952	0.021	2.231	39.642	14.368	15.256	8.225	0.046	0.040	0.032	96.874
Sadanagaite	0.039	11.288	1.966	0.210	3.901	0.036	2.299	39.732	14.722	15.075	7.976	0.071	0.027	0.000	97.468
Sadanagaite	0.025	11.030	2.019	0.181	3.899	0.016	2.256	40.036	14.512	15.286	8.177	0.058	0.019	0.026	97.644
Sadanagaite	0.041	11.084	2.020	0.186	3.982	0.039	2.103	39.099	14.230	15.112	8.287	0.068	0.051	0.009	96.397
Sadanagaite	0.033	10.973	2.023	0.149	3.923	0.020	2.194	39.913	14.670	15.506	8.085	0.100	0.039	0.008	97.727
Sadanagaite	0.035	10.977	2.017	0.160	3.888	0.015	2.264	40.090	14.526	15.514	8.311	0.057	0.030	0.031	97.992
Sadanagaite	0.017	10.880	1.977	0.121	3.936	0.044	2.231	39.932	14.572	15.369	7.996	0.084	0.018	0.006	97.251
Sadanagaite	0.045	10.857	2.004	0.154	3.803	0.052	2.233	39.666	14.528	15.299	8.321	0.120	0.026	0.006	97.188
Sadanagaite	0.042	11.175	1.953	0.166	3.941	0.015	2.196	40.181	14.545	15.502	8.455	0.085	0.038	0.027	98.433
Sadanagaite	0.040	11.113	1.992	0.176	3.902	0.015	2.201	40.219	14.755	15.568	8.341	0.063	0.046	0.015	98.533
Sadanagaite	0.030	10.921	1.996	0.091	3.900	0.030	2.237	39.650	14.838	15.508	8.289	0.081	0.034	0.001	97.660
Sadanagaite	0.042	11.043	2.021	0.189	3.911	0.029	2.171	39.864	14.474	15.521	8.272	0.075	0.019	0.016	97.732
Sadanagaite	0.027	10.963	2.038	0.171	3.859	0.010	2.131	39.066	14.146	15.006	8.288	0.063	0.025	0.000	95.879
Sadanagaite	0.039	10.913	1.992	0.131	3.890	0.023	2.188	40.161	14.671	15.320	8.210	0.076	0.056	0.000	97.755
Sadanagaite	0.029	11.007	1.968	0.144	3.962	0.015	2.160	39.692	14.324	15.156	8.193	0.066	0.043	0.000	96.841

Sadanagaite	0.032	10.958	2.139	0.175	3.804	0.019	2.058	39.394	14.047	15.310	8.019	0.108	0.025	0.009	96.151
Sadanagaite	0.032	10.941	1.999	0.147	3.888	0.011	2.143	39.068	14.174	15.058	8.150	0.091	0.037	0.006	95.835
Sadanagaite	0.037	9.732	1.808	0.000	3.507	0.000	2.149	40.974	16.748	15.518	7.256	0.100	0.003	0.006	97.883
Sadanagaite	0.019	11.063	2.049	0.180	3.910	0.018	2.149	39.898	14.554	15.330	8.269	0.098	0.036	0.015	97.707
Sadanagaite	0.024	10.883	1.995	0.147	3.936	0.021	2.291	40.527	14.699	15.502	8.059	0.117	0.047	0.000	98.334
Sadanagaite	0.032	10.869	2.032	0.169	3.943	0.003	2.218	39.661	14.578	15.402	8.196	0.087	0.038	0.043	97.324
Sadanagaite	0.031	10.884	2.038	0.178	3.889	0.036	2.162	39.839	14.581	15.538	8.203	0.097	0.069	0.020	97.658
Sadanagaite	0.031	10.868	2.048	0.140	3.854	0.041	2.326	40.049	14.650	15.365	8.191	0.095	0.033	0.022	97.774
Sadanagaite	0.031	10.858	1.949	0.115	3.863	0.004	2.253	40.158	14.673	15.501	8.241	0.068	0.020	0.011	97.824
Sadanagaite	0.038	10.909	1.998	0.187	3.828	0.041	2.203	39.198	14.453	15.200	8.242	0.056	0.038	0.010	96.457
Sadanagaite	0.029	11.037	2.004	0.189	3.901	0.037	2.179	39.787	14.536	15.096	8.265	0.112	0.019	0.000	97.228
Sadanagaite	0.018	11.150	2.035	0.152	3.898	0.019	2.218	40.333	14.954	15.406	8.292	0.095	0.003	0.026	98.689
Sadanagaite	0.051	10.950	1.997	0.215	3.918	0.011	2.290	39.389	14.369	15.153	8.217	0.061	0.036	0.017	96.805
Sadanagaite	0.032	10.992	2.010	0.183	3.835	0.026	2.224	39.388	14.383	15.084	8.142	0.075	0.028	0.004	96.508
Sadanagaite	0.031	11.241	2.004	0.204	3.937	0.009	2.220	39.505	14.475	15.171	8.274	0.068	0.026	0.004	97.258
Sadanagaite	0.033	11.049	2.002	0.184	3.899	0.026	2.237	39.350	14.483	14.905	8.310	0.106	0.023	0.000	96.729
Sadanagaite	0.029	11.206	2.029	0.304	3.873	0.008	2.421	38.916	14.125	14.948	7.764	0.099	0.027	0.002	95.841
Sadanagaite	0.044	10.918	1.987	0.128	3.866	0.019	2.180	39.608	14.398	14.947	8.214	0.072	0.046	0.007	96.504
Sadanagaite	0.036	11.002	2.012	0.164	3.872	0.003	2.348	40.815	14.776	15.512	8.191	0.063	0.055	0.028	98.962
Sadanagaite	0.012	11.070	2.043	0.182	3.918	0.050	2.234	39.762	14.629	15.285	8.319	0.085	0.033	0.013	97.712
Sadanagaite	0.030	11.126	1.993	0.160	3.911	0.026	2.202	39.696	14.755	15.056	8.323	0.103	0.048	0.008	97.552
Sadanagaite	0.028	11.065	1.978	0.149	3.860	0.019	2.274	39.798	14.613	15.197	8.086	0.079	0.037	0.018	97.283
Sadanagaite	0.038	11.076	1.978	0.160	3.906	0.021	2.262	39.790	14.628	15.162	8.318	0.095	0.070	0.025	97.644
Sadanagaite	0.021	11.113	1.965	0.190	3.898	0.040	2.337	39.925	14.596	15.185	8.139	0.063	0.040	0.029	97.636
Sadanagaite	0.021	11.084	2.003	0.188	3.913	0.023	2.205	39.958	14.659	15.289	8.263	0.091	0.021	0.000	97.790
Sadanagaite	0.024	11.202	1.980	0.181	3.835	0.000	2.156	39.404	14.345	14.725	8.188	0.080	0.030	0.011	96.257
Sadanagaite	0.026	11.099	1.985	0.145	3.857	0.027	2.302	39.649	14.725	15.328	8.359	0.090	0.059	0.026	97.769
Sadanagaite	0.027	11.154	2.010	0.194	3.814	0.011	2.241	39.776	14.697	15.189	8.315	0.087	0.033	0.001	97.626
Sadanagaite	0.016	10.960	1.977	0.189	3.900	0.018	2.278	39.654	14.422	15.225	8.258	0.096	0.028	0.015	97.158

Sadanagaite	0.026	11.003	2.014	0.116	3.890	0.044	2.325	40.272	15.013	15.823	8.196	0.100	0.037	0.012	99.022
Sadanagaite	0.036	11.200	1.985	0.169	3.875	0.039	2.218	39.813	14.536	15.128	8.179	0.089	0.050	0.030	97.441
Sadanagaite	0.020	11.095	1.956	0.162	3.889	0.006	2.205	39.916	14.535	15.137	8.155	0.095	0.021	0.000	97.264
Sadanagaite	0.027	11.121	1.994	0.136	3.851	0.016	2.236	39.936	14.743	15.252	8.177	0.069	0.031	0.006	97.704
Sadanagaite	0.028	11.013	1.955	0.253	3.949	0.014	2.305	39.416	14.364	14.909	8.228	0.079	0.032	0.000	96.630
Sadanagaite	0.024	11.090	1.974	0.185	3.888	0.000	2.208	39.661	14.669	15.265	8.197	0.084	0.045	0.018	97.432
Sadanagaite	0.030	11.059	2.025	0.210	3.821	0.016	2.192	39.189	14.345	14.987	8.236	0.093	0.029	0.010	96.346
Sadanagaite	0.027	10.984	1.979	0.211	3.875	0.029	2.153	40.097	14.681	15.462	8.200	0.073	0.034	0.011	97.922
Sadanagaite	0.024	11.061	2.072	0.205	3.812	0.019	2.146	39.112	14.377	14.912	8.222	0.088	0.036	0.020	96.205
Sadanagaite	0.045	11.110	2.009	0.213	3.808	0.021	2.258	39.535	14.413	14.889	8.363	0.093	0.039	0.020	96.925
Sadanagaite	0.028	10.984	1.939	0.196	3.880	0.026	2.113	39.553	14.435	15.047	8.138	0.068	0.042	0.030	96.547
Sadanagaite	0.023	11.133	1.975	0.213	3.961	0.015	2.245	39.865	14.768	15.302	8.162	0.098	0.025	0.000	97.865
Sadanagaite	0.034	11.059	2.013	0.193	3.872	0.010	2.348	40.232	14.653	15.204	8.131	0.059	0.041	0.002	97.988
Sadanagaite	0.031	11.030	2.024	0.201	3.903	0.021	2.259	39.141	14.207	14.824	7.950	0.095	0.050	0.012	95.846
Sadanagaite	0.025	11.065	2.009	0.184	3.865	0.031	2.254	39.775	14.844	15.220	8.297	0.107	0.020	0.000	97.794
Sadanagaite	0.031	11.034	2.044	0.151	3.852	0.015	2.347	40.592	14.719	15.415	8.195	0.083	0.028	0.012	98.601
Sadanagaite	0.021	11.047	1.991	0.197	3.873	0.024	2.040	39.238	14.335	14.837	8.214	0.079	0.015	0.000	95.977
Sadanagaite	0.033	11.459	1.980	0.223	4.020	0.001	2.467	39.023	14.345	14.794	7.982	0.085	0.007	0.026	96.542
Sadanagaite	0.027	11.086	2.006	0.152	3.830	0.023	2.299	40.647	15.101	15.468	8.149	0.073	0.021	0.011	98.970
Sadanagaite	0.029	10.961	2.011	0.162	3.940	0.026	2.270	40.471	14.881	15.312	8.043	0.079	0.028	0.015	98.347
Sadanagaite	0.037	11.007	1.974	0.184	3.862	0.028	2.249	40.274	14.936	15.180	8.243	0.088	0.003	0.000	98.111
Sadanagaite	0.019	10.965	1.991	0.139	3.869	0.010	2.288	40.371	14.743	15.443	8.206	0.086	0.024	0.038	98.296
Sadanagaite	0.028	11.040	2.010	0.221	3.877	0.005	2.201	39.629	14.499	14.988	8.306	0.083	0.046	0.000	97.016
Sadanagaite	0.032	10.942	1.968	0.191	3.880	0.000	2.165	39.831	14.515	15.126	8.243	0.079	0.007	0.032	97.092
Sadanagaite	0.040	10.846	1.995	0.224	3.862	0.029	2.224	39.409	14.329	15.070	8.002	0.051	0.030	0.011	96.211
Sadanagaite	0.030	11.168	1.998	0.209	3.930	0.005	2.223	39.642	14.562	15.222	8.315	0.076	0.045	0.002	97.510
Sadanagaite	0.026	11.173	2.067	0.141	3.892	0.005	2.105	39.495	14.330	15.065	8.231	0.102	0.060	0.000	96.757
Sadanagaite	0.039	11.044	2.031	0.163	3.897	0.047	2.203	39.559	14.403	15.274	8.176	0.079	0.035	0.002	97.046
Sadanagaite	0.026	11.035	1.993	0.236	3.843	0.024	2.179	39.124	14.299	14.795	8.159	0.073	0.046	0.000	95.956

Sadanagaite	0.025	10.961	1.988	0.180	3.920	0.024	2.255	40.273	15.050	15.539	8.342	0.074	0.035	0.015	98.780
Sadanagaite	0.029	11.093	2.006	0.197	3.960	0.019	2.205	39.787	14.383	14.983	8.192	0.082	0.020	0.008	97.051
Sadanagaite	0.020	11.014	2.001	0.169	3.897	0.014	2.164	39.397	14.366	15.021	8.215	0.118	0.014	0.007	96.500
Sadanagaite	0.034	10.919	1.978	0.194	3.881	0.016	2.122	39.396	14.359	14.961	8.306	0.082	0.044	0.002	96.370
Sadanagaite	0.024	11.161	1.984	0.189	3.928	0.024	2.201	39.830	14.595	14.980	8.286	0.093	0.039	0.020	97.443
Sadanagaite	0.039	11.108	1.943	0.193	3.904	0.036	2.179	39.428	14.235	15.052	8.213	0.081	0.012	0.023	96.507
Sadanagaite	0.030	11.071	2.020	0.203	3.819	0.011	2.244	40.410	14.742	15.385	8.250	0.092	0.036	0.005	98.409
Sadanagaite	0.026	11.005	1.973	0.158	3.854	0.011	2.187	39.236	14.399	14.684	8.258	0.064	0.025	0.005	95.960
Sadanagaite	0.024	11.089	1.979	0.129	3.933	0.023	2.239	40.055	14.534	15.208	8.373	0.076	0.018	0.037	97.813
Sadanagaite	0.039	11.052	2.023	0.210	3.844	0.016	2.288	40.110	14.816	15.362	8.253	0.095	0.038	0.005	98.248
Sadanagaite	0.023	11.020	2.034	0.182	3.907	0.018	2.143	39.128	14.200	14.866	8.291	0.103	0.053	0.000	96.078
Sadanagaite	0.038	11.085	2.028	0.176	3.882	0.019	2.175	39.561	14.372	14.975	8.241	0.062	0.014	0.000	96.716
Sadanagaite	0.033	11.047	1.946	0.173	3.880	0.034	2.229	40.565	14.686	15.455	8.258	0.105	0.044	0.016	98.533
Sadanagaite	0.031	10.987	1.977	0.206	3.933	0.000	2.196	39.611	14.583	15.250	8.231	0.117	0.002	0.000	97.191
Sadanagaite	0.041	11.171	2.017	0.187	3.874	0.034	2.132	39.001	14.223	14.901	8.253	0.090	0.027	0.000	96.056
Sadanagaite	0.049	11.036	1.992	0.185	3.826	0.021	2.264	40.028	14.794	15.380	8.144	0.111	0.045	0.013	97.980
Sadanagaite	0.066	11.076	1.985	0.206	3.869	0.016	2.189	39.052	14.218	14.864	8.218	0.090	0.010	0.007	95.937
Sadanagaite	0.046	11.065	1.971	0.210	3.831	0.005	2.201	40.151	14.655	15.277	8.244	0.068	0.025	0.009	97.806
Sadanagaite	0.046	11.099	1.995	0.153	3.861	0.018	2.227	40.100	14.618	15.178	8.359	0.098	0.036	0.000	97.841
Sadanagaite	0.072	10.847	2.010	0.175	3.772	0.006	2.317	39.343	14.475	15.001	8.100	0.130	0.048	0.000	96.386
Sadanagaite	0.026	11.130	1.989	0.184	3.884	0.020	2.277	39.973	14.931	15.318	8.348	0.109	0.050	0.028	98.357
Sadanagaite	0.040	11.076	1.998	0.210	3.855	0.013	2.367	39.504	14.406	15.222	8.075	0.098	0.048	0.007	97.018
Sadanagaite	0.056	11.139	2.037	0.217	3.838	0.027	2.376	39.582	14.351	14.932	8.091	0.071	0.018	0.017	96.922
Sadanagaite	0.048	11.065	1.980	0.189	3.846	0.024	2.211	39.665	14.456	15.262	8.133	0.067	0.025	0.020	97.074
Sadanagaite	0.033	11.101	2.024	0.205	3.968	0.019	2.225	39.426	14.509	14.989	8.269	0.090	0.012	0.003	96.985
Sadanagaite	0.035	11.083	2.021	0.135	3.874	0.021	2.408	40.882	15.243	15.708	8.292	0.093	0.056	0.006	99.909
Sadanagaite	0.040	11.110	2.001	0.174	3.966	0.026	2.255	40.424	14.847	15.473	8.221	0.107	0.051	0.000	98.791
Sadanagaite	0.038	11.159	1.982	0.207	3.917	0.019	2.220	39.697	14.511	15.198	8.253	0.078	0.041	0.009	97.406
Sadanagaite	0.050	10.916	1.932	0.113	3.864	0.019	2.232	39.580	14.886	14.962	8.075	0.099	0.031	0.022	96.870

Sadanagaite	0.031	11.098	1.961	0.192	3.970	0.038	2.122	39.749	14.598	15.093	8.329	0.111	0.028	0.000	97.449
Sadanagaite	0.034	11.009	1.990	0.135	3.907	0.039	2.183	39.979	14.520	15.448	8.247	0.082	0.046	0.042	97.763
Sadanagaite	0.034	11.063	2.042	0.172	3.883	0.006	2.236	40.258	14.592	15.294	8.192	0.090	0.061	0.000	98.068
Sadanagaite	0.029	11.186	2.004	0.182	3.977	0.008	2.145	39.679	14.445	14.979	8.148	0.106	0.037	0.032	97.055
Sadanagaite	0.032	11.145	1.988	0.149	3.948	0.024	2.221	39.981	14.602	15.260	8.256	0.110	0.018	0.025	97.894
Sadanagaite	0.040	11.166	2.100	0.179	3.896	0.026	2.193	39.496	14.300	15.126	8.352	0.091	0.025	0.000	97.118
Sadanagaite	0.025	11.043	2.036	0.156	3.956	0.019	2.203	39.881	14.581	15.155	8.262	0.069	0.013	0.037	97.525
Sadanagaite	0.031	11.070	1.971	0.183	3.965	0.039	2.126	39.117	14.165	14.962	8.271	0.071	0.025	0.000	96.060
Sadanagaite	0.031	11.235	1.991	0.192	3.910	0.022	2.154	39.297	14.351	14.880	8.197	0.096	0.029	0.046	96.549
Sadanagaite	0.036	11.071	1.985	0.149	3.911	0.009	2.240	40.137	14.534	15.322	8.176	0.096	0.009	0.041	97.771
Sadanagaite	0.028	11.167	2.058	0.142	3.942	0.021	2.208	40.597	14.741	15.432	8.175	0.096	0.016	0.000	98.746
Sadanagaite	0.037	11.040	1.995	0.155	3.979	0.032	2.123	39.650	14.441	15.253	8.253	0.082	0.011	0.012	97.141
Sadanagaite	0.047	11.127	2.011	0.157	3.852	0.036	2.274	40.297	14.940	15.412	8.131	0.058	0.046	0.000	98.524
Sadanagaite	0.065	11.099	2.050	0.172	3.877	0.026	2.149	40.076	14.528	15.249	8.203	0.086	0.025	0.000	97.651
Sadanagaite	0.050	11.098	2.010	0.155	3.987	0.023	2.145	39.736	14.347	15.163	8.348	0.103	0.035	0.000	97.264
Sadanagaite	0.057	11.005	1.991	0.161	3.910	0.000	2.195	40.194	14.531	15.554	8.228	0.076	0.015	0.000	97.979
Sadanagaite	0.059	11.178	2.001	0.177	3.901	0.029	2.202	40.054	14.381	15.247	8.144	0.092	0.054	0.024	97.627
Sadanagaite	0.037	10.961	1.988	0.132	3.913	0.026	2.223	40.305	14.782	15.331	8.303	0.091	0.018	0.021	98.203
Sadanagaite	0.051	11.115	2.033	0.189	3.946	0.038	2.315	40.446	14.601	15.476	8.263	0.061	0.017	0.000	98.657
Sadanagaite	0.033	10.884	1.796	0.066	3.881	0.047	2.324	38.441	13.471	14.345	9.482	0.111	0.009	0.001	95.017
Sadanagaite	0.039	10.869	1.806	0.129	3.847	0.026	2.369	38.954	13.694	14.545	9.273	0.091	0.012	0.000	95.734
Sadanagaite	0.023	11.087	1.917	0.055	4.028	0.012	2.400	39.191	14.160	14.581	8.502	0.124	0.029	0.009	96.267
Sadanagaite	0.027	11.085	1.892	0.082	4.069	0.030	2.409	39.425	14.298	14.770	8.625	0.087	0.021	0.033	96.954
Sadanagaite	0.031	11.009	1.845	0.027	3.929	0.027	2.423	39.197	13.953	14.640	8.804	0.096	0.019	0.003	96.093
Sadanagaite	0.023	10.874	1.887	0.037	3.895	0.025	2.491	40.200	14.194	15.245	8.764	0.098	0.031	0.014	97.862
Sadanagaite	0.026	10.945	1.856	0.061	4.018	0.000	2.300	39.363	14.029	14.829	8.930	0.089	0.000	0.001	96.556
Sadanagaite	0.036	11.027	1.869	0.069	3.905	0.028	2.475	39.684	14.159	14.760	8.906	0.107	0.022	0.015	97.182

APPENDIX 4: EASYMELTS MODELLING

Fractionation of Trachybasalt

Note: each new composition was taken from the previous fractionated liquid

Fractionation ↓	Temperature (°c)	Pressure (bar)	SiO2 %	TiO2 %	Al2O3 %	Fe2O3 %	Cr2O3 %	FeO %	MnO %	MgO %	CaO %	Na2O %	K2O %	P2O5 %
	1375	10000	47.41	2.02	15.35	1.77	0.04	10.18	0.19	8.58	7.95	3.99	1.93	0.59
	1325	10000	47.11	2.11	15.93	1.83	0.02	10.18	0.20	7.48	8.28	4.20	2.03	0.62
	1275	10000	46.79	2.40	17.74	1.90	0.00	10.29	0.24	5.29	7.28	4.97	2.46	0.65
	1225	10000	47.84	2.60	19.33	1.89	0.00	10.06	0.30	3.23	5.17	6.01	3.08	0.48
	1175	10000	51.88	2.23	20.28	1.51	0.00	7.11	0.37	1.71	3.58	7.17	3.78	0.38
	1125	10000	53.82	1.89	20.08	1.10	0.00	4.15	0.75	1.34	2.34	8.81	5.34	0.38
	1075	10000	54.16	1.55	20.06	0.90	0.00	2.86	1.12	0.98	1.59	10.84	5.58	0.36
	1025	10000	54.11	1.34	20.03	0.82	0.00	2.20	1.39	0.62	1.10	12.92	5.17	0.31
	975	10000	60.26	0.74	12.58	1.14	0.00	2.30	1.16	0.30	0.93	17.00	3.32	0.26
	925	10000	62.93	0.45	9.66	1.33	0.00	2.02	0.85	0.14	0.79	19.01	2.58	0.24

Melting Arrays of Peridotite

*Note: * indicates lost data. FeO & Fe_2O_3 calculated from FeO(t) assuming 85% of Fe^{2+} is FeO, and 15% of FeO(t) is Fe^{3+}.*

Peridotite Melting at 10kbar. QFM = 0. No H2O				
Temp (°c)	1240	*	*	*
Melt	1%	3%	5%	10%
SiO2	54.54	49.17	46.99	45.87
TiO2	0.39	0.61	0.63	0.50
Al2O3	20.66	18.07	16.16	14.12
FeO	1.79	5.47	7.15	8.40
Fe2O3	0.47	1.11	1.34	1.51
Cr2O3	*	*	*	*
MnO	*	*	*	*
MgO	3.38	8.87	11.68	13.87
CaO	4.21	9.20	11.44	12.97
Na2O	7.37	4.73	2.98	1.78
K2O	6.54	2.29	1.27	0.67
P2O	0.55	0.33	0.18	0.10

Peridotite Melting at 8kbar. QFM = 0. No H2O				
Temp (°c)	1200	*	*	*
Melt	1%	3%	5%	10%
SiO2	55.79	50.70	48.49	47.08
TiO2	0.34	0.58	0.62	0.49
Al2O3	20.65	18.88	17.23	14.80
FeO	1.52	4.53	6.08	7.42
Fe2O3	0.41	0.95	1.18	1.37
Cr2O3	*	*	*	*
MnO	*	*	*	*
MgO	3.00	7.88	10.44	13.07
CaO	4.02	8.86	11.11	13.12
Na2O	7.59	4.88	3.18	1.73
K2O	6.05	2.26	1.31	0.63
P2O	0.56	0.32	0.19	0.09

Peridotite Melting at 5kbar. QFM = 0. No H2O				
Temp (°c)	1190	*	*	*
Melt	1%	3%	5%	10%
SiO2	55.91	53.66	50.97	49.71
TiO2	0.46	0.51	0.59	0.52
Al2O3	20.62	20.44	18.50	16.75
FeO	1.67	3.10	4.56	5.54
Fe2O3	0.42	0.69	0.92	1.08
Cr2O3	*	*	*	*
MnO	*	*	*	*
MgO	3.71	6.11	8.93	10.84
CaO	5.67	7.93	10.85	12.56
Na2O	5.86	5.22	3.12	1.98
K2O	4.85	2.31	1.22	0.72
P2O	0.76	0.33	0.17	0.10

1% Peridotite Melt at 10kbar, subtracting 5, 10, & 20% of amphibole composition for amphibole fractionated melt compositions				
	1% Melt	-5% Amphibole	-10% Amphibole	-20% Amphibole
SiO2	54.54	55.33	56.18	58.19
TiO2	0.39	0.20	-0.01	-0.51
Al2O3	20.66	20.95	21.26	21.99
FeO	1.79	1.63	1.31	0.55
Fe2O3	0.47	0.29	0.23	0.10
Cr2O3	*	*	*	*
MnO	*	*	*	*
MgO	3.38	2.80	2.16	0.63
CaO	4.21	3.85	3.45	2.50
Na2O	7.37	7.64	7.93	8.64
K2O	6.54	6.78	7.05	7.69
P2O	0.55	0.63	0.61	0.68

APPENDIX 5: NEWLY MAPPED SOUTHERN PEAK RANGE PETROGRAPHY

Below are petrographical descriptions of the newly mapped bodies in the southern Peak Range which are summarised in Table 2.1. Spatial locality of these bodies is shown in Figure 2.3, form characteristics are based on Mollan (1965) shown in Figure A, and rock type is based on the TAS Classification diagram shown in Figure 4.9.

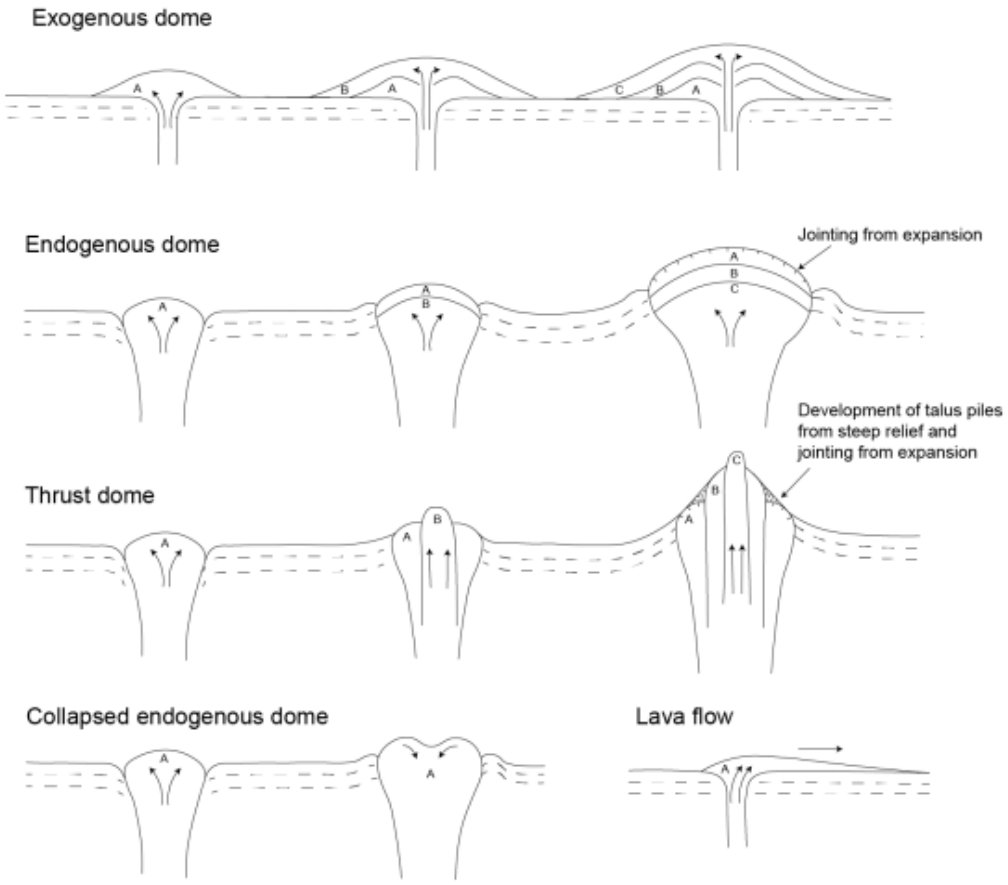

Figure A: Dome and flow morphologies of the southern Peak Range modified from Mollan (1965), taken from Chandler (2018)

Christmas Dome

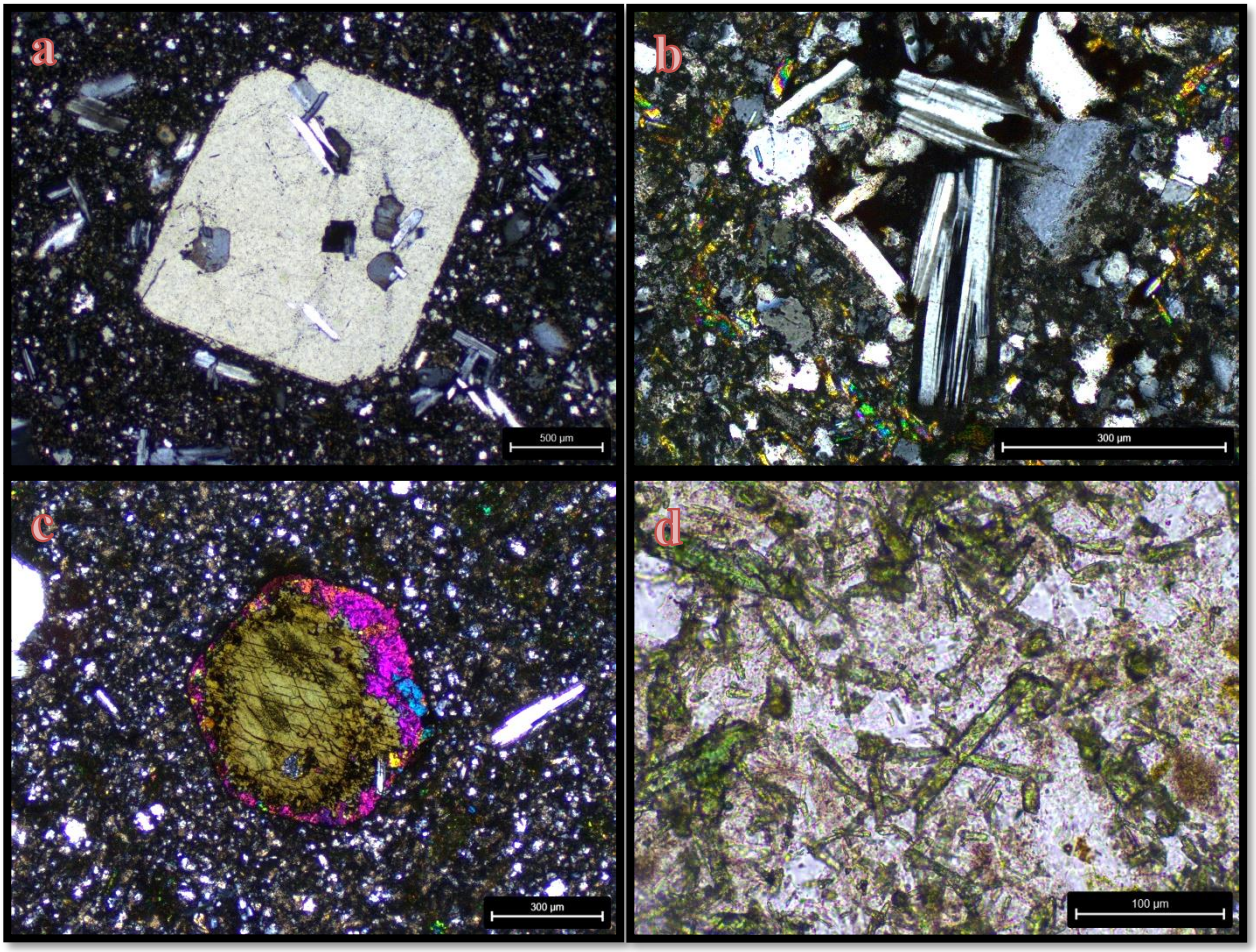

Figure B: Micrographs of aegirine rhyolite of Christmas Dome. a) Thin section of euhedral quartz (cream) phenocryst with alkali feldspar (grey to white) inclusion under XPL. b) Thin section of glomeroporhyritic cluster of albite (tabular), sanidine (grey) and quartz (rounded) under XPL. c) Thin section of euhedral amphibole (brownish green) rimmed by pyroxene (purple/blue) under XPL. d) Thin section of aegirine (green) rhyolite under PPL (colourless is alkali feldspar and quartz).

Christmas Dome is a sunken endogenous cumulo-dome measuring 0.7 km in diameter. The dome is characterised by aegirine rhyolite, and moderate flow banding of aegirine grains in the groundmass. The flow banding is restricted to the southern portion of the dome, and brecciated rhyolite is found on the NE edge, likely due to the nature of extrusion.

The aegirine rhyolite is characterised by a phenocryst assemblage of euhedral quartz (up to 1.2 mm) (Figure A.a), glomeroporhyritic albite, sanidine, quartz clusters (Figure A.b), and sparse euhedral amphibole occasionally rimmed by pyroxene (0.4 – 0.5 mm) (Figure A.c). The fine-grained groundmass is mainly quartz, alkali feldspar, and aegirine with minimal amounts of Na-amphibole. The abundance of aegirine gives outcrop and hand samples of

Christmas Dome its distinct green colour. When aegirine-poor, the rhyolite is cream in colour, and when it appears bluer in colour, then Na-amphibole is usually present in some quantity.

Thin sections show variability of quartz, feldspar, aegirine and Na-amphibole in the groundmass across a NE-SW transect on the southern side of the dome. Most fine-grained and flow banded samples have a quartz and aegirine-rich groundmass. Feldspar and aegirine-rich groundmasses appear to be concentrated to samples undergoing magma mingling. The brecciated rhyolite is quartz-rich and contains more Na-amphibole than aegirine in its ground mass. It should be noted that some samples have approximately even amounts of aegirine and Na-amphibole in the groundmass, or no Na-amphibole at all.

Due to very fine grain size, the exact Na-amphibole species was unable to be identified in Christmas Dome, and the Southern Ridge.

Southern Ridge

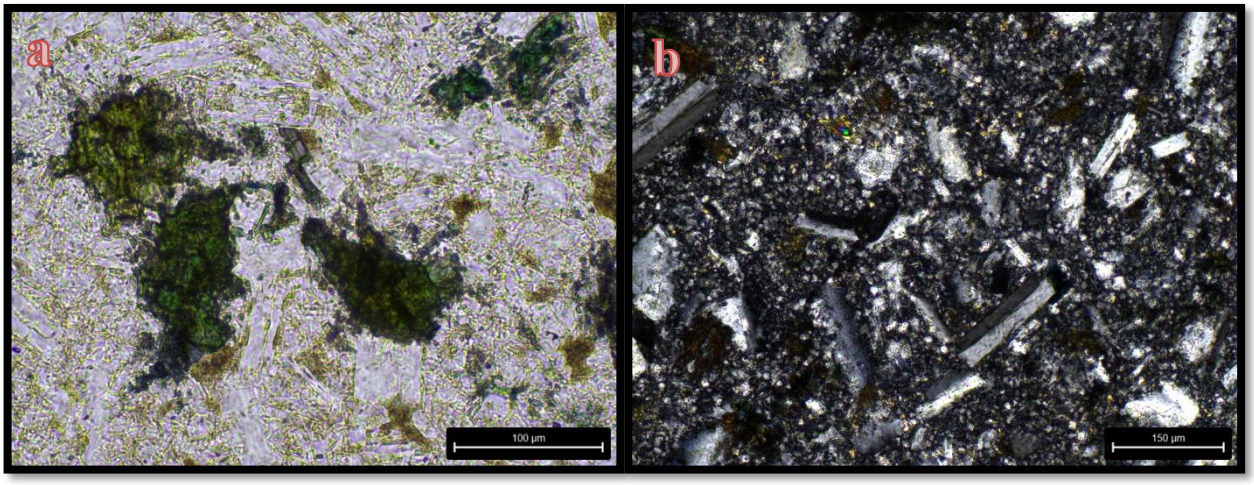

Figure C: Micrographs of aegirine rhyolite of the Southern Ridge. a) Thin section of aegirine (green) rhyolite groundmass with minor Na-amphibole (blue) under PPL (colourless is alkali feldspar and quartz). b) Thin section of sanidine (tabular) phenocrysts amongst aegirine (yellow to blue) and fine-grained alkali feldspar and quartz under XPL.

The Southern Ridge is a ridge-shaped lava flow spanning only 0.6 km in length (Figure 2.3). It consists mainly of magma mingling between aegirine/Na-amphibole rich and poor rhyolite,

with small areas of aphanitic aegirine rhyolite. The groundmass is alkali feldspar (predominantly sanidine) and quartz. Anhedral quartz (up to 0.5 mm) phenocrysts are found sparingly across the dome. The rhyolite at the very top of the dome is contains clasts of grey, vesicular pumice containing quartz and feldspar infill. Hand samples of the Southern Ridge range from fine-grain blue/white and green/white magma mingling, and fine-grained, blueish green aphanitic rock.

The Southern Ridge strangely has a patch of Permian sandstone in between the rhyolitic rock types, and a quartzite "dyke" running N-S below the eastern part of the dome (purple in Figure 2.3) estimated to be ~500 m long. The sandstone is coarse grained and reddish in colour, characteristic of the sandstone the volcanoes have protruded through. The quartzite is white, and sugary. Outcrop of the quartzite is minimal and was only seen when walking along the sandstone surrounding it.

Crescent Hill

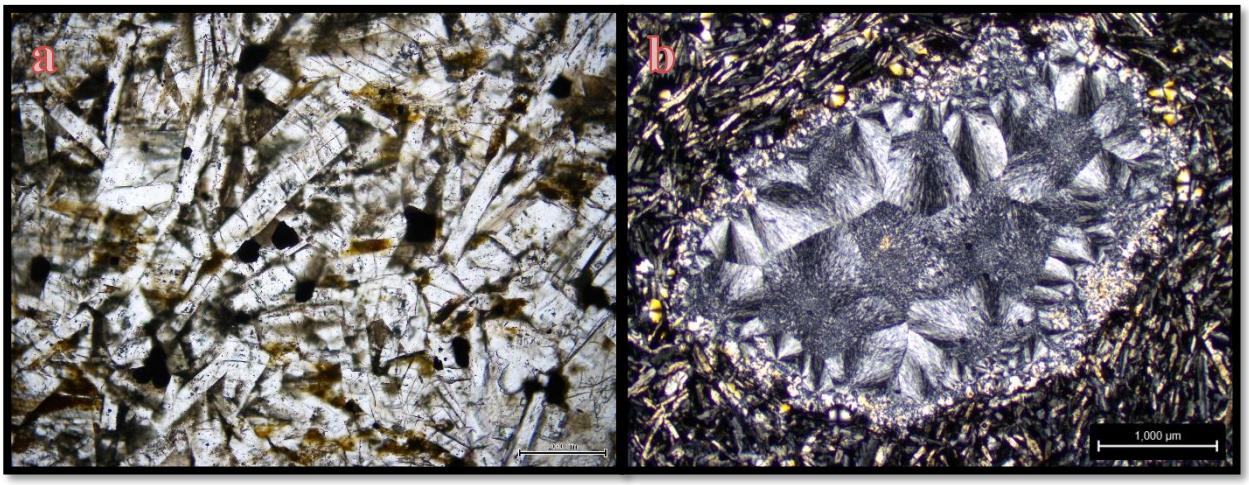

Figure D: Micrographs of trachyte of Crescent Hill. a) Thin section of sanidine (tabular) trachytic texture with opaque oxides (black) under PPL. b) Thin section of infilled vesicle with spherulitic texture of feldspar and quartz under XPL.

Crescent Hill is a barchan-shaped dome, 1.4 km in length (Figure 2.3), and likely represents a collapsed dome developed over an arcuate fissure (Mollan 1965). The dome is aphanitic trachyte, with infilled vesicles of various sizes (up to 1cm) present only in a small area of the

dome (NW). The groundmass consists of ~0.5 mm alkali feldspar grains (predominantly sanidine) arranged in a trachytic texture and commonly showing Carlsbad twinning, also sub-opaque matrix, and opaque oxides (up to 0.2 mm).

The infilled vesicles display spherulitic textures, a degassing feature that produces aggregates of radiating fibrous arrays made up of two minerals, quartz and feldspar (Figure B.b). It is unknown as to why the spherulitic textures is only present in such a small area of the dome.

In outcrop and hand samples, the rock is weathered orange. Fresh rock is hard to find, but it is usually fine grained, and blue in colour with yellowish vein-like weathering.

Gibson Hill

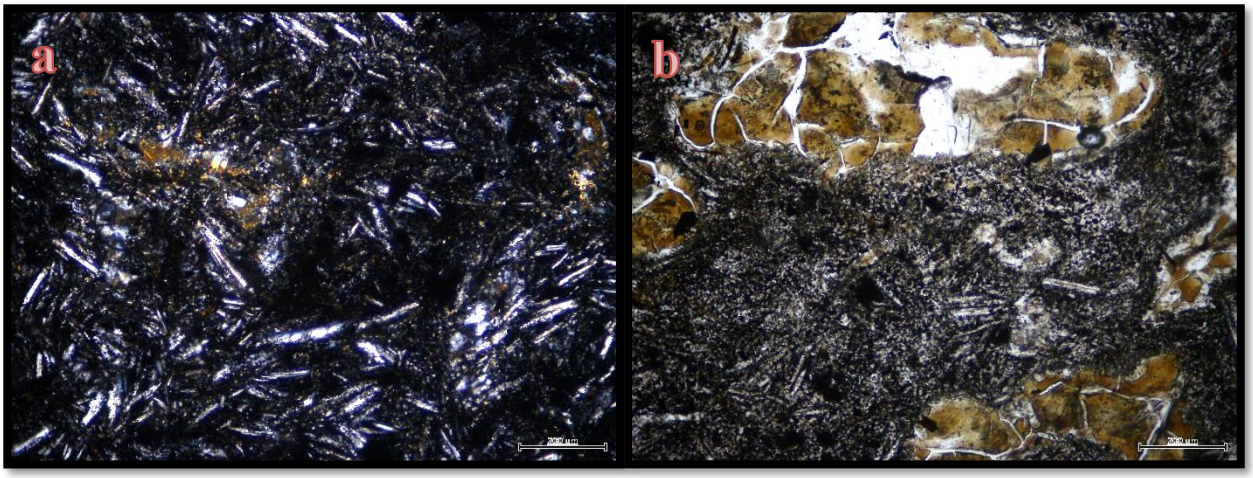

*Figure E: Micrographs of basaltic trachyandesite of Gibson Hill. a) Thin section of basaltic trachyandesite groundmass under XPL *thin section too thick. b) Thin section of unknown brown mineral within Gibson Hill under XPL.*

Located at the turn off to Gibson Downs on Colorado Road is a small hill (Gibson Hill in Figure 2.3) consisting of basaltic trachyandesite. It can be classified further depending on K_2O and Na_2O content. When Na_2O is $2.0 \leq K_2O$, the rock is shoshonite, and when Na_2O is $2.0 \geq K_2O$, the rock is mugearite, which is what is found at Gibson. The appearance of Gibson Hill is close to a sunken dome (similar to a smaller version of Christmas) and is only 150 metres wide. The groundmass is difficult to distinguish through thin section. Typical

mugearite is characteristic of oligoclase, olivine, and opaque oxides. Hand samples are dark grey, crystalline rocks with slight yellow/brown weathering.

Mollan (1965) identified the flood basalts of the Peak Range to consist mainly of alkalic and tholeiitic olivine basalts. Since Gibson Hill is similar to the alkaline basalts that Mollan described, it will be assumed that Gibson Hill is a gradual hill of flood basalt.

Mount Lowe

Figure F: Micrographs and field photos of trachyte and textures of Mount Lowe. a) Thin section of sanidine (tabular) trachytic texture with opaque oxides (black) under XPL. b) Thin section of glomeroporhyritic cluster of Sanidine amongst sanidine (tabular) trachytic groundmass under XPL. c) Onionskin texture of a trachyte hand specimen. d) Unknown green alteration within quarry at Mount Lowe.

Mount Lowe is a trachytic exogenous dome measuring 1.10 km x 1.45 km (Figure 2.3), characterised by a groundmass of ~0.2 – 0.5 mm alkali feldspar grains (predominantly sanidine) arranged in a trachytic texture and commonly showing Carlsbad twinning, as well

as opaque oxides (up to 0.4 mm). Sparse glomeroporhyritic clusters of sanidine, and ~0.7 mm phenocrysts of subhedral quartz are observed throughout. The petrography of Mount Lowe is similar to that of Crescent Hill, though outcrop of Mount Lowe is characteristic of onion skin weathering (Figure F.c), and green 'alteration' concentrated in a quarry at the SW side (Figure F.d).

Outcrops and hand samples of Mount Lowe are usually very weathered, greenish in colour and have phenocrysts being weathered out. Fresh rock is fine-grained, blue/grey in colour with visible tabular feldspar phenocrysts.

Boat Race Cluster

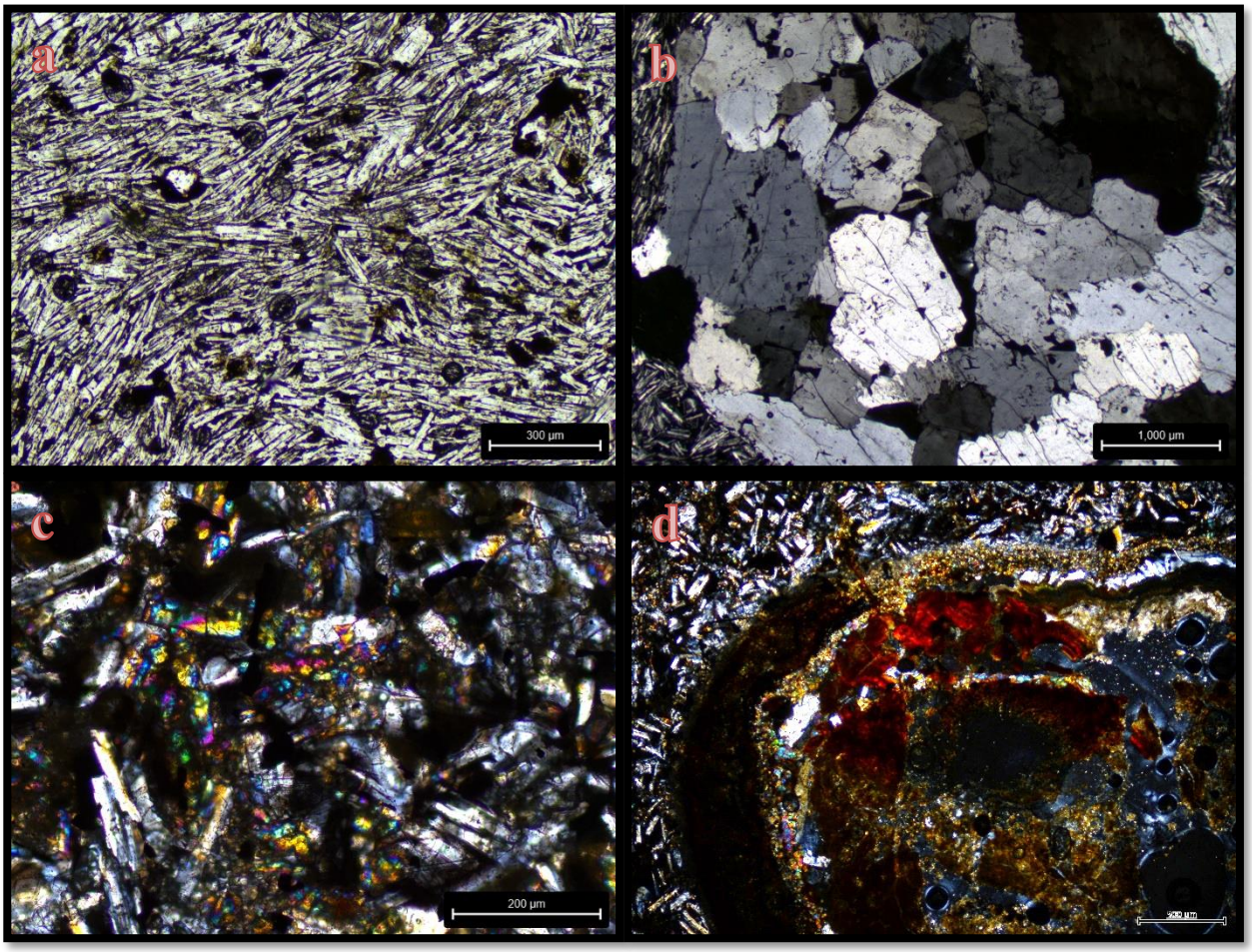

Figure G: Micrographs of trachyte and basaltic andesite of the Boat Race Cluster. a) Thin section of sanidine (tabular) trachytic texture with opaque oxides (black) and minor aegirine (green) under PPL. b) Thin section of granoblastic phenocryst of quartz (black, grey, white) within the trachyte under XPL. c) Thin section of basaltic andesite groundmass; sanidine (tabular), olivine (purple/blue), pyroxene (yellow/orange) and opaque oxides

(black) under XPL. d) Thin section of olivine phenocryst altered to iddingsite (brown) amongst basaltic andesite groundmass under XPL. Remnant olivine (purple/blue) is found rimming the iddingsite.

The Boat Race Cluster (Figure 2.3) is also barchan-shaped (0.9 km in size) but is likely originally an exogenous trachytic dome that had collapsed after a successive extrusion of another trachytic flow which breached the east wall and continued to flow eastwards (Mollan 1965). In the northern area of the dome is a small section consisting of basaltic andesite. It is likely that this is a dyke or flood basalt, as it is similar to the tholeiitic basalts that Mollan (1965) described. The groundmass consists of olivine, alkali feldspar (likely sanidine), pyroxene, and opaque oxides (Figure G.c). Figure G.d shows a large phenocryst of olivine (heavily altered to iddingsite) which is found sparingly throughout the rock. The basaltic andesite is crystalline, dark grey rock with visible brown iddingsite after olivine phenocrysts, 4 – 8 mm in length.

The rest of the dome consists of equigranular trachyte characterised by ~0.2 mm alkali feldspar grains (predominantly sanidine) arranged in a trachytic texture and infrequently showing Carlsbad twinning, as well as minor aegirine and a sub opaque matrix. Large phenocrysts of granoblastic quartz (up to 8 mm) are present throughout the dome (Figure G.b). The quartz phenocrysts can be seen amongst a blue/green fine groundmass in a fresh rock face.

APPENDIX 6: AMPHIBOLE NOMENCLATURE

The general chemical formula of amphiboles can be written as $A\ B_2\ C_5\ T_8\ O_{22}\ W_2$, where

A = □, Na, K, Ca, Pb, Li;
B = Na, Ca, Mn^{2+}, Fe^{2+}, Mg, Li;
C = Mg, Fe^{2+}, Mn^{2+}, Al, Fe^{3+}, Mn^{3+}, Cr^{3+}, Li;
T = Si, Al, Ti^{4+}, Be;
W = (OH), F, Cl, O^{2-}.

as of the classification system of IMA 2012 (Hawthorne et al. 2012). All amphiboles in this study have been named under calcium amphiboles via this system. Ca-amphiboles are classified as $^{B}(Ca + \Sigma M^{2+})/\Sigma B \geq 0.75$, $^{B}Ca/\Sigma B \geq B\Sigma M^{2+}/\Sigma B$, and further classified via the compositional boundary plot defined by $C = {}^{C}(Al+Fe^{3+}+2Ti)$ apfu vs $A = {}^{A}(Na+K+2Ca)$ apfu. Average composition of amphibole found in the peridotite is as follows: SiO_2 41.67, TiO_2 1.32, Al_2O_3 14.75, Cr_2O_3 1.47, $FeO_{(t)}$ 6.44, MnO 0.11, MgO 17.04, CaO 10.40, Na_2O 3.18, and K_2O 0.69. Once apfu of each element is calculated, it can then be placed in the structure above:

T= Si(5.98) Al(2.02)
C= Mg(3.59) Fe2+(0.71) Mn(0.01) Al(0.33) Fe3+(0.00) Cr(0.14) Ti(0.14)
B= Na(0.42) Ca(1.58)
A= Na(0.42) K(0.13)
For classification, C = Al(0.33) + Fe3+(0.00) + 2* Ti(0.14), and A = Na(0.42) + K(0.13).

Average composition of the amphibole found as xenocrysts in the trachybasalt is as follows: SiO_2 39.72, TiO_2 3.96, Al_2O_3 15.25, Cr_2O_3 0.03, $FeO_{(t)}$ 8.65, MnO 0.09, MgO 14.27, CaO 10.95, Na_2O 2.30, and K_2O 1.92. Once apfu of each element is calculated, it can then be placed in the structure above:

T= Si(5.72) Al(2.28)
C= Mg(3.14) Fe2+(0.46) Mn(0.01) Al(0.37) Fe3+(0.61) Ti(0.40)
B= Na(0.27) Ca(1.73)
A= Na(0.39) K(0.36)
For classification, C = Al(0.37) + Fe3+(0.61) + 2* Ti(0.40), and A = Na(0.39) + K(0.36).

Below is the Ca-amphibole compositional plot (Hawthorne et al. 2012) with all data values of each amphibole grain found (Figure H). Amphibole in the peridotite is pargasite, and the amphibole xenocrysts are sadanagaite.

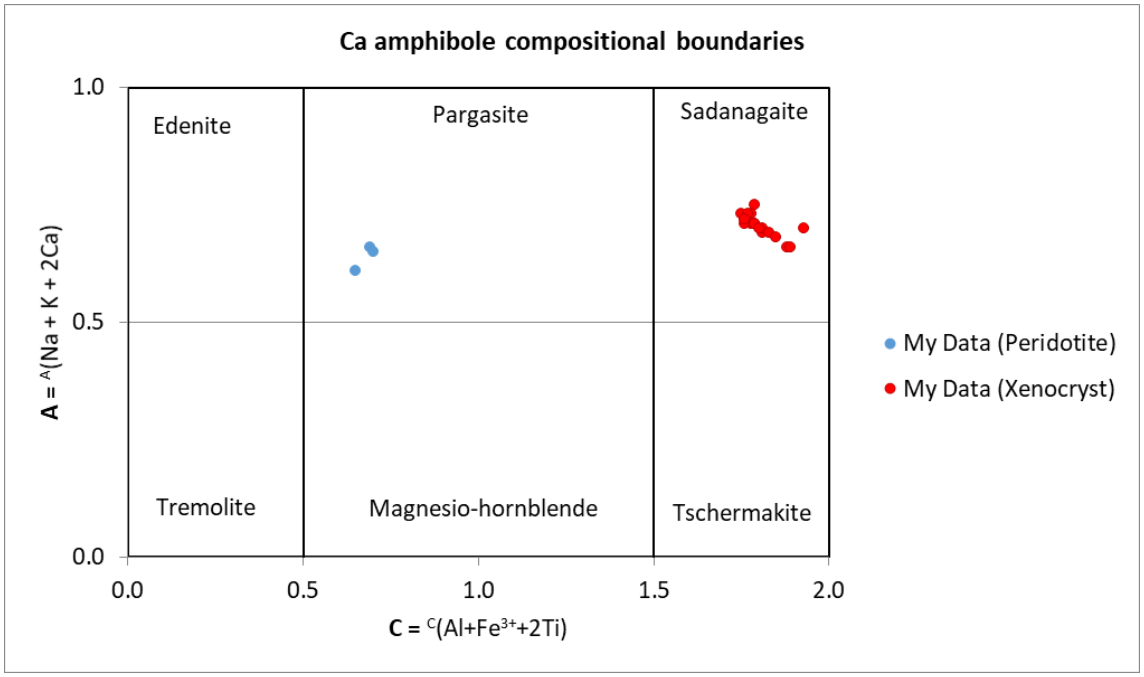

Figure H: Calcium amphiboles and their compositional boundaries after Hawthorne et al. (2012).

When discovered in 1984, sadanagaite was first described as a new silica-poor amphibole. Sadanagaite in 1984 is now classified as potassic-ferro-sadanagaite. Na and Fe^{2+} dominant amphiboles described as sadanagaite between 1997 and 2012 are now ferro-sadanagaite, and the material described by Banno et al (2003) as magnesio-sadanagaite is now defined as sadanagaite.

APPENDIX 7: ADDITIONAL CLASSIFICATION

Alumina Saturation Index

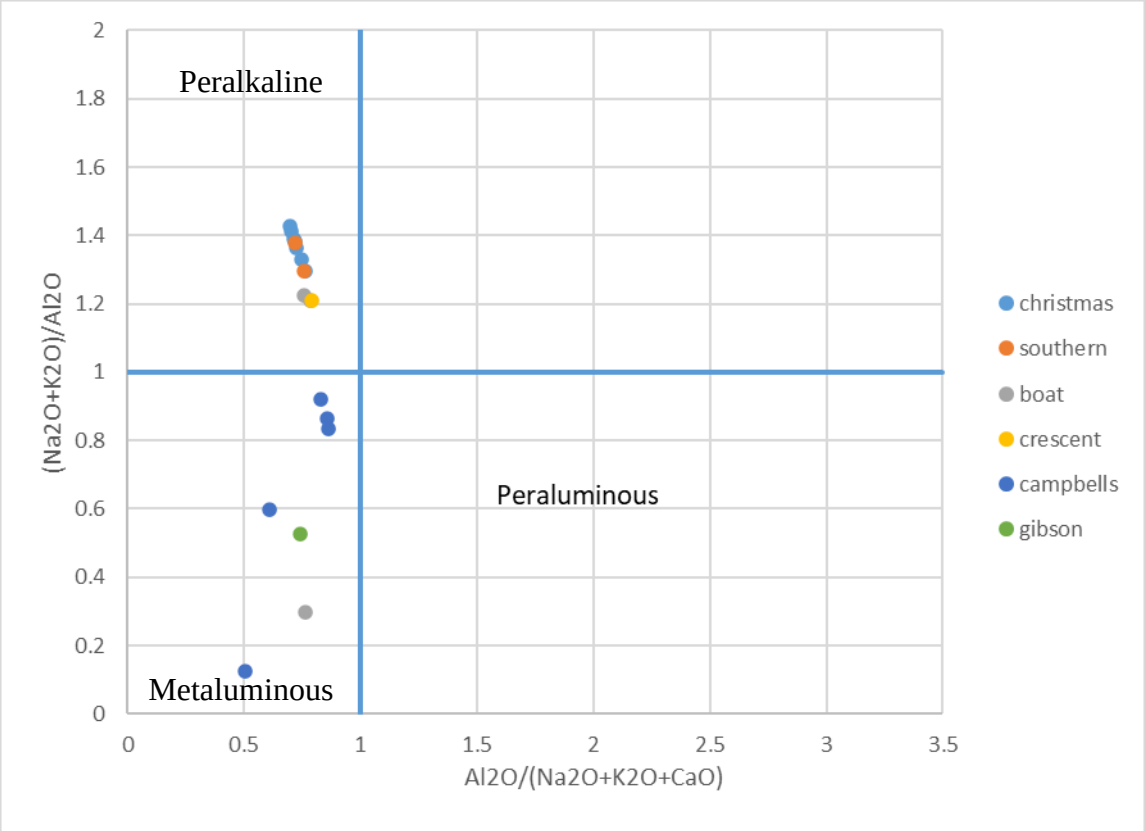

Figure I: Alumina saturation index (Al2O3/(Na2O+K2O+CaO) vs (Na2O+K2O)/Al2O3) plot for all samples.

Above is an alumina saturation index (Al2O3/(Na2O+K2O+CaO) vs (Na2O+K2O)/Al2O3) plot for all samples (Figure I). This plot shows that all values that plot below 1 in Figure 4.10 are metaluminous and confirming that values above 1 are peralkaline.

Zeolite Composition Comparison (MSA)

As mentioned in Section 4.1, the zeolite minerals are classified only based on comparison of the Mineralogical Society of America's database. The table below shows the comparison between the zeolites found at Campbell's Peak with MSA data to confirm the classification of natrolite and analcime.

Comparison of zeolite found at Campbell's Peak with the zeolite compositions of MSA.

	Natrolite (MSA)	Natrolite (Tephriphonolite)	Analcime MSA)	Analcime (Trachyandesite)
SiO_2	47.60	48.30	54.58	54.79
Al_2O_3	27.40	28.74	23.05	25.03
MgO	n/a	0.02	0.10	0.02
CaO	0.13	0.37	0.45	0.45
Na_2O	15.36	14.89	13.50	11.84
K_2O	0.23	0.13	0.00	0.34
H_2O^+	9.47	~7.00	8.70	~7.00
Total	100.19	92.59	100.38	92.63

Note: water content (red) of the zeolite from Campbell's is based of the total.